STRUCTURE-FUNCTION RELATIONSHIPS AND ACTION MECHANISM OF KRAIT NATRIURETIC PEPTIDE

SINDHUJA SRIDHARAN

B.Tech. (Hons.), SASTRA University

A THESIS SUBMITTED
FOR THE DEGREE OF DOCTOR OF PHILOSOPHY

DEPARTMENT OF BIOLOGICAL SCIENCES

FACULTY OF SCIENCE

NATIONAL UNIVERSITY OF SINGAPORE

2014

Declaration

I hereby declare that the thesis is my original work and it has been written by me in its entirety. I have duly acknowledged all the sources of information which have been used in the thesis.

This thesis has also not been submitted for any degree in any university previously.

Sindhuja Sridharan

23rd January 2014

Acknowledgements

At the outset I would like to thank the almighty to have blessed me with the best parents, teachers and friends, without whom I would not be who I am today. The encouraging words, enlightening talks, endless fun with them has made the journey memorable and enjoyable. I would like to extend my sincere thanks to National university of Singapore for having given me the opportunity to conduct my research in the Department of Biological sciences with financial assistance.

I would like to express my gratitude to my mentor Prof. Manjunatha Kini for his constant guidance and support. Under his supervision, I have not just learnt protein chemistry but the art of conducting independent research. His critical comments and informative discussions have honed my rational thinking and questioning abilities. The freedom that I have experienced in his lab has given me a platform to learn a lot, think differently, design my own experiments and most importantly, evolve into a confident scientist.

I would like to thank Prof. Peter Wong from the Department of Pharmacology, for letting me use his lab space and equipment to conduct my research. My sincere thanks to Prof. Arthur Mark Richards and Dr. Y T Chen, for giving me the opportunity to perform my cell culture experiment in Cardiovascular Research Institute. My sincere appreciation and thanks to my inspiring peers, Ms. Su Jing and Ms. Sheena Foo for imparting me the skills of surgery and isolated tissue experiments.

My heartfelt thanks to my teachers, Mrs. Sundari, Mrs. Hemalatha, Mrs. G. Vijayalakshmi, Dr. Uma Maheshwari, Dr. Adeline Princy, Dr. Rajan, Dr. Sridharan, Dr. H. M. Shankar who have given a strong foundation in the field of biology and chemistry.

My appreciation and thanks to my lab officers Ms. Tay Bee Ling, Ms. Xu Liyuan and Mrs. Ting who have been prompt in helping me order reagents and for helping me find different equipment. Thanks to Ms. Reena and Ms. Priscilla for easing the administrative processes.

I would like to express my heartfelt thanks to all the past and present members of my lab for having created a friendly and positive environment for work. Million thanks to my seniors Bhaskar, Girish, Angie Ng, Sheena, Reza and Amrita, who have been instrumental in imparting different techniques and skills. My sincere thanks to my lab twin, Bidhan who has taught me nuances of different equipment. I would not have been able to grow as a researcher if not for the scientific discussions with these people. I have learnt a lot of troubleshooting and experiment design from Bhaskar and Girish. Their constructive suggestions have improved my technical skills. I want to thank Ryan (my lab bench buddy) and Angelina for their help and valuable suggestions. I would like to thank all my peers Summer, Ritu, Janaki, Varuna, Norrapat, Feng Jian, Ben, Chen Wan, Shifali and Shiyang for their timely help and support. I have had the opportunity to mentor several undergraduate and exchange students. I would like to thank them for helping me to become a better teacher.

The journey of PhD had a number of frustrating moments. But rejuvenating back to a cheerful strive was only possible because of my friends. My block 511 buddies, Tanujaa, Pratibha, Swetha, Shridhivya, Soumya and Devika had created home away from home. They always had ears to listen to my long mind-numbing stories and have encouraged me in depressing times. Life would not have been as fun-filled if not for the outings and crazy chats we have had. My housemates and my other friends Divya Shankari, Akila, Lavanya, Omar, Srinath, Shreenath, Vignesh and Rohit have made my stay in Singapore the most memorable and fun-filled. Thanks guys!!

A special thanks to my family; I'm extremely grateful to my mother Mrs. Sowmithri and my father Mr. C. Sridharan who have been encouraging and supporting me always. They have been motivating me all through my hardships and had belief in me. Another person desires special thanks, my sister and my friend Ms. Swetha who I have tried to emulate from childhood. She has been the best critic and has helped me in every walk. Finally I would like to thank all my other friends and family members for all their encouragement. Thank you all!

Sindhuja Sridharan

January 2014

Table of contents

Summary

Natriuretic peptides (NPs) are a class of potent vasoactive peptide hormones, which maintain circulatory pressure/volume homeostasis through mediating vasodilation and decreasing vascular fluid volume. These regulatory peptides mediate their function through binding to membrane bound guanylyl cyclase receptors. There are three mammalian NPs, namely ANP, BNP and CNP that are well characterized. Snake venom NPs are structurally similar to mammalian endogenous NPs with a 17-residue ring but with C-terminal extension of varying lengths that confers altered biological activities.

Transcriptome of red-headed krait venom gland revealed the presence of a unique NP; called KNP. Structurally, this NP is distinct from mammalian and other venom NPs. It has a 38 residues long C-terminal tail in contrast to 4-6 residues in mammalian NPs. Further, this tail has the propensity to form an α-helix, unlike other NPs. This thesis documents the mode of action and structure-function relationships of KNP.

KNP was heterologously expressed and purified from *E.coli* and its activity was assessed using in-vivo, ex-vivo and in-vitro assays. KNP induced relaxation of pre-contracted aortic strips in ex-vivo organ bath experiments by a mechanism independent of NP receptors. It induced vasodilation via endothelium-dependent pathways in contrast to ANP which mediated vasodilation via endothelium-independent mechanisms. In experimental animals, infusion of ANP caused a rapid drop in blood pressure which recovered within 30 min after the infusion was stopped. In contrast, KNP caused a sustained drop in blood pressure which did not recover within the experimental period (40 min). Also ANP caused a marked increase in urine

volume while KNP had no renal effects. These results showed that KNP exerted its biological activity through a different mechanism than canonical NPs such as ANP.

The activities of various deletion mutants revealed the presence of two functional pharmacophores; the KNP Ring and the putative C-terminal helix. The ring functions like a classical NP while the putative helix induces vasorelaxation in an endothelium-dependent manner like intact KNP. Thus, the helical segment in the C-tail in KNP confers its function. The ring of KNP has receptor binding ability, but the presence of its tail blocked its interaction with NP receptors. Further, using various inhibitors, KNP was found to require nitric oxide, prostacyclins and hyperpolarization factor from endothelium to evoke vasodilation.

KNP showed a remarkable resistance to degradation by neutral endopeptidase (> 150 min). Also, Ring of KNP showed increased half-life (12 min) compared to ANP (1.8 min). Using different mutants D3, R4 and D14 residues were identified to be responsible for the increased half-life of Ring.

Thus this study has lead to the understanding of the mode of action of a unique NP-like peptide using structure- based activity approaches.

List of tables

Chapter 1

Chapter 2

List of Figures

Chapter 1

Chapter 2

Chapter 3

Chapter 4

Appendix

Abbreviations

Single and three letter abbreviations of amino acids were followed as per the recommendations of the IUPAC-IUBMB Joint Commission on Biochemical Nomenclature.

Chemicals and reagents

HEPES	4-(2-Hydroxyethyl)piperazine-1-ethanesulfonic acid
Ach	Acetylcholine
APS	Ammonium persulfate
BCA	Bichinchonic acid
BSA	Bovine serum albumin
CaCl2	Calcium chloride
DCM	Dichloromethane
DIPEA	N-N-diisopropylethylamine
DMEM	Dulbecco's Modified Eagle's Medium
DMF	N-N- dimethyl formamide
dNTP	Deoxyribonucleotide triphosphate
DTT	Dithiothreitol
EDT	Ethylenediamine tetraacetic acid
EDT	1,2-ethanedithiol
FA	Formic acid
FBS	Fetal bovine serum
Fmoc	9-fluorenylmethoxycarbonyl
HCl	Hydrochloric acid
IBMX	3-Isobutyl-1-methylxanthine
IPTG	Isopropyl β-D-thiogalactoside
KCl	Potassium chloride
KH_2PO4	Potassium di-hydrogen phosphate
LB	Luria bertani
L-NAME	L- arginine methyl ester hydrochloride
$MgCl_2$	Magnesium chloride
$MgSO_4$	Magnesium sulphate
NaCl	Sodium Chloride

$NaHCO_3$	Sodium bicarbonate
NaOH	Sodium hydroxide
NMP	N-methyl pyrrolidine
ODQ	1H-[1,2,4]oxadiazolo[4,3-a]quinoxalin-1-one
PBS	Phosphate-buffered saline
PE	Phenylephrine
SDS	Sodium dodecyl sulphate
TEMED	N,N,N′,N′-Tetramethylethylenediamine
TFA	Trifluoroacetic acid
TIS	Triisopropylsilane
Tris	Tris(hydroxymethyl)-aminomethane

Units

Å	Angstrom
cm	Centi meter
CPS	Counts per second
Da	Daltons
°C	Degree Celsius
U	Enzyme unit
g	Gram
h	Hour
kDa	Kilo Daltons
kg	Kilo gram
l	Litre
µg	Micro gram
µl	Micro litre
µM	Micro molar
µmol	Micro mole
µm	Micron
mAU	Milli absorbance unit
mg	Milli gram
ml	Milli liter

mm	Milli meter
mm Hg	Milli meter mercury
mM	Milli molar
min	Minute
M	Molar
ng	Nano gram
nm	Nano meter
nmol	Nano mole
nM	Nano molar
rpm	Revolutions per minute
s	Second
V	Volt

Others

ANP	Atrial natriuretic peptide
ATP	Adenosine triphosphate
BNP	B-type natriuretic peptide
BPM	Beats per minute
Ca^{2+}	Calcium
cDNA	Complementary DNA
cGMP	cyclic guanosine monophophate
CIEX	Cation exchange chromatography
CNP	C-type natriuretic peptide
CO2	Carbon dioxide
COX	Cyclooxygenase
C-terminus	Carboxy terminus
DAG	Diacylglycerol
DNP	Dendroaspis natriuretic peptide
EC_{50}	Effective concentration 50
ESI-MS	Electrospray ionization-mass spectrometry
GC	guanylyl cyclase
GTP	Guanosine triphosphate
IP	Intraperitoneal
IP3	Inositol-3-phosphate

K^+	Potassium ion
KHD	Kinase homology domain
KNP	Krait natriuretic peptide
LC-MS	Liquid chromatography- mass spectrometry
m/z	Mass to charge ratio
MAP	Mean arterial pressure
NEP	Neutral endopeptidase
NO	Nitric oxide
NOS	Nitric oxide synthase
NP	Natriuretic peptide
NPR	Natriuretic peptide receptor
N-terminus	Amino terminus
OD600	Optical density at 600 nm
PCR	Polymerase chain reaction
PDE	Phosphodiesterase
pGC	particulate guanylyl cyclase
pI	Isoelectric point
PKG	Protein kinase G
PLC	Phospholipase C
PP	Pulse pressure
RAAS	Renin-angiotensin-aldosterone system
RP-HPLC	Reverse phase-high performance liquid chromatography
SDS-PAGE	Sodium dodecyl sulfate polyacrylamide gel electrophoresis
SEM	Standard error mean
sGC	soluble guanylyl cyclase
SPPS	Solid phase peptide synthesis
TEV	Tobacco-etch-virus
Trx	Thioredoxin
α	Alpha
β	Beta
Δ	Delta

List of Publications/ Conferences

Publications

"Tail wags the dog- C-terminal tail of KNP redirects it away from natriuretic peptide receptor." S Sridharan, R M Kini (Manuscript under preparation)

Conferences

Gene Structure and regulation mechanism of BPP-CNP gene from *Sistrurus catenatus tergiminus.* Sridharan S, Kini. R.M. Poster presented at **15th Biological Science Graduate Congress**, University of Malaya, Kuala Lumpur, December 2010.

Structural and functional characterization of a novel Natriuretic peptide from *Bungarus flaviceps*. Sridharan S, Kini. R.M. Poster presented at **6th International Conference for Structural Biology and Functional Genomics**, National University of Singapore, Singapore, December 2010.

Action Mechanism and Structure-function relationship of Krait Natriuretic peptide. Sridharan S, Kini. R.M. Oral presentation at **16th Biological Science Graduate Congress**, National University of Singapore, Singapore. December 2011.

Structure-function relationship and Action mechanism of Krait Natriuretic Peptide (KNP). Sridharan S, Kini. R.M. Oral presentation at **17th Biological Science Graduate Congress**, Chulalongkorn university, Thailand. December 2012.

KNP- A non-classical natriuretic peptide. Sridharan S, Kini. R.M. Poster presentation at **6th International conference on cGMP**, Erfurt, Germany, June 2013

Structure-function relationship and Action mechanism of Krait Natriuretic Peptide (KNP). Sridharan S, Kini. R.M. ePoster Presentation at **27th ISTH Congress**, Amsterdam, Netherlands. July 2013.

Natriuretic peptides from snake venom. Sridharan S, Kini. R.M. Oral Presentation at 5th International conference on **Exogenous factors affecting thrombosis and haemostasis**, Amsterdam, Netherlands. July 2013

CHAPTER 1

Central role of natriuretic peptides- An Introduction

Chapter 1: Central role of natriuretic peptides – An Introduction

1.1. Blood pressure regulation

Blood flow is one of the vital processes for the survival of a vertebrate organism. Constant flow of blood ensures distribution of oxygen and nutrients to all tissues and organs. This is sustained by repeated, rhythmic contraction of heart, which pushes blood into the blood vessels for dissemination throughout the body. Blood circulation is a pressure driven phenomenon, like any other fluid driven by a pump. The pressure in this system is due to the force exerted by blood on the walls of the blood vessel, commonly known as blood pressure (BP), defined by Ohm's law of fluid dynamics (pressure = flow X resistance). Flow is directly dependent on the amount of blood that is squeezed into circulation by heart, called cardiac output (CO) and resistance depends on the contractile state of arteries and arterioles, called systemic vascular resistance (SVR).

An array of stabilizing mechanisms such as neural, renal or humoral, modulate CO and SVR to keep BP within certain limits. Of these regulatory processes sympathetic nervous system (SNS) and kidneys play a major role. On a short time scale (seconds to hours), the variation in BP due to day to day activities (feeding, exercise, emotions, etc.) is effectively buffered by the SNS which senses the pressure changes with its afferent sensors (Sunagawa *et al.*, 1998). Regulation of arterial pressure in hours or longer is heavily dependent upon the kidneys, which dictate fluid-electrolyte balance.

Momentary changes in blood pressure are detected through three different sympathetic afferents, namely baroreceptors, thermoreceptors and

chemoreceptors, which sense pressure, temperature and oxygen levels respectively (Guyenet, 2006). Changes in these parameters result in an autonomic reflex feedback which signals heart and blood vessels to restore BP to its normal value (Guyenet, 2006). Within minutes to hours after a disturbance in BP, mechanisms that modulate fluid volume such as movement of intravascular fluid into interstitial space are activated. These short-term regulatory signals, reset the BP perturbation partly towards the normal level, but does not restore back completely to baseline (Hall *et al.*, 2012). In such circumstances, long-term regulatory processes play a key role. Thought to be a kidney-centric phenomenon, long-term BP control alters body fluid volume through excretion to bring the system back towards baseline. Body fluid volume is determined by the balance between intake and excretion of salt and water (through kidneys, skin, gut and airways). Higher fluid volume imposes higher load on heart and hence, it is critical to maintain an appropriate salt and water levels to sustain normal BP. Thus, in response to rising BP, normally excretion of water and salts through the kidneys is increased. This regulatory mechanism is modulated by various hormonal and neural controls. Out of the exhaustive number of endocrinal secretions, renin-angiotensin-aldosterone system (RAAS) and natriuretic peptides (NPs) have influential roles. RAAS promotes sodium and water reabsorption and causes vasoconstriction. Excessive activation of this system elevates BP and circulating volume, which increases the transmural distending pressure experienced by cardiac muscles. This force exerted on the heart induces the production of NPs. These peptides cause vasodilation and increased excretion of water and salt as a part of a homeostatic negative feedback. Thus, according to the Guytonian concept of

BP control, no disturbance can render a sustained alteration in BP unless the renal – pressure – volume relationship is reset.

Pathophysiological state such as hypertension (HTN), the elevated BP increases stress on heart. It is one a major causes for cardiovascular, cerebrovascular and renal disorders like chronic heart failure (CHF), stroke, kidney failure etc., which are associated with high morbidity and mortality.

Heart failure (HF) is a clinical syndrome, which is associated with impaired ability of the ventricles of the heart to fill (diastolic dysfunction) or eject (systolic dysfunction) blood (Yancy *et al.*, 2013). It is estimated that about 5.1 million in the U.S. have HF (Go *et al.*, 2014) which accounts for 7% of total deaths due to cardiovascular disorders (Manickavasagam *et al.*, 2009). HTN increases the risk of development of HF and is precedent in 75% of HF patients (Chobanian *et al.*, 2003). Drugs with antihypertensive properties such as angiotensin converting enzyme inhibitors (ACEI), Angiotensin-II- receptor blockers (ARBs), β-blockers, Ca-channel blockers, diuretics, aldosterone-receptor blockers, vasodilators etc., have shown to decrease mortality due to HF (Manickavasagam *et al.*, 2009). The potential strategies for antihypertensive therapy include, lowering CO and SVR along with increased urinary excretion of salt and water. Since multiple counter-acting mechanisms control BP, the antihypertensive action of a drug is evaluated not only based on its primary target but as well by its efficacy to regulate the compensatory processes. Table 1.1 lists the present targets for antihypertensive agents used for HF treatment.

1.2. Antihypertensive therapy

1.2.1. Systemic hemodynamics as target

1.2.1.1. Anti-adrenergics

This class of drugs lowers the blood pressure by limiting the activity of neurotransmitters – epinephrine and norepinephrine. Activation of β1-adrenergic receptors on the specialized conductive tissue of the heart by norepinephrine increases heart rate and contractibility. On the blood vessels, norepinephrine binds to α1-adrenergic receptors resulting in vasoconstriction (Del Bo *et al.*, 1985). Circulating epinephrine binds to β2-adrenergic receptors on the blood vessels to stimulate vasodilation (Del Bo *et al.*, 1985).

Peripheral receptor blocking drugs belong to two major classes; β-blockers and α-blockers. These drugs prevent the neurotransmitters from binding to their receptor, thereby reducing heart rate and blood pressure (Stokes *et al.*, 1974). Owing to the negative inotropic effects and ability to cause bradycardia, β-blockers are not considered as the first-line medication in case of HF (Remme and Swedberg, 2001). However, current guidelines prescribe the use of β-blockers for systolic dysfunction only after stabilization using ACEI therapy (Dickstein *et al.*, 2010).

Apart from the peripheral receptor blockers, drugs that act on central and peripheral nerve fibers are in use. Centrally acting drugs such as clonidine and methyldopa prevent the stimulation of SNS in response to increased BP while the peripheral drugs deplete the autonomic nerves of the neurotransmitter norepinephrine.

1.2.1.2. Renin- Angiotensin inhibitors

RAAS system produces potent vasoconstricting hormones, which induce the reabsorption of sodium and water through the kidneys. This system involves the production of angiotensin I (Ang I) from its precursor angiotensinogen through the action of renal protease renin. Further Ang I is proteolytically cleaved by angiotensin converting enzyme (ACE) to form the bioactive angiotensin II (Ang II). Ang II binds to its receptors AT1 to cause vasoconstriction in smooth muscles, increased reabsorption of water and sodium by the kidneys and synthesis of aldosterone by adrenal cortex. Thus the primary targets inhibited in this system are, drugs that block renin secretion, ACE inhibitors (ACEI), AT1 receptor blockers (ARB) and aldosterone receptor. These drugs are predominantly used for hypertension, as they are associated with marked decrease in SVR without significant change in CO, along with favorable renal effects (de Boer *et al.*, 2003). ACEI therapy is recommended for patients with systolic dysfunction and is proven to have reduced mortality and hospitalization rate (Manickavasagam *et al.*, 2009). ACEIs remain the first choice drugs with ARBs as alternative drugs in case of HF (Remme and Swedberg, 2001).

1.2.1.3 Direct vasodilators

These are drugs cause the relaxation of arteries. These drugs act quickly and are used in emergencies, as they are associated with potential hypotension and fluid retention. These drugs cause an elevation of cGMP in vascular smooth muscles. This increase in cGMP dilates blood vessels, which in turn cause reduction in arterial pressure, stroke volume and cardiac output (Kawakami *et al.*, 1995). The current guidelines recommend the infusion of

Table 1.1. List of antihypertensive drugs and their targets

Class of drug	Effect	Primary target	Examples of drugs in market
Centrally acting drugs	Reduce sympathetic neurotransmission	Cardiac and vascular sympathetic drive affecting HR, CO and SVR	Methyldopa Clonidine
Anti-adrenergic drugs			
- α-adrenoceptor blocker	Antagonism of α- adrenoceptor	CO, heart rate, inhibition of renin release	Prazosin and doxazosin Betaxolol , bisprolol
- β-adrenoceptor blocker	Antagonism of β- adrenoceptor		
ACE inhibitors	Reduce formation of Ang II	SVR and water-salt reabsorption	Captopril, enalapril, imidapril
AT1 receptor blocker	Blocks receptor subtype 1 of Ang II	SVR and water-salt reabsorption	Irbesartan, candesartan cilexetil, Valsartan
Vasodilators	Relax blood vessels	SVR	Nitroglycerine, itramin, propatylnitrate , Natriuretic peptides
Ion channel modulators		SVR and HR	
- Potassium channel openers	Hyperpolarization		Nicorandil Verapamil
- Calcium channel blockers	Reduce intracellular calcium		Nifedipine, Felodipine, Amlodipine
Diuretics	Block nephron tubular sodium reabsorption	Vascular fluid volume	
- Loop			Furosemide, Bumetanide
- Thiazide			Metolazone, Indapamide
- Potassium-sparing			Amiloride, Spironolactone, Eplerenone

Co: cardiac output, SVR: systemic vascular resistance

nitroglycerin, nitroprusside or nestritide (B-type natriuretic peptide) in case of absence of symptomatic hypotension in patients with HF (Lindenfeld *et al.*, 2010).

1.2.1.4 Ion channel modulators

These drugs cause hyperpolarization of smooth muscles, which initiates relaxation. Potassium channel openers and calcium channel blockers are the potential drugs (MacGregor *et al.*, 1987; Richer *et al.*, 1990). These drugs cause an indirect elevation of cGMP by decreasing intracellular Ca^{2+} ions. Thus resulting in reduction in SVR, heart rate and stroke volume, which reduces BP. Calcium channel blockers such as Amlodipine and Verapamil are used for diastolic dysfunction (Manickavasagam *et al.*, 2009).

1.2.2. Kidney as target: Diuretics

1.2.2.1 Loop and thiazide diuretics

These are the oldest drugs, which have been used for antihypertensive therapy. These drugs aid elimination of water and salts by the kidneys. This process reduces fluid volume, and hence, lowering the load on heart thereby reducing BP. The diuretic drugs commonly target Na-K-2Cl cotransporters in different locations within the kidney. Loop diuretics prevent the reabsorption of sodium and chloride in the Henle loop of nephron while the Thiazide diuretics act on distal loop. Usage of diuretics is usually associated with potassium depletion, necessitating dietary supplements (Swedberg *et al.*, 2005). This class of drugs is used only in patients with fluid overload as in pulmonary congestion or peripheral oedema and is usually given in combination with ACEIs (Remme and Swedberg, 2001).

1.2.2.2 Potassium-sparing diuretics

Aldosterone antagonists or mineralocorticoid antagonists such as spironolactone and eplerenone inhibit the reabsorption of sodium by the collecting ducts of the nephron. These drugs interfere with the sodium/potassium exchange, thereby minimizing potassium excretion and weakly increasing water excretion (Epstein and Calhoun, 2011). These drugs are prescribed only to patients who have hypokalaemia when administered with ACEIs (Remme and Swedberg, 2001).

1.3. Effects of antagonism of neuro-hormonal activation during HF

During HF, the increasing stress on the heart activates the production of NPs. Despite the increase in plasma NP levels, the system exhibits resistance to their biological activity due to the exaggerated counter-regulatory neuro-hormonal activation. Drugs used for the treatment of HF counteract the detrimental effects of these neuro-hormonal factors. Some of these drugs such as β-blockers, ACEIs, ARBs and spironolactone modulate the levels of circulating NPs (Richards *et al.*, 2002) and increase their biological activity (Clerico *et al.*, 2000). Treatment with certain ACEIs and ARBs like enalapril or candesartan or valsartan decrease the plasma levels of NPs which match the indices of reverse ventricular remodeling (Kasama *et al.,* 2006). In response to certain β-blockers like carvedilol or bisoprolol, the hypotensive action of ANP is enhanced because of increasing plasma ANP and downregulation of processes that degrade the NP (van den Meiracker *et al.*, 2003; Yoshimoto *et al.,* 1998). Thus in retrospection to the findings it seems that the therapy for

HF targets a) the overactivity of counter-regulatory mechanism, which when abolished causes the NP levels to decrease, or b) a stimulatory effect of plasma NPs. Thus, levels of NPs during HF therapy serve as a prognostic tool (van Veldhuisen *et al.*, 2013) as well as add on to the beneficial action of the drug. More recently, studies are focused on enhancement of the activity of NPs as an alternative approach for HF therapy. This goal has been attempted by administering exogenous NPs in healthy subjects and HF failure patients that has resulted in favorable effects (Schmitt *et al.*, 2004).

1.4. Natriuretic peptides

Natriuretic peptides (NPs) are vital hormones participating in pressure/volume homeostasis in both health and disease. NPs counteract the blood pressure elevating effects of the RAAS by inducing vasodilation, natriuresis, diuresis and increasing endothelial permeability. Three decades of extensive studies on NPs have shed light on their molecular mechanisms, further extending to the understanding of its role in pathophysiological conditions.

Marked reduction in blood pressure accompanied by increased water and sodium excretion, was observed for the first time when atrial extracts were intravenously injected into rats (de Bold *et al.*, 1981). This seminal experiment progressed the understanding of the existing humoral link between heart and kidney. Subsequently, the factors involved in this regulatory process were identified and sequenced. These peptide hormones were called "Natriuretic peptides". The first isolated peptide of cardiac origin was atrial natriuretic peptide (ANP) (Kangawa and Matsuo, 1984). Following which BNP and CNP were identified from brain (Matsuo and Kangawa, 1984; Sudoh *et al.*, 1988; Sudoh *et al.*, 1990; Ueda *et al.*, 1987). These peptides have a conserved 17-

residue ring with variable N- and C- terminal extensions (Matsuo and Kangawa, 1984) (Figure 1.1). The ring structure is held together by a disulphide bridge between two flanking Cys residues. This feature is shown to be essential for NPs to retain their biological activity (Olins *et al.*, 1988).

In a system level, NPs exhibit smooth muscle relaxing ability and increased fluid-electrolyte excretion, which are associated with increased cGMP levels in different tissues (Waldman *et al.*, 1984; Winquist *et al.*, 1984). Following this observation, chemical cross-linking and pull down experiments led to the identification of the natriuretic peptide receptors namely NPR-A, NPR-B and NPR-C (Takayanagi *et al.*, 1987). Among the three receptor subtypes A and B are linked to guanylyl cyclase (GC) (Chang *et al.*, 1989). NP binding to these two receptors elevates cGMP levels. These receptors have ligand specificity; ANP and BNP bind to NPR-A (Suga *et al.*, 1992) while CNP binds to NPR-B (Koller *et al.*, 1991). The third receptor subtype C lacks the GC domain. NPR-C is involved the clearance of NPs (Maack *et al.*, 1987). This receptor can bind to all three NPs. Thus, a physiological response to a NP is mediated by specific receptors.

1.4.1. Atrial natriuretic peptide (ANP)

ANP is the first peptide to be isolated and characterized among the NP family. This peptide is majorly synthesized and stored in atria. RNA transcripts of ANP encode a 151-amino acid residue preprohormone (Kangawa *et al.*, 1985) which is proteolytically processed to remove the N-terminal signal peptide to form 126-amino acid residue prohormone. Both prepro-ANP and pro-ANP are stored as dense granules in atrial myocytes. In response to atrial wall stretch or increasing transmural distending pressure in the cardiac chambers, secretion of

pro-ANP is stimulated (de Bold, 1985; de Bold *et al.*, 1986), which is hydrolyzed by membrane-bound serine protease, corin, to release the bioactive 28 amino acid residue peptide (Vuolteenaho *et al.*, 1985; Yan *et al.*, 2000). Other hormones such as endothelin, angiotensin and vasopressin also increase ANP secretion (Lachance *et al.*, 1986). Mature ANP has a 6-residue long N-terminal extension and a 5-residue long C-terminal tail flanking the 17-residue ring. In the kidney, alternately processed pro-ANP, results in a mature peptide with longer N-terminus extension, called urodilatin, which acts as local regulator of sodium-water balance (Forssmann *et al.*, 1998).

Upon entering the bloodstream, ANP circulates and acts via NPR-A in a number of tissues to cause vasodilation, decreased renal reabsorption of water and sodium, decreased release of renin and increased endothelial permeability. These responses reduce blood pressure and volume. Genetic knock out mouse model studies involving targeted deletion of ANP (-/-) or NPR-A (-/-) exhibited chronic arterial hypertension, cardiac hypertrophy and death (John *et al.*, 1996; Oliver *et al.*, 1997). This observation led to the understanding that ANP mediated NPR-A signaling has an important role in maintaining circulatory homeostasis.

The plasma half-life of ANP is reported to be approximately 2 min (Yandle *et al.*, 1986), with neutral endopeptidase (NEP) and NPR-C actively involved in the clearance of the peptide. NEP cleaves ANP between Cys7 and Phe8 (Abassi *et al.*, 1994), thereby linearizing the peptide, while NPR-C causes internalization mediated degradation on binding. Despite its rapid clearance, plasma levels of ANP increases to about 10-30 fold during pathophysiological conditions such as heart failure (Cody *et al.*, 1986).

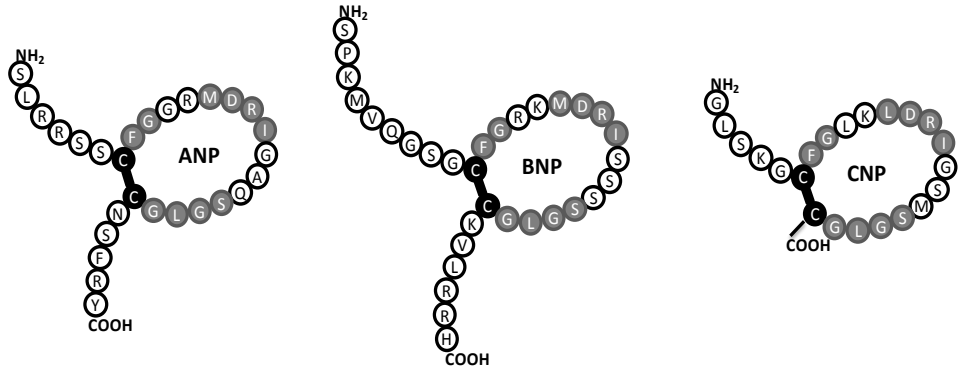

Figure 1.1. Schematic representation of mammalian natriuretic peptides
All three isoforms have a 17-residue ring held by a disulphide bond (●–●), with conserved residues shown in●. These peptides differ in their C- and N-terminal extensions. ANP and BNP have 5 and 6 residues in their C-tail respectively, while CNP lacks tail. Variable residues within these peptides are represented in○.

1.4.2. B-type natriuretic peptide (BNP)

BNP was first isolated from porcine brain tissue, but later found to be expressing in much higher concentration in cardiac ventricles of patients or animals undergoing cardiac stress such as congestive heart failure (Mukoyama *et al.*, 1991). Hence, brain natriuretic peptide was renamed as B-type natriuretic peptide. Like ANP, BNP is synthesized as a preprohormone, which is cleaved by proteases to release a 32- amino acid residue functional peptide. Although BNP is stored in atrial granules along with ANP (Nakamura *et al.*, 1991), the mRNA level of BNP transcript is higher in ventricle compared to atria (Nakao *et al.*, 1990). BNP is not stored in ventricular tissues but is transcriptionally activated in response to wall stretch (Potter *et al.*, 2009).

BNP binds to NPR-A with 3.5 fold lower affinity compared to ANP (Kambayashi *et al.*, 1990). Genetic knockout mice model studies involving targeted deletion of BNP do not result in observation similar to ANP deletion. Mice without BNP do not manifest hypertension or cardiac hypertrophy,

instead shows ventricular fibrosis, with increased expression of angiotensin converting enzyme, transforming growth factor-β and pro-α-1 collagen – factors that promote fibrosis (Tamura *et al.*, 2000). Although BNP signals through the same receptor as ANP, the knockout mice experiments suggest that they have distinct biological roles. Under physiological conditions, plasma levels of BNP are lower than ANP. Further, BNP has lower affinity to NPR-A compared to ANP (Bennett *et al.*, 1991) and exhibits markedly lower vasodilatory potency (van der Zander *et al.*, 1999). Thus, BNP is thought to be acting as a local paracrine antifibrotic factor within heart as fibroblasts express both NPR-A and NPR-B (Cao and Gardner, 1995).

Plasma half-life of BNP is longer compared to ANP (20 min) (Holmes *et al.*, 1993). It has lower susceptibility to NEP hydrolysis and lower affinity for NPR-C. But during pathophysiological states such as congestive heart failure, its level elevates up to 200-300 fold (Mukoyama *et al.*, 1991). In clinical practice BNP and its N-terminal propeptide (NT-proBNP) are used as a marker for acute heart failure and to monitor control of chronic heart failure (Cheung, 1994).

1.4.3. C-type natriuretic peptide (CNP)

The most abundant NP in brain, namely CNP was first identified from the porcine brain extracts (Sudoh *et al.*, 1990). Later CNP was found to be widely expressed in endothelial cells. Synthesized as a preprohormone like the other two NPs, enzymatic processing of precursor CNP results in a 53-amino acid residue pro-CNP, which is abundantly found in tissues, while a shorter 22-residue CNP dominates in the circulation (Wu *et al.*, 2003). Both the isoforms can interact with NPR-B and cause an elevation of cGMP. CNP is not stored

in granules, but secreted in response to a range of stimuli including growth factors and shear stress in endothelial cells (Suga *et al.*, 1993).

CNP levels in plasma are low (1-2 pM) under normal physiology, but are elevated during cardiac stress (Kalra *et al.*, 2003). The elevated levels are still low compared to ANP/BNP during a pathophysiological condition. Pharmacological experiments show that CNP is a weak arterial vasodilator but potent venodilator compared to ANP and notably have no natriuretic effects (Barletta *et al.*, 1998). Further CNP-deficient mice do not exhibit arterial hypertension. These observations suggest that CNP/ NRP-B system might not be as crucial as ANP/ NPR-A or NO/sGC systems in regulating vascular tone (Chusho *et al.*, 2001).

Interestingly, CNP signaling has anti-proliferative effects on endothelial cells, suggesting a possible inhibitory role in angiogenesis (Komatsu *et al.*, 1996). Further CNP deletion in mice causes severe dwarfism and early death due to impaired endochondral ossification (Chusho *et al.*, 2001). Thus, CNP is thought to be a paracrine and autocrine factor that exerts a major influence on growth and differentiation along with its role in maintaining vascular tone (Yamahara *et al.*, 2003).

1.5. Natriuretic peptide receptors (NPRs)

Three subtypes of receptors have NP binding properties, namely NPR-A, NPR-B and NPR-C (Takayanagi *et al.*, 1987). All three receptors exist as homo-dimers or -tetramers. These receptors have a large extracellular domain (~450 residues) and a single transmembrane region (~20 residues). Receptors A and B have large intracellular domains which include, the kinase homology domain (KHD), dimerization domain, and carboxy terminal guanylyl cyclase

(GC) domain (Potter, 2005). Binding of NP to these two receptors leads to activation of GC, thereby increasing cGMP, the recognized secondary messenger of the NP system (Lowe *et al.*, 1989). The third subtype, NPR-C, has 37 residues intracellular domain and lacks any GC domain.

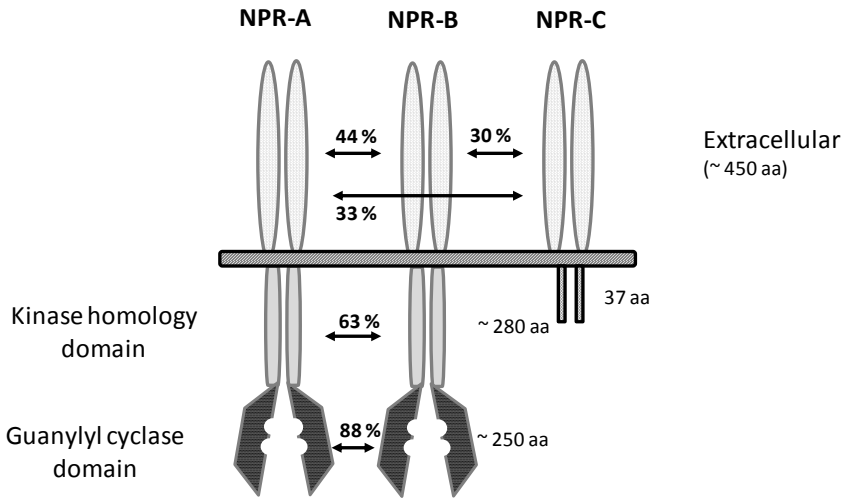

Figure 1.2. Schematic representation of natriuretic peptide receptors
There are three isoforms of natriuretic peptide receptors, namely NPR-A, NPR-B and NPR-C. All three receptors exist as homo-dimers or -tetramers in their native state, with relatively similar exterior topology. NPR-A and NPR-B are linked to a guanylyl cyclase domain via a kinase homology domain (highly conserved between both receptors), while NPR-C lacks the GC domain. The intracellular region of NPR-C is a 37 amino acid residue segment. The percentages represent the extent of similarity between domains in different receptors.

Hence, receptor-C is thought to be involved in regulating local concentration of NPs, by receptor-mediated internalization (Maack *et al.*, 1987; Nussenzveig *et al.*, 1990). Although, in the recent years, G-protein dependent down regulation of cAMP levels has been reported for NPR-C activation, its biological functions are unclear (Anand-Srivastava, 2005).

1.5.1. Natriuretic peptide receptor-A (NPR-A)

NPR-A is the primary receptor responsible for the bioactivity of ANP and BNP. It is expressed in different tissues including, kidney, lung, adipose, adrenal, brain, heart, testis and vascular smooth muscle (Lowe *et al.*, 1989).

The receptor oligomerizes as homodimers or homotetramers in a ligand independent manner in native state. The receptor binds to the ligand in 2:1 stoichiometry with affinities ranked as ANP ≥ BNP >> CNP (Suga *et al.*, 1992). Sedimentation experiments show that dissociation constant K_d for the receptor dimer is ~500 nM which decreases to ~10 nM in the presence of ANP, suggesting that dimerization is favored in the presence of the ligand (Ogawa *et al.*, 2010).

The extracellular domain (ECD) contains three disulphide bonds and five N-linked glycosylation sites, which are shown to be important for receptor function (Miyagi *et al.*, 2000). The ECD has a highly conserved chloride ion binding site near the dimerization interface. The binding of chloride ions is necessary for the activation of NPR-A. Further, ECD has a structurally conserved juxta-membrane motif, which links it to the transmembrane region (Huo *et al.*, 1999; Ogawa *et al.*, 2010). This motif consists of Pro-417, Cys-423 (in disulphide bond with Cys-432) and Phe-425, conserved in all GCase (Miyagi and Misono, 2000). This segment is responsive to hormone binding and transmits the conformational change of ECD to intracellular domains.

The kinase homology domain (KHD) in the inner side of the membrane is phosphorylated at four serine and three threonine residues in basal condition. Phosphorylation of the KHD is necessary for receptor activation, while dephosphorylation is a mechanism for desensitizing the receptor on prolonged exposure to ligand (Potter and Hunter, 1998). ATP has been shown to augment the activation of the GC domain on ANP binding (Kurose *et al.*, 1987; Schroter *et al.*, 2010), but the mechanism was unclear until recently.

Crystal structures of apo NPR-A and ANP bound NPR-A reveal the mechanism of receptor activation. The apo receptor structure shows certain hydrophobic interaction (Trp74 A with Trp74 B and Phe96 A with Phe96 B between monomers A and B) and hydrogen bonds (Asp71 A and His99 B, His99 A and Asp71 B) that holds the receptor as dimer (Ogawa *et al.*, 2004; van den Akker *et al.*, 2000). Upon ANP binding, all interactions at the receptor dimer interface except the [Phe96 A - Phe96 B] hydrophobic interactions are disrupted. ANP binds in an asymmetric fashion with N-terminal segment interacting with monomer A and its C-terminal portion interacts with monomer B. This binding confers no significant change to the intramolecular distances, but largely affects the quaternary structure of the receptor. The receptor undergoes a twist motion that opens membrane distal region, while translocating the juxtamembrane motif in opposite direction; bringing them nearly 10 Å closer. This change in the orientation is thought to result in the movement of to the intracellular domains, which brings the GC domains in head to tail fashion. This rearrangement opens two GTP binding sites in the GC dimer, thus activating the receptor (Ogawa *et al.*, 2004).

ANP binding leads to activation of GC, which is further enhanced in the presence of ATP. Earlier ATP was thought to bind to KHD and allosterically augment the hormone-mediated response (Thorpe *et al.*, 1996). But, recently, Potter *et al*., have shown that ATP competes for one of the GTP binding sites in the GC domain and decreases the K_m of GTP in the presence of ANP (Robinson and Potter, 2012).

Thus, activation of GC-linked NPR-A involves; hormone-induced structural changes of the ECD, which orients the GC domains in a head to tail fashion.

This conformational change results in the opening up of two GTP binding sites. ATP binding to one these sites allosterically enhances GC activity (Robinson and Potter, 2011, 2012). The hormone-bound domains of NPR-A lose their affinity for ligand, promoting its dissociation from the receptor. Finally dephosphorylation of regulatory sites in KHD desentisizes the receptor. The desensitization of NPR through dephosphorylation of KHD is stimulated on prolonged exposure to ANP/ BNP or by peptide hormone which have antagonistic role to NP, such as angiotensin, endothelin, basic fibroblast growth factor, etc. (Potter and Garbers, 1992).

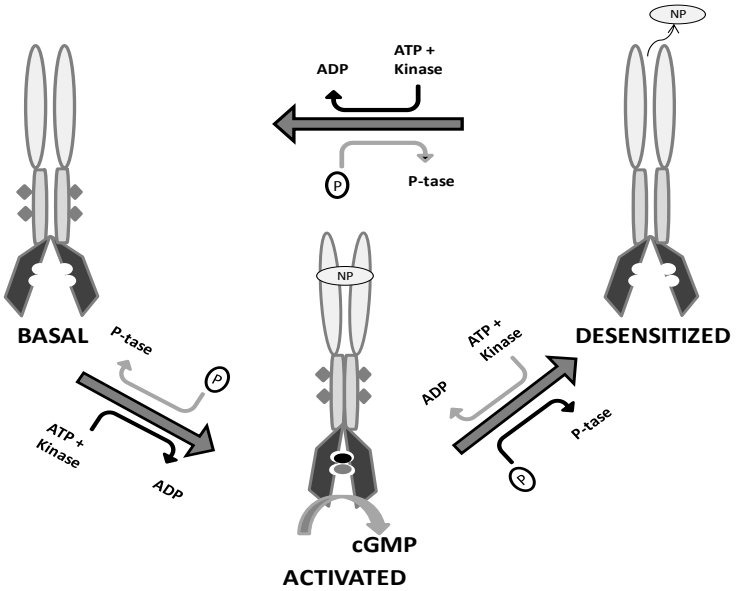

Figure 1.3. Model of NPR-A and NPR-B activation and desensitization

The NPRs are thought to go through three states in the cycle of activation. These states have been represented as "basal", "activated" and "desentisized". Receptors in basal state are predominantly, dimers or tetramers, and are phosphorylated in 5 to 6 residues in their KHD domain. *Grey color diamonds* represent phosphorylated residues. The binding of NP to the inactive basal receptors induces a twist rotation of the ECD, which is transmitted intracellularly causing dimerization of GC domains. This process opens up two ligand pockets in GC, of which ATP (*Black sphere*) binds to one of the binding pockets and allosterically increasing affinity for GTP (*grey sphere*). Prolonged exposure to ligand causes dephosphorylation of KHD and results in the loss of affinity to NP. Hence, dissociation of NP from NPR and dephosphorylation of KHD domains desensitize the receptor. The colors (grey: slower, black: faster) of the *arrows* between two receptor states represent the rate at phosphorylation or dephosphorylation. This model of NPR- A and NPR-B activation shows phosphorylation as "license" for receptor to be turned on by the hormone.

1.5.2. Natriuretic peptide receptor-B (NPR-B)

NPR-B is the second GC- linked receptor of the NPR family. It is involved in CNP signaling (Koller *et al.*, 1991). The overall topology of this receptor is similar to NPR-A. The ECD is 43% identical with disulphide bonds and potential glycosylation sites retained. The intracellular domains are 78% identical and phosphorylation sites are conserved in the KHD (Potter and Hunter, 1999). The ligand affinities are ranked as CNP >> ANP > BNP (Suga *et al.*, 1992). The mechanism of activation of NPR-B is thought to be the same as of NPR-A. There are no structural studies on isolated NPR-B. This receptor is expressed in lung, ovary, adrenal, uterus and brain. NPR-B seems to be the predominant receptor in brain (Hirsch *et al.*, 2003). Deletion of NPR-B in mice resulted in dwarfism, accumulation of white adipose tissue and infertility (Tsuji and Kunieda, 2005), suggesting CNP/NPR-B signaling to have key role in tissue remodeling, reproduction and brain functions (Lopez *et al.*, 1997). Another study showed that transgenic rats expressing dominant negative mutation of NPR-B had cardiac hypertrophy providing a link between NPR-B signaling and cardiac growth.(Langenickel *et al.*, 2006).

1.5.3. Natriuretic peptide receptor-C (NPR-C)

The intracellular domain of this receptor lacks both KHD and GC, instead has a 37-residue peptide. Ligand binding exhibits no enzyme activity, but is thought to mediate certain cellular responses through inhibitory G-protein activation (Anand-Srivastava *et al.*, 1996). All three NPs have high affinity for NPR-C with relative ranking of ANP > CNP > BNP (He *et al.*, 2001). Unlike NPR-A and NPR-B, receptor subtype-C is known to bind to ring deleted analogs of ANP with higher affinity (Anand-Srivastava *et al.*, 1990). Crystal structure of apo NPR-C and its complex with ANP, BNP and CNP are known (He *et al.*, 2006). Comparison of these structures reveals the degeneracy versus specificity of hormone binding properties of different NPRs**.**

Table 1.2. Affinity constants of ANP, BNP and CNP towards different NPRs

	Dissociation constants		
Receptors	ANP	BNP	CNP
NPR-A	1.9 pM	7.3 pM	> 500 nM
NPR-B	5.4 nM	30 nM	7 pM
NPR-C	2.6 pM	13 pM	10.8 pM

Data as described in (Bennett *et al.*, 1991)

The interaction interfaces in the complex crystal structure of the three NPs with NPR-C are almost identical, suggesting NPR-C uses a single conformation to bind to all three NPs, instead of adapting its local structure according to the differences in the ligand. Thus, the promiscuous nature of

NPR-C is attributed to its conformational rigidity in its binding sites (He *et al.*, 2006).

Functionally, NPR-C is associated with clearance of these peptides; thereof controlling the amount of circulating NPs (Jaubert *et al.*, 1999; Maack *et al.*, 1987). Internalization followed by degradation is the mechanism through which clearance occurs. NPR-C is the most abundant receptor among NPRs and it accounts for about 90% of total NPRs in important target tissues such as the kidney. NPR-C knockout mice show reduced ability to clear ANP, reduced ability to concentrate urine and lone bone overgrowth (Jaubert *et al.*, 1999). In other words, animals lacking NPR-C, have exaggerated effects of NPR-A and NPR-B signaling leading to hypotension and gigantism. Thus, these results suggest that NPR-C is involved in clearance and possibly mediate other functions of NPs. In the recent years, binding of NP to this receptor has been associated with inhibition of adenylyl cyclase activity and activation of phospholipase C in a G_i protein dependent manner and causes a reduction in intracellular cAMP (Anand-Srivastava *et al.*, 1996).

1.5.4. Structure- function relationships of NP and NPR

Several studies have looked into the structural requirement of a NP for binding to its receptor. Before the NPR-A –ANP crystal structure was solved different approaches were used to delineate important amino acid residues in ANP binding. Truncation of N- and C- termini extensions of ANP decreased the amount of cGMP produced in rat endothelial cells, suggesting that these segments influenced the interaction (Olins *et al.*, 1988). Although deletion of the N-termini extension is tolerated, the C-terminal tail has profound influence on ANP activity.

The disulphide linkage within the peptide confers rigidity to the molecule. Disruption of the cyclic structure, reduces the affinity of the peptide to GC-coupled receptor by more than 1000 fold, thus it is an important structural feature associated with its bioactivity (Olins *et al.*, 1988). Although linearized NPs do not bind to NPR-A/NPR-B, they do bind to the non-GC coupled NPR-C with high affinity (Bovy, 1990). Thus, linear ANP analog differentiated between GC and non-GC receptors (Anand-Srivastava *et al.*, 1990).

Alanine scan mutagenesis improved the understanding of the contribution of each residue to receptor binding. Residues F8, M12, D13, R14, I15, L21 and R27 had greater influence on receptor binding (Li *et al.*, 1995). The structure of ANP by nuclear magnetic resonance gave further information about the solution structure of the peptide (Li *et al.*, 1995). Using a structure based approach, ring minimization strategies were used to develop mini-ANP, which had 7.2 times lower affinity compared to wild type (Li *et al.*, 1995).

The crystal structure of ANP in complex with NPR-A gave clear molecular details of residue level interaction. ANP binds to NPR-A in an asymmetric fashion with N-terminal portion of the peptide interacting with one subunit while the C-terminal portion interacts with the other subunit. The structure reveals the key interaction between peptide and receptor, with R14 forming hydrogen bonds with D62B and E119A, F8 of ANP with a hydrophobic pocket created by Y154A, F165A, V168A and Y172A. The third set of interactions is between N24 through F27 of ANP, which runs in partial β-sheet with receptor residues Q186B and F188B. These interactions perfectly correlated with the previous studies, thus identifying the key amino acids involved in ligand-receptor interaction (Ogawa *et al.*, 2004).

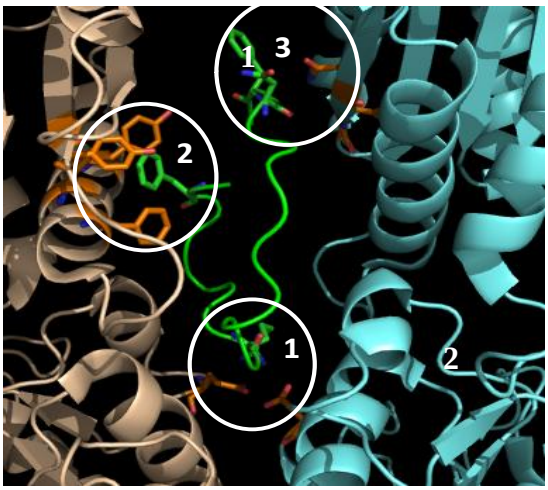

Figure 1.4. Intermolecular interactions of ANP with NPR-A
Three crucial interaction sites between ANP and NPR-A are shown in the figure. (1) R14 of ANP is involved in hydrogen bonding with D62B and E119A of NPR-A. (2) F7 of ANP fits into a hydrophobic pocket constituting Y154A, F165A, V168A and Y172A. (3) The C-terminal residues of ANP, N24, S25, F26, R27 runs in parallel β-sheet with Q186B and F188B.

1.6. Physiological functions of NPs

NPs are vital hormones that maintain circulatory homeostasis. Most of the known physiological response is due to interaction of NP with its NPR, which elevates intracellular levels of the secondary messenger cGMP. Hence, the downstream effectors that interact with cGMP determine the physiological response of the NP.

cGMP is known to interact with three important protein targets. The first and principal mediator among these is a cGMP dependent protein kinase (PKG) (Schlossmann *et al.*, 2005). Two different genes of PKG are known, of which PKG I, a cytosolic protein, which is expressed in cardiac myocytes, endothelial cells, brain, kidney and adrenal glands (Pfeifer *et al.*, 1998). The second variant PKG II, a membrane bound protein, which is not expressed in the cardiovascular system, but in bones, brain, intestine, lung and kidney

(Pfeifer *et al.*, 1996). Thus two PKG isoforms may be involved in mediating entirely different physiological response to NPs.

The second target, relevant to the cardiovascular system is the Na^{+} and Ca^{2+}, cyclic nucleotide gated ion channels (Light *et al.*, 1990). Although the specific channels modulated in response to NP binding are not known, it is evident that they are involved in NP mediated hyperpolarization and intracellular Ca^{2+} decrease in vascular smooth muscle and inhibition of sodium reabsorption in the distal tubules of the nephron.

The third group of proteins which bind to cGMP are the phosphodiesterases (PDE), which are crucial regulators of cGMP signaling (Rybalkin *et al.*, 2003). PDEs hydrolyze cyclic nucleotides to nucleotide monophosphates, thereby regulating their concentrations. NP-mediated cGMP increase has been shown to activate PDE 2, a specific enzyme that degrades cAMP. AngII causes an increase in intracellular Ca^{2+} through cAMP, which activates PDE 3 that degrades cGMP (Beavo, 1995).

Thus PDEs play a major role in regulation and crosstalk of signals transmitted by both cAMP and cGMP (Figure 1.5).

By triggering various cGMP-dependent cellular processes, NPs trigger vasodilation, natriuresis, diuresis, endothelial permeability and tissue remodeling which aids in the regulation of intra-vascular and total body fluid volume and blood pressure.

This thesis mainly focuses on the cardiovascular effects of NPs.

Table 1.3. Physiological functions of natriuretic peptides

Target system	Biological effects
Vascular	• Vasorelaxation (Brenner *et al.*, 1990) • Increased endothelial permeability (Sabrane *et al.*, 2009; Skryabin *et al.*, 2004) • Decrease cardiac preload and after load (Shapiro *et al.*, 1986)
Cardiac	• Reduction of cardiac output (Breuhaus *et al.*, 1985) • Inhibition of cardiac remodeling (Kapoun *et al.*, 2004)
Renal	• Increase glomerular filtration rate by dilating afferent arterioles and constricting efferent arterioles (Harris *et al.*, 1987a; Marin-Grez *et al.*, 1986) • Increased excretion of sodium by inhibiting proximal and distal tubule and collecting duct Na+ channels (Light *et al.*, 1990) • Induction of diuresis by inhibiting the incorporation of aquaporins (Harris *et al.*, 1987b; Kishimoto *et al.*, 1996)
Endocrine	Suppress the production of : • Renin- angiotensin- aldosterone (Richards *et al.*, 1988) • Sympathetic nerve stimulation (Thoren *et al.*, 1986) • Arginine vasopressin (Burrell *et al.*, 1991) • Endothelin(Hu *et al.*, 1992)
Proliferation	Inhibit growth factor induced cardiac hypertrophy and fibrosis (Cao and Gardner, 1995; Takahashi *et al.*, 2003)

1.6.1. Vascular and cardiac effects of NPs

Predominant vascular effects of NPs include endothelial permeability and vascular smooth muscle relaxation. The exact mechanism by which NPs increase endothelial permeability is unclear. Genetic knockout mice with endothelial NPR-A deletion have raised BP (10-15 mmHg higher) and are 11-13 % volume expanded compared to wild type animals, while animals with complete NPR-A knockout were severely hypertensive (30-40 mmHg) and are 30 % volume expanded (Sabrane *et al.*, 2005). Further endothelial NPR-A

knockout were not able to clear radio iodine labeled albumin in an ANP dependent manner in contrast to wild type animals (Sabrane *et al.,* 2009). These experiments suggest that NP increases endothelial permeability to decrease intravascular fluid volume.

NPs are potent vasodilators. These peptides cause the relaxation of smooth muscles via the activation of NPRs. In mice with complete NPR-A deletion, ANP do not cause relaxation of aortic strip in an ex-vivo system and exhibit no reduction in blood pressure in response to bolus injections of ANP (Holtwick *et al.,* 2002; Lopez *et al.,* 1997). The downstream signaling cascade of NPR-A activation that leads to muscle relaxation is well understood (Carvajal *et al.,* 2000). It is a PKG dependent phenomenon, which leads to decrease in intracellular Ca^{2+}, thereby inhibiting Ca^{2+} dependent contraction. PKG opens big conductance calcium activated K^{+} channels, which facilitates hyperpolarization of the vascular smooth muscles (Alioua *et al.,* 1998). Further, PKG phosphorylates inositol 3-phosphate receptor on sarcoplasmic recticulum which prevents the efflux of Ca^{2+} to the cytosol (Komalavilas and Lincoln, 1996). Subsequently PKG causes the phosphorylation of Ca^{2+} sensitive targets such as myosin light chain which prevents the contraction (Nakamura *et al.,* 1999). These cellular events lead to relaxation of the vascular smooth muscle (Figure 1.5), which counteracts the action of AngII, arginine vasopressin and α1- adrenergic stimulation. Further in an NPR-A dependent fashion, the synthesis of endothelin – a vasoconstricting peptide from the endothelial cells, is inhibited by NP (Hu *et al.,* 1992). Thus, by inducing relaxation and inhibiting the secretion of opposing constrictor effectors, NP reduces blood pressures and volumes. This reduces intra-cardiac

volumes and pressures completing the negative feedback loop in association with decreased cardiac preload and afterload.

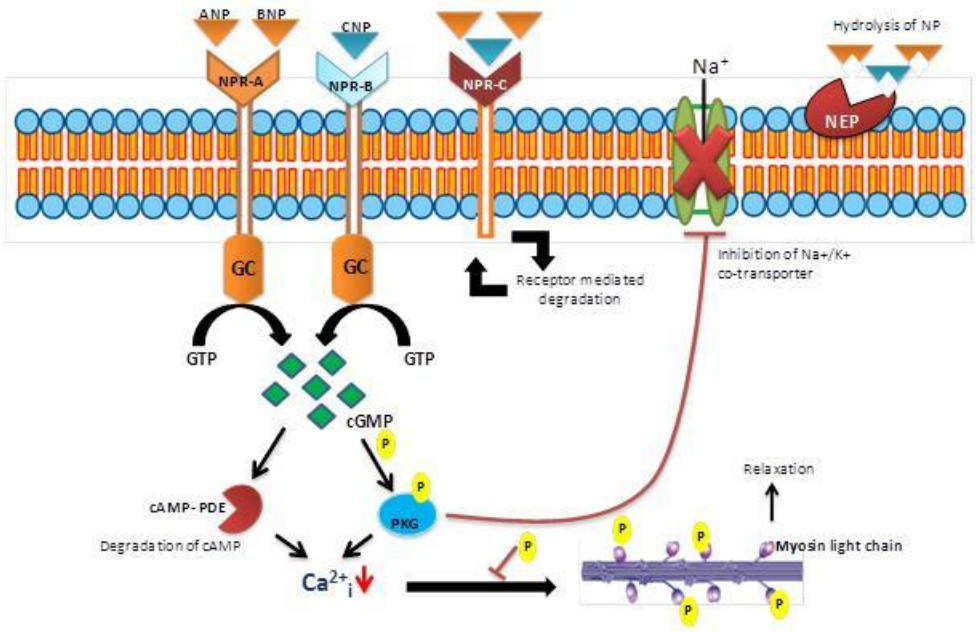

Figure 1.5. NP signaling and degradation
NPs signal by elevating intracellular cGMP levels. Three main protein targets that are activated or repressed by cGMP are Protein Kinase G (PKG), Phosphodiesterase (PDE) and cGMP gated ion channels. These protein targets are responsible for different physiological responses. PKG and PDE decrease intracellular Ca^{2+} levels and lead to phosphorylation of myosin light chain. This process aids the relaxation of smooth muscle. In the renal tubules cGMP directly as well as in PKG dependent manner causes the closure of Na^{+}/K^{+} co-transported to prevent the reabsorption of Na^{+}. Active degradation of NPs occurs through receptor-mediated internalization and hydrolysis by NEP. Circulating levels of NPs are maintained by these active clearance mechanisms.

NPs exhibit antiproliferative effects on the site of its synthesis, the heart. Mice lacking ANP/NPR-A show cardiac hypertrophy (enlarged heart) while ANP/NPR-A overexpressing animals have smaller hearts (Holtwick *et al.*, 2002). This phenotype had an ambiguity of whether ANP/NPR-A signaling was directly involved in the growth inhibitory effects of cardiac myocytes or whether it is the response of high blood pressure when ANP/NPR-A is disrupted. In a study, mice lacking NPR-A were treated with anti-hypertensive drugs right from their birth (Holtwick *et al.*, 2003). The elevation in blood

pressure was reduced while the cardiac overgrowth did not diminish supporting the fact that NP systems are involved in inhibition of cardiac myocyte growth.

1.6.2. Renal effects of NPs

Kidneys are an important target for long-term regulation of blood pressure as they play a key role in maintaining body fluid-electrolyte balance. In response to hemodynamic parameters, hormones and neuro-signals, the reabsorption of water and sodium is triggered (Kishimoto *et al.*, 1996). Retention of sodium leads to blood volume expansion and this may result in cardiac overload. This phenomenon is counter regulated by NPs which vasodilate to allow accommodation of volume with little pressure rise and also inhibit reabsorption of water and sodium (Maack *et al.*, 1986).

NPs are involved in hemodynamic and glomerular changes in the kidneys. It exerts vasodilation of afferent arterioles whilst constrict the renal efferent arterioles, which increases intra-glomerular capillary pressure, glomerular filtration rate and filtration fraction (Marin-Grez *et al.*, 1986; Potter *et al.*, 2006). These changes in the hemodynamics are accompanied by changes in the absorption leading to natriuresis and diuresis. NPs inhibit Na^+/H^+ exchanger, Na^+/Cl^- co-transporter and other Na^+ channels (Light *et al.*, 1990) preventing the reabsorption of sodium and inhibit the recruitment of aquaporin thereby increasing the water excretion (Harris *et al.*, 1987b).

Apart from the direct changes in reabsorption, NPs cause inhibition of renin-angiotensin-aldosterone production. Increase in plasma ANP levels in a physiological context causes the inhibition of renin and aldosterone secretion (Chartier *et al.*, 1984; Richards *et al.*, 1988). At birth, NPR-A lacking mice

have higher levels of renin and aldosterone (Burnett *et al.*, 1984; Shi *et al.*, 2001). The systemic levels of these factors decrease in adult NPR-A null mice, suggesting other compensatory mechanisms in response to elevated blood pressure might be in place (Shi *et al.*, 2001).

Thus by modulating intravascular fluid volume and pressure through different mechanisms, NP reduce cardiac load.

1.7. Degradation of NPs

The reported half-life of ANP in different species varies between 0.5-4 min (Yandle *et al.*, 1986), with the organ preference for ANP extraction as lung> liver>kidney (Hollister *et al.*, 1989). BNP in circulation is reported to have longer half-life (20 min) (Richards *et al.*, 1993) while CNP has a short half-life as that of ANP (2.6 min) (Palmer *et al.*, 2009). Circulating NPs are continuously cleared by three main processes; (1) receptor-mediated internalization and degradation, (2) proteolytic inactivation and (3) secretion of peptide into urine or bile. Although not much information is known about the latter process, detailed studies have been conducted to investigate the mechanism of clearance via receptor and proteolysis.

1.7.1. Receptor-mediated clearance of natriuretic peptides

It is of immense interest that there exists an entirely separate receptor for the clearance of NPs – a unique mechanism in the cardiovascular system (Cohen *et al.*, 1996). Receptor-mediated degradation mechanics of NPR-C involves clathrin-dependent endocytosis of the receptor followed by lysosomal

degradation of the peptide bound to the receptor and the recycling of the receptor back to the membrane(Nussenzveig *et al.*, 1990).

NPR-C is a promiscuous receptor. It has lesser selectively for its ligand compared to NPR-A and NPR-B. Crystal structure of NPR-C with ANP, BNP and CNP has revealed that the receptor uses a single interface to bind to all three hormones (He *et al.*, 2006). The structural rigidity imposed by the receptor forces the flexible ligand to adopt a conformation that would overcome the unfavorable entropic penalty (He *et al.*, 2001). CNP bound to NPR-C takes up an extended conformation compared to ANP and BNP. The conformation of the different ligands utilizes different subset of residues within the receptor surface. In comparison to NPR-A, NPR-C seems to have weak interaction with the C-terminal residues of ANP and BNP. Further subtle changes in the common binding pockets that interact with the residues in the ring between NPR-A and NPR-C have given insightful information about NPR-C's degeneracy. Pocket I of NPR-C that interacts with F2 in the ring is more spacious compared to NPR-A to accommodate the side chain conformations of both ANP and CNP. Pocket II which interacts with residue at position 12 in the ring is shallower compared to NPR-A, providing less specific interactions which do not discriminate between the side chains in the three ligands.

Isothermal titration calorimetry and radioligand binding studies gave CNP = ANP > BNP as the order of the NPs affinity to NPR-C, which matches their half-life data (He *et al.*, 2001).

1.7.2. Proteolytic degradation of natriuretic peptides

Neutral endopeptidase or Neprilysin (E.C.3.4.24.11) is a zinc dependent membrane bound metalloprotease which was identified as key player in the degradation of NPs (Stephenson and Kenny, 1987). This enzyme cleaves at the amino terminus of hydrophobic residues. Stephenson *et al.* have shown that the C7-F8 peptide bond is the first cleavage site during ANP degradation by NEP (Stephenson and Kenny, 1987). Cleavage of this bond results in opening up of the ring, which inactivates the peptide. Like ANP, CNP is efficiently cleaved by NEP, but BNP is a relatively poor substrate for NEP (Gerbes and Vollmar, 1990; Norman *et al.*, 1991). The degradation profile of BNP shows cleavages sites located in the N- and C-terminal extensions and the bond between R14-I15 (Norman *et al.*, 1991). The renal isoform of ANP, urodilatin, which has four extra residues on the N-terminus of ANP, is less susceptible to hydrolysis by NEP compared to ANP (Abassi *et al.*, 1994).

A familial mutation on ANP rendered a variant ANP with 17-residue long C-terminal tail that showed an increased half life (Dickey *et al.*, 2009). Thus the susceptibility of the known NPs to NEP may be ranked as CNP=ANP > Urodilatin >> BNP. These observations showed that the longer the N- and C-termini of the NP, the less vulnerable it is to degradation. A possible mechanism for NEP mediated hydrolysis has been predicted using a modeled interaction site of NP with NEP (Pankow *et al.*, 2009). Figure 1.6 shows that NEP interior cavity represented in light green, has two recognition sites R222 and D372 opposite to the active site (depicted in yellow). NP slips into this pocket to orient the lytic bond (C7-F8) near the active site. It is thought that D13 and R14 of the NP interact with R222 and D372 of NEP electrostatically

to position the lytic bond. In the case of peptides with longer N- and C-termini, accommodation of the entire molecule within the pocket leads to spatial clashes, which confer resistance to cleavage (Pankow *et al.*, 2009).

Oral NEP inhibitors are shown to elevate plasma NP levels and increase sodium excretion during HF in various animal and human models (Wegner *et al.*, 1995). Although NP levels in mice lacking neprilysin have not been reported, these animals do not show any obvious signs of increased NPR activation suggesting other degradation pathways compensating for the loss of NEP (Lu *et al.*, 1995).

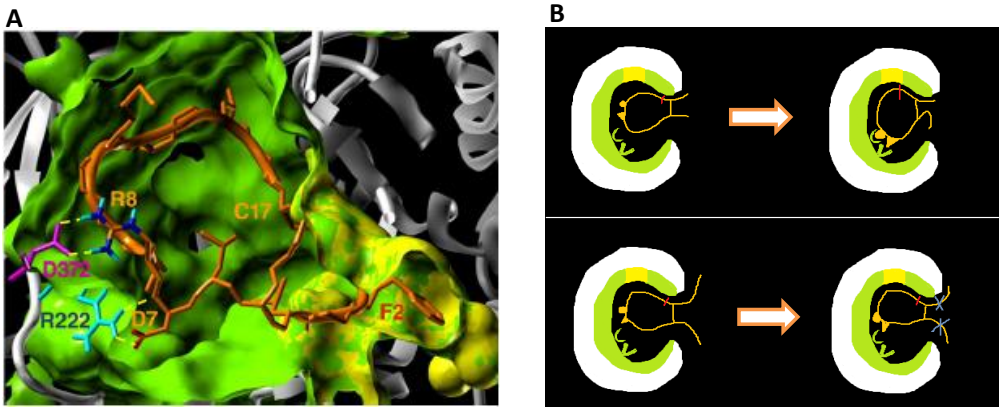

Figure 1.6. Hypothetical mechanism of NEP mediated hydrolysis
A- Modeled active site of NEP. R222 and D372 of NEP binding pocket interacts with D13 and R14 of NP respectively, which aid the positioning of the lytic bond C7-F8 near the active site.
B- NP with short N- and C- terminal segments are accommodated with the active site while the ones with longer extension provide steric hindrance to be accommodated within the binding pocket which hampers the positioning of the lytic peptide bond.

NPs are also cleaved by another zinc metalloprotease called insulin-degrading enzyme (IDE) (Johnson *et al.*, 1989). This enzyme is found in both cytoplasmic and membrane fractions and has a wide substrate specificity. It cleaves ANP at S25-F26 peptide bond in the C-terminal tail (Johnson and Foster, 1990) which is followed by the lysis of R3-R4, D13-R14 and C7-F8

(Muller *et al.*, 1992). Among the three NPs, ANP is the preferred substrate for IDE while BNP is relatively a poor substrate (Muller *et al.*, 1992). In mice lacking IDE, amyloid-β protein and insulin levels are increased, but no record of NP levels are available (Farris *et al.*, 2003). Hence, the physiological role of IDE in NP clearance is not clearly understood.

The relative contribution of both NPR-C and NEP mediated degradation are equal for clearing NPs (Charles *et al.*, 1996). It is thought that under pathophysiological condition where plasma levels of NPs are markedly elevated and NPR-C may be saturated, NEP plays a major role in degradation. Hence, strategies to improve half-lives of NPs pertain to increasing the N- and C-termini of these peptides or use of NEP inhibitors (Brandt *et al.*, 1997).

1.8. Pathophysiological role of NPs

Increasing intravascular fluid volume due to higher water and sodium retention, a resultant of lowered cardiac output, is the phenomenon that provokes congestion of heart. The levels of NPs are the highest during such pathophysiological conditions (Rubattu *et al.*, 2008). Despite the increase of NP, the exaggerated neuro-hormonal activation during cardiac dysfunction is not compensated. This apparent discrepancy has been attributed to one of the following reasons, but the exact mechanism is not understood yet: the release of non-active forms of NPs, increased clearance by proteolytic degradation, down regulation of NPRs, and increased antagonist mechanisms of RAAS, vasopressin and endothelin (Brockhoff *et al.*, 2000). In view with this observation, BNP and its N-terminal propeptide (NT-proBNP) are used as diagnostic markers for the detection of HF in clinical practice (Anwaruddin *et al.*, 2006; Cheung, 1994). Measurement of BNP and NT-proBNP is sensitive

and specific for the disease and is performed at a reasonable cost (Collinson *et al.,* 2004). Several studies have observed a correlation between BNP and NT-ProBNP levels and impaired left ventricular ejection fraction or systolic dysfunction (Gustafsson *et al.*, 2005). Similarly, along with other diagnostic methods, level of NT-proBNP is used for detection of diastolic dysfunction (Lubien *et al.,* 2002). Further, the plasma levels of these peptides are used for prognosis of treatment for HF. Among hospitalized HF patients, decrease in plasma levels of NT-proBNP indicated an improvement in their status compared to patients with no significant change or increase of NT-proBNP (Bettencourt *et al.*, 2004).

Also in experimental animals and healthy human volunteers, infusion of ANP/BNP resulted in marked reduction in blood pressure, increased natriuresis and diuresis, whereas in models and human with CHF renal responses were not as significant as normal subject but effectively contributed to the reduction in peripheral vascular resistance and blood volume (Burnett *et al.*, 1986; Florkowski *et al.*, 1994).

1.9. Venom NPs

NPs have been identified in all vertebrates. All these peptides have strikingly similar structures and are thought to have similar function. Apart from the well-studied mammalian NPs, other NPs from the venom of reptiles are new molecules with intriguing pharmacological functions. Venoms of snakes and lizards contain an ensemble of toxins, which are used for debilitation of prey. Venom NPs have similar 17- residue ring structure with variable N- and C-termini. Certain peptides characterized from venom have distinct pharmacological action.

The first NP from venom, identified from the green mamba snake, Dendroaspis natriuretic peptide (DNP) was reported in 1992 (Schweitz *et al.*, 1992). Since its discovery extensive studies have been done to investigate and compare this peptide from venom to the mammalian peptides. DNP possesses a similar 17- residue ring, but with a longer (14 residues) C-terminal extension compared to mammalian NPs. It relaxes pre-contracted aortic strips and induces cGMP response in rat aortic myocytes and endothelial cells equivalent to that of ANP (Schweitz *et al.*, 1992). Through radiolabelled ligand studies, DNP has been shown to bind to NPR-A with a similar affinity as ANP, thus ranked as DNP = ANP > BNP > CNP (Singh *et al.*, 2006). Despite the analogous properties of DNP to ANP, it shows 5-fold weaker binding to NPR-C (K_d values: DNP 4.1 nM and ANP 0.8 nM) (Johns *et al.*, 2007) and exhibits greater resistance to NEP hydrolysis ($t_{½}$: DNP > 150 min and ANP = 2.5 min) (Dickey and Potter, 2011). These distinct characteristics of DNP are attributed to its C-terminal tail. Further, infusion of DNP in dogs significantly reduced mean arterial pressure and caused natriuresis and diuresis effects together with an increase in plasma and urine cGMP (Lisy *et al.*, 1999). Owing to the higher resistance of DNP to hydrolysis, the tail of DNP has been used to generate chimeric NP with CNP called CD-NP, which is attributed with potentially better clinical properties and is presently undergoing clinical trials (Lisy *et al.*, 2008).

Since DNP, several NPs from snake venom have been isolated and characterized. Proteomic analysis of *Macrovipera lebetina* venom revealed the presence of two NPs in its venom, lebetin 1 and 2 (Bazaa *et al.*, 2005). Although structurally similar to NPs, lebetins exhibited potent anti-platelet

activity (EC_{50}: 100 nM) and the N-terminal extension of the peptide was identified as the region responsible for this activity (Barbouche *et al.*, 1996). Following the identification of lebetin, a NP from *Pseudocersates persicus* called PNP was isolated. This peptide was shown to have both anti-platelet activity and NPR-A binding ability (Amininasab *et al.*, 2004). PNP shares a similar N-terminal extension sequence as lebetin that is thought to explain the observation. Three isoforms of NPs from *Oxyranus microlepidotus* namely-TNP-a, TNP-b, TNP-c, have been identified (Ref). These peptides have longer C-terminal tails similar to DNP. Among three isoforms TNP-a and TNP-b, do not possess any vasorelaxation ability while TNP-c shows similar activity that of ANP and DNP (Fry *et al.*, 2005). This difference in activity has been attributed to the presence of Pro residue replacing the conserved hydrophobic residue at the third position within the ring of TNP-a and TNP-b.

In the following year, NP specific cDNA amplification from Australian elapids, *Pseudonaja textilis* and *Pseudechis australis* revealed the presence of several NP isoforms, of which Pt-NP-a and Pa-NP-c were recombinantly expressed and characterized. These two NPs, showed a weak interaction with NPR-A, despite their structural similarity. They exhibited a dose-dependent inhibition of angiotensin converting enzyme (ACE). These peptides have a Pro residue at position 5 within the ring, which may be attributed to the structural disruption responsible for weak receptor binding (St Pierre *et al.*, 2006).

In addition to the atypical NPs from elapids described above, recent studies have aided the characterization of distinct NPs from viperids.

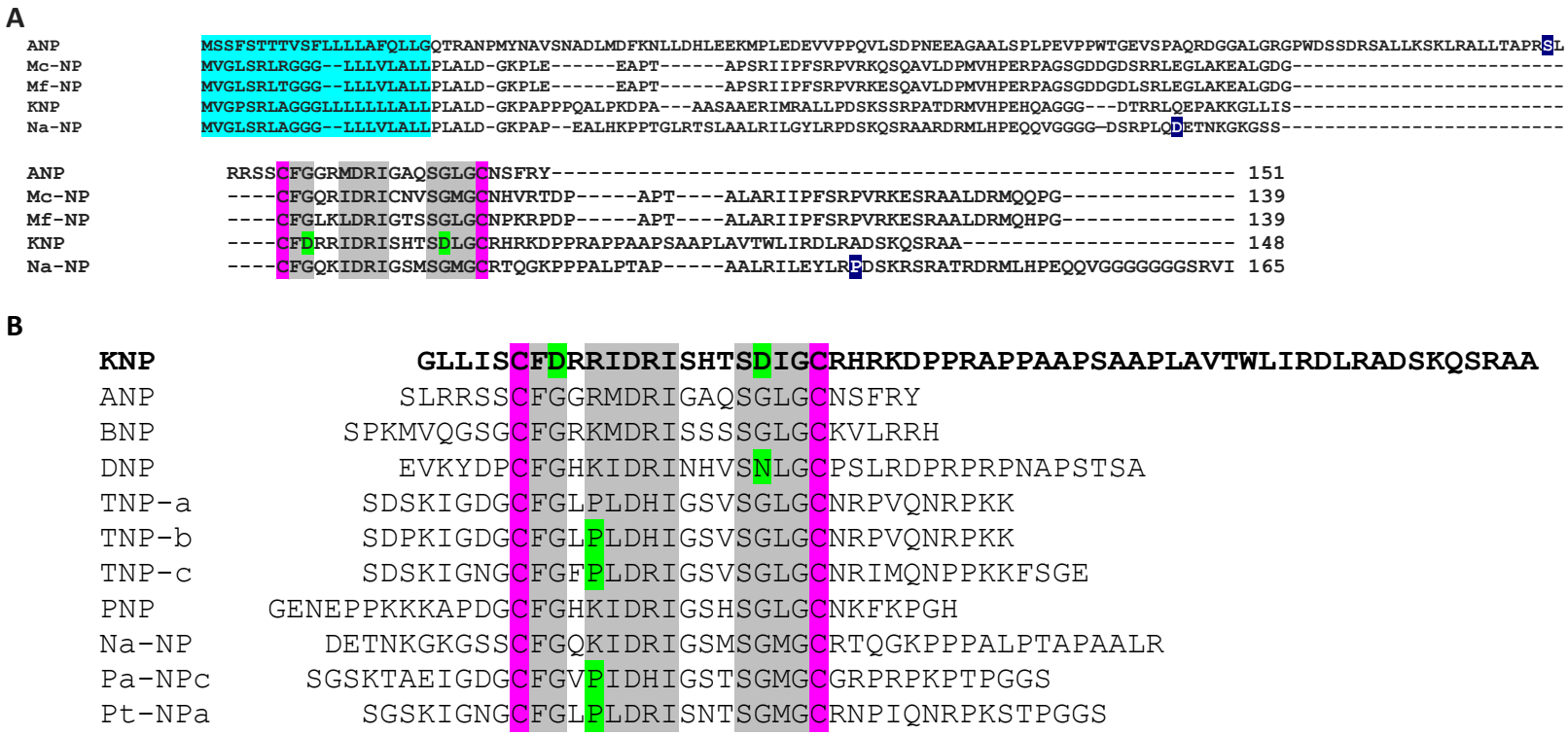

Figure 1.7. Sequence comparision of KNP with mammalian and venom NPs

A: Presursor NP found from the mRNA/ transcriptome of the following species Na–NP (ADK12001*)* from *Naja atra*, KNP (ADF50041) from *Bungarus flaviceps*, Mf-NP (AAZ39879) from *Micrurus fulvius* and Mc-NP (AAC60341) from *Micrurus coralline* have been aligned. Signal peptide Start of the mature protein

B: Mature NPs from elapid snakes and human are aligned. TNP-a (P83226), TNP-b (P83229), TNP-c (P83231) identified from Oxyuranus species, PtNP-a (DQ116724) from *Pseudonaja textilis*, PaNP-c (DQ116727) from *Pseudechis australia*, Na–NP (ADK12001*)* from *Naja atra*, Mc-NP (AAC60341) from *Micrurus coralline*, DNP (AAB22476) from *Dendroaspis augusticeps*, KNP (ADF50041) from *Bungarus flaviceps*, ANP (AAA35529), Human BNP (AAH25785) and human CNP (NP_077720) have been compared. Cys in disulphide bond Evolutionarily conserved residues Non- conserved, non-synonymous substitutions

A number of viperids express CNP-like peptides along with multiple bradykinin potentiating peptides (BPP). BPPs inhibit ACE, the enzyme that degrades bradykinin. ACE inhibition has been one of the attractive targets for hypertension and captopril (the prototype ACE inhibitor preceding the array of ACEI, now in clinical use) is a peptidomimetic of BPPs (Murayama *et al.*, 1997). Although several viperids produce BPP-CNP, recent studies have shown the presence of ANP-like NPs from venoms of *Crotalus durissus casacavella* and *Crotalus oreganus abyssus (Evangelista et al., 2008).*

Venom NPs exhibit an array of subtle changes compared with mammalian NPs that confer entirely different pharmacological effects. Exploring the activity of these peptides provide molecular details of specific NP action.

1.10. Therapeutic potential of NPs

Both ANP and BNP are produced by myocardial cells in response to increasing transmural distending pressure which is exaggerated during HF. These peptides activate NPR-A thereby increasing intracellular cGMP, which mediates natriuresis, inhibition of renin and aldosterone as well as vasorelaxation, anti-fibrotic, anti-hypertrophic and other effects (Ahluwalia *et al.*, 2004; Potter *et al.*, 2006). CNP through activation of NPR-B induces vasorelaxation, inhibition of vascular smooth muscle cell proliferation (Furuya *et al.*, 1991), suppression of aldosterone (Wennberg *et al.*, 1999) and prevention of cardiac remodeling, although it lacks significant natriuresis (Stingo *et al.*, 1992). With such favorable cardiac and renal protection properties, NP system acts as a pivotal compensatory mechanism against the neuro-hormonal activation during HF (Lee and Burnett, 2007b). This gives a

strong justification for the use of exogenous NPs for cases of acute heart failure syndromes.

Both ANP and BNP are clinically used. Human recombinant ANP (Carperitide) was approved in Japan in 1995 for acute HF (Gheorghiade *et al.*, 2005) and human recombinant BNP (Nesiritide) was approved in the U.S. in 2001 (Lee and Burnett, 2007a). Table 1.4 lists the NPs, which are in use and in clinical trials for HF.

Cody *et al.* and Saito *et al.* have demonstrated that intravenous infusion of ANP in patients with HF induced natriuresis, diuresis, inhibited the release of aldosterone, decreased systemic BP and pulmonary capillary wedge pressure (PCWP). But, they observed that the renal response was reduced in patients with HF compared to normal subjects (Cody *et al.*, 1986; Saito *et al.*, 1987). In a recent report on safety of using carperitide, an evaluation for a period of 6 years with 3,777 patients who were treated with a median concentration of 0.085 µg/kg/min of this synthetic peptide, 82% clinically improved (Abraham *et al.*, 2005; Suwa *et al.*, 2005).

Infusion of BNP resulted in decreased PCWP and systemic vascular resistance, increased stroke volume index, increased urine volume and sodium excretion and decreased plasma aldosterone levels (Yoshimura *et al.*, 1991). In the efficacy trials involving 127 HF patients, infusion of BNP resulted in decreased PCWP, improvement in global clinical status, reduced dyspnea and reduced fatigue (Colucci, 2000). Another study reported that BNP may worsen renal functions in patients with HF (Sackner-Bernstein *et al.*, 2005). Thus a panel of experts have recommended the use of BNP only to patients with acute

decompensated HF with dyspnea at rest and have suggested not to use BNP as diuretics.

A challenge in the use of NPs is the route of administration. Owing the peptide nature, NPs are degraded in the gut with low oral bioavailability, thereby necessitating intravenous infusion or subcutaneous administration (Brunner-La Rocca *et al.*, 2001; Chen *et al.*, 2000). Newer long acting fusion hormones have been developed using BNP and human serum albumin called AlbuBNP, which have plasma half-life of 12-16 h (Wang *et al.*, 2004). Further infusion of BNP along with furosemide, a loop diuretic in HF animal models have been reported to exhibit natriuresis and diuresis, improved glomerular filtration rate and attenuation of aldosterone production compared to furosemide or BNP infused alone (Cataliotti *et al.*, 2004).

Table 1.4. Comparison of doses and half-lives of NPs in therapeutics

Peptide in market	Therapeutic concentration (µg/kg/min)	Median duration (h)	In-vitro half-life (min)	Plasma terminal half-life (min)
Carperitide (Synthetic human ANP)	0.085	12- 65	2	13.3
Nesiritide (synthetic human BNP)	0.015	6- 60	8	18
Chimeric CD-NP	0.025	4- 12	15	18.4

As described in (Lee and Burnett, 2007a)

Apart from the usage of classical mammlain NPs, Burnett *et al*. have developed the concept of chimeric NPs. These NPs are designed to have N-terminal and C-terminal extensions of a certain NP, while the ring of a

different NP, so as incorporate the properties of both peptides. Vasonatrin is a chimera of the CNP ring with the ANP C-terminal tail that exhibits vasodilation characteristic of both the parent NPs (Wei *et al.*, 1993). A similar strategy has been used to develop CD-NP, a chimera of the CNP ring with the DNP 15-residue tail (Lisy *et al.*, 2008). This chimera binds to both NPR-A and NPR-B (Dickey *et al.*, 2008), attributes from the parent NPs, and hence was able to elicit venodilation, vasodilation, natriuresis and diuresis (Martin *et al.*, 2012). Although CD-NP had 60 times lower potency compared ANP and BNP, at pharmacologically relevant concentration, CD-NP retained its renal properties in an animal HF model (Lee *et al.*, 2009). Also, this chimeric peptide is reported to have longer in-vitro half life (Dickey and Potter, 2011). This property CD-NP makes a promising therapeutic agent and is currently under clinical trials.

Based on the existing studies, it is evident that NPs have favourable cardiorenal protection properties which could be put to use in the case of acute HF. However, further additional studies to elevate the efficacy and adverse effects of NPs are required to establish their effectiveness as pharmacological agents. Also, the discovery of NPs from non-mammalian sources add on to the knowledge, which would aid the creation of novel therapeutic molecules with improved pharmacological effects.

1.11. Krait natriuretic peptide (KNP)

The present thesis focuses on the characterization of a peculiar NP identified from krait. Kraits (*Bungarus* species) are large, highly venomous snakes inhabiting parts of south and South-east Asia. Predominantly nocturnal, these

reptiles feed on skinks, lizards, frogs, small mammals and snake eggs. A number of classical neurotoxins have been characterized from these species.

Red-headed krait (*Bungarus flaviceps*), the species of krait from which the candidate molecule has been identified, has distinct body coloration, with a blue or black body and red colored head, neck and tail. The venom of *B. flaviceps* is more lethal than that of *B. fasciatus* and comparable to that of *B. candidus*. Except for a few neurotoxins isolated and characterized (Yanoshita *et al.*, 2006), the venom of *B. flaviceps* is largely unexplored. A transcriptome analysis of the venom of this snake revealed the presence of several three-finger toxins, neurotoxin and Kuntiz type serine protease inhibitors (Siang *et al.*, 2010). Along with these a low abundant NP transcript was found. The identified NP transcript, namely KNP or Bf-NP (Krait natriuretic peptide) encodes a 148-amino acid residue protein with the first 27 residues predicted to be a signal peptide (Fig. 1.7A). The precursor has a long C-terminal tail (38 residues); although it is similar in length to *Micrurus coranillus* (Mc-NP), *Micrusus fulvius fulvius* (Mf-NP) and *Naja atra* (Na-NP), it has a unique sequence (Fig. 1.7A). The C-tail of KNP has no sequence similarity against the non-redundant database on NCBI. The last 21 residues of the tail have the ability to form an α-helix when predicted using PSI-PRED. This propensity to form a secondary structure in the C-terminal extension has not been previously reported. Apart from the unique C-terminal tail, there are two substitutions of residues within the ring, which are conserved Gly residues in all other NPs.

Thus with such unique characteristics, KNP may have different biological functions compared to all venom or mammalian NP characterized to date.

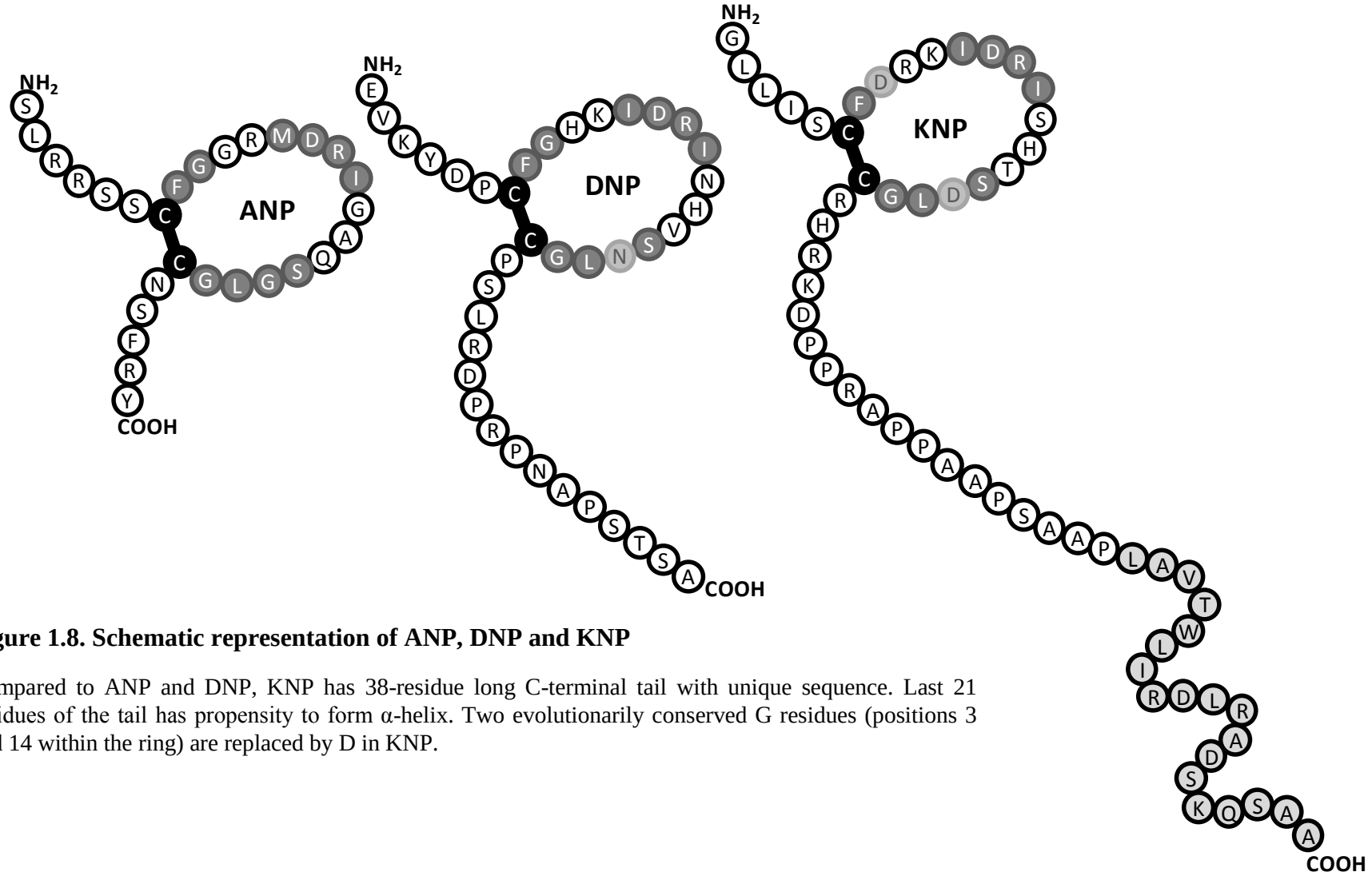

Figure 1.8. Schematic representation of ANP, DNP and KNP

Compared to ANP and DNP, KNP has 38-residue long C-terminal tail with unique sequence. Last 21 residues of the tail has propensity to form α-helix. Two evolutionarily conserved G residues (positions 3 and 14 within the ring) are replaced by D in KNP.

1.12. Aim and scope of the study

NPs from snake venom have distinct biological characteristics. Understanding their biological functions has lead to the design of newer and better pharmacological agents. To date, few venom NPs have been isolated and characterized. Hence, exploration for novel NPs from an exogenous source as snake venom, will serve in understanding the diversity of NPs and design of NPs with therapeutic potential.

The transcriptome of the venom gland of *Bungarus flaviceps* revealed the presence of a NP with a long C-terminal tail, "KNP". This peptide has a unique sequence with a propensity to form α- helix in its C-terminal segment. Also, Gly residues at positions 3 and 14 within the ring that are conserved in all other NPs, are replaced by Asp in case of KNP. Hence, this thesis focuses to understand the mode of action of KNP using structure-function relationships of the molecules. The objectives of this thesis are:

1. To document the biological function of KNP
    - Heterologous expression and purification of KNP
    - Evaluation of vasodilator actions of KNP
    - Evaluation of in-vivo activity of KNP: effect on blood pressure and urine output

2. To delineate the mechanism of action of KNP
    - Assessment of structure- function relationships
    - Evaluation of downstream signaling cascade

3. To investigate the stability of KNP to degradation
    - Role of residues involved in conferring resistance to proteolysis and clearance receptor binding

CHAPTER 2

Tail wags the dog: C-terminal tail redirects KNP away from natriuretic peptide receptor

Chapter 2: Tail wags the dog: C-terminal tail redirects KNP away from natriuretic peptide receptor

2.1. Introduction

Snake venoms are a cocktail of pharmacologically active proteins. They have evolved to aid prey capture and deterrence. These protein toxins target different physiological systems resulting in neuromuscular and respiratory paralysis, loss of consciousness, hemorrhage, localized pain etc., in their prey (Gaffney *et al.*, 1979). In the last few decades, with the advent of specialized techniques a number of toxins have been identified. One such toxin, identified from the venom gland of red-headed krait (*Bungarus flaviceps*) named Krait natriuretic peptide (KNP), is investigated in the present study.

B. flaviceps is a highly venomous elapid snake found in South and Southeast Asia. Transcriptomic analysis revealed the presence of a full length precursor NP (Bf-NP or KNP) (Siang *et al.*, 2010). KNP has a 17-residue ring as have all known NPs. However the 38-residue long C-tail is the longest such tail known among NPs. In-silico analysis suggest the C-tail has propensity to form an α-helix (Figure 1). The amino acid residues of the C-tail of KNP are unique. Further, Gly residue at positions 3 and 14 which is conserved within the ring of all NPs has been substituted with Asp residue in KNP. **With distinct features – unique sequence, propensity to form α-helix and possessing much longer C-tail than any known NP – KNP is hypothesized to exhibit a distinct biological actions.** The unusual C-terminal makes KNP an interesting candidate to evaluate its function. KNP showed an endothelium-dependent vasorelaxation, in contrast to classical NPs. Infusion of KNP in experimental rats resulted in sustained and prolonged decrease in blood

pressure and heart rate while did not influence the renal function in contrast to ANP. These observations connote the existence of a unique mode of action for KNP. A structure based functional studies revealed the putative helix region to be involved in conferring this action.

2.2. Materials and Methods

2.2.1. Materials

Materials used in the experiments described below were obtained from the following sources:

Codon optimized Synthetic DNA of KNP cloned in pUC-57 from Genescript corporation (Piscataway, NJ, USA), pET-32a vector (Novagen, Merck biosciences), DNA oligos for amplification from1st Base Asia (Singapore), Hifi polymerase (Kapa Biosystem, Cape Town, South Africa), Kpn1 and Sac1 restriction enzymes (Fermentas Fast Digest, Ontario, Canada), QIAquick gel extraction kit (Qiagen, Hilden, Germany), T4 DNA fast Ligase (Fermentas, Canada), DNA Gene ruler (Fermentas, Ontario, Canada), plasmid extraction kit (GeneAll plasmid miniprep kit, Korea), Big Dye (Life Technologies, Carlsbad, USA), Luria burtani- broth and agar (Q.BIOgene,Irvine, CA, USA), Precision Plus Protein™ Dual-Colour Standards (Hercules, CA, USA), Acetonitrile and trifluoroacetic acid, Formic acid (Merck KGaA,Darmstadt, Germany), RP- Jupiter C18 columns (300 Å, 5 µm, 250 mm X 21.2 mm and 250 mm X 10 mm) from Phenomenex (Torrance, CA, USA), Hiprep 26/10 desalting column and Hi-Trap-Sulfopropyl (SP)-Sepharose column (GE healthcare, Little chatfont, UK), Tris-HCl, Urea, NaCl from 1st Base Asia (Singapore, Singapore), TGA, TGR, pre-loaded Wang resin (Novabiochem,

Merck chemicals, NY,USA), Fmoc-protected amino acids (Anaspec, China, Novabiochem or GL Biochem, China), Solvents N-N-dimethylformamide (DMF), Dichloromethane (DCM), piperidine, N-methyl pyrrolidine (NMP), N-N-diisopropylethylamine (DIPEA), 1,2-diethylether, methanol, Acetonitrile, trifluroacetic acid and formic acid (Merck chemicals, NY, USA).

CHO-K1 cell line (American Type Culture Collection,Manassas, VA, USA), L-NAME,Indomethacin, Dulbecco's Modified Eagle's Medium (DMEM), IBMX, BSA (Sigma-Aldrich ,St. Louis, MO, USA), Penicillin-Streptomycin, Trypsin and trypsin neutralizer (GIBCO, Invitrogen, CA, USA), ODQ (Cayman Chemical,Ann Arbor, MI, USA), Tissue culture plates (Corning, NY, USA), saline, heparin (5000 IU/ml), sodium pentobarbital (NUS, pharmacy, Comparitive medicine).

Animals

Animals (Sprague Dawley rats) were obtained from Invivos and acclimatized in the Comparitive Medicine, Animal Holding Unit for a minimum of one day before the experiments. The animals were kept under standard conditions with food and water available *ad libitum* in a light-controlled room (12 h light/dark cycle, light on 07:00 h) at 23°C and 60% relative humidity.

2.2.2. Cloning of KNP and deletion mutants

The DNA sequence encoding KNP was optimized for expression in *Escherichia coli* and synthesized. Obtained synthetic gene was cloned in pUC57 vector. This fragment was amplified using forward primer 5’ GGTACCGAAAACCTGTACTTCCAATCGGGCCTGCTGATTT 3’ which had Kpn1 restriction site followed by tobacco etch virus (TEV) protease

recognition sequence followed by the 5' end of the gene of interest and reverse primer 5'GAGCTCTTATTAATGCGGCACGGCTCTGTTTACTATC3' which had complementary sequence to 3' of the gene and Sac1 restriction site. Synthetic DNA (0.1 µg) containing plasmid was mixed with 1 µl of 10 µM primer stock, 1 µl of 10 mM dNTPs, 1 unit of Kapa HiFi polymerase and 10 µl of 5X PCR buffer containing $MgCl_2$ in a 50 µl reaction. The cycling parameters were set as one cycle of 98ºC for 2 min, 35 cycles of 98ºC for 10 s, 60ºC for 30 s and 72ºC for 45 s, and a final extension at 72ºC for 7 min. The amplified product was analysed using 1% (w/v) agarose gel electrophoresis. The obtained product was extracted from gel using the Qiagen gel extraction kit using manufacturer's protocol.

Both the DNA fragment and pET-32 a (vector into which the DNA fragment is to be cloned) were double digested using Kpn1 and Sac1 enzymes (1 unit enzyme per µg DNA) for 30 min at 37°C. Digested pET-32a was run on 1 % (w/v) agarose gel and band corresponding to the linear plasmid was extracted from the gel. The double digested DNA fragment of KNP was subjected to PCR purification. Concentrations of the purified digested DNA fragment and the vector were determined by measuring using NanoDrop ND-1000 Spectrophotometer (NanoDrop Technologies) with software ND-1000 V3.3.0. Insert and vector were ligated at 3:1 molar ratio. To the DNA mixture, 1 unit of T4 DNA ligase along which the 2 µl of 5X ligase buffer was set up for a reaction of total volume 10 µl and was incubated 4°C overnight.

2.2.3. Preparation of competent cells and transformation

Before transformation, the competent cells for *E. coli* JM109 (copy number increase strain) and BL21DE3 (expression strain) were prepared. The stock of

these cells was thawed and streaked on LB agar plates without any antibiotic and was grown at 37°C for 16 h. The following day, a single colony from plate was inoculated in 2 ml of LB broth without any antibiotics and was culture at 37°C, 200 rpm, 16 h. 1 ml from the overnight culture was used to inoculate 100 ml of LB broth without any antibiotic and was grown until the optical density at 600 nm reached value between 0.6-1 OD at 37°C, 200 rpm. The culture was transferred to an ice-cold falcon tube and spun at 2000 g, 4°C for 10 min. The culture supernatant was discarded and the cells were resuspended in 1 ml of 100 mM $CaCl_2$ which was further diluted to 50 ml with the same solution. This mixture was incubated on ice for 40 min, following which it spun at 2000 g, 4°C for 10 min. The cell pellet was gently resuspended in 8-10 ml of 100 mM $CaCl_2$ containing 10% glycerol (sterilized) and was split into pre-chilled 1.5 ml Eppendorf tubes as 50 µl aliquots.

The prepared competent cells were used for transformation. A vial of the cells was thawed on ice and the ligation mixture was added to it and incubated on ice for 30 min. After the incubation, the cells were subjected to heat shock at 42°C for 90 sec and were immediately transferred on ice for 5 min. This was followed by the addition of 200 µl of LB broth and recovery of cells by incubating at 37°C, 200 rpm for 30 min. This transformation mixture was spread on LB agar plate containing 100 µg/ml ampicillin. The plates were incubated at 37°C for 16- 18 h.

2.2.4. Plasmid isolation and DNA sequencing

Isolated transformants for the plates were inoculated in 2 ml LB broth containing 100 µg/ml ampicillin and cultured for 16 h at 37°C, 200 rpm. Plasmids were isolated from the cultured bacterial cells using GeneAll™

plasmid extraction kit, using protocol recommended by the manufacturer. The concentration of DNA was measured as described previously.

DNA sequencing of the plasmid was performed using ABI PRISM® Big Dye™ Terminator Cycle Sequencing Ready Reaction Kit (version 3.0) (PE-Applied Biosystems, CA, USA). Each reaction contained 100 ng of plasmid DNA which was mixed with 2 µl of Bigdye and 1 µM T7 promoter or terminator primers in a volume of 5 µl. The reactions were amplified using the following cycling conditions: 25 cycles of denaturation at 96ºC for 10 s, annealing at 50ºC for 5 s and extension at 60ºC for 4 min. The PCR product was cleaned using Cleanseq magnetic beads and the purified DNA was dissolved in 40 µl of autoclaved water. This DNA mixture was loaded on to automated ABI PRISM® 3130XL Genetic Analyzer (Applied Biosystems, Foster City, CA, USA). The obtained sequences were analyzed using FinchTV and Generunner softwares.

2.2.5. Expression of KNP

After verifying the sequence, clones encoding the fusion protein were transformed into *E. coli* expression strain BL21 DE3 as described previously. A single colony was inoculated in 100 ml LB Broth containing 100 µg/ml of ampicillin and grown for 16 h at 37°C at 200 rpm. This culture was used to inoculate 1 l LB broth containing 100 µg/ml ampicillin in 1: 100 (culture: broth) ratio and was growth at 37°C, 200 rpm until the cell density reached ~ 0.6 OD at 600 nm. Protein expression was then induced using 0.1 mM IPTG (isopropyl β-D-thiogalactoside) and further grown at 16°C, 150 rpm for 16-18 h. The cells were harvested by spinning them at 5,000 g for 15 min at 4°C.

The cell pellets were stored at -80°C until further processing. The expression of recombinant protein was analyzed using SDS-PAGE on a 15% polyacrylamide gel.

Bio-Rad Mini-PROTEAN™ gel system was used for running SDS-PAGE. Samples were prepared by mixing 20 µl of sample and 5 µl of 5X loading dye and incubating the mixture at 100°C for 10 min. The samples were spun at 10, 000 g and 10 µl of this mixture was loaded on to the gel. On the first lane molecular weight ladder, Precision Plus Protein™ Dual-Colour Standards (5 µl) was run. Electrophoresis was carried at 120 V until the dye front reaches the bottom of the gel. The gel was stained with Coomassie Brilliant Blue-R250.

2.2.6. Purification of KNP

To purify the expressed protein, the harvested cells were resuspended in native lysis buffer (50 mM Tris-HCl, 150 mM NaCl pH 8) and were subjected to ultrasonication (pulse frequency 1 s ON and 1 s OFF) for 5 min. The lysed cells were spun at 12,000 g and pellet was washed with wash buffer (50 mM Tris-HCl, 150 mM NaCl, 2 M urea pH 8). The slurry was spun at 12,000 g and the pellet was solubilized in denaturation buffer (50 mM Tris-HCl, 150 mM NaCl, 8 M urea pH 8) overnight at 4°C. After the solubilizing the protein solution was spun at 12,000 g to remove particulate matter. These samples were run on SDS-PAGE to assess the presence of the protein. Hence, the crude protein mixture from the solubilized pellet was syringe filtered and purified by reversed-phase chromatography using Jupiter C18(5 µm, 300 Å, 250 X 21.2 mm) preparative grade HPLC column using 0.05 % formic acid (FA) as buffer A and 100 % acetonitrile with 0.05 % FA as buffer B on Akta

purifier system (GE Healthcare Life Sciences, Little Chatfont, UK). A linear gradient of 40-70 % B was used to achieve required separation of the protein peaks and the quality of the fusion protein was analyzed using Electrospray-ionization (ESI) - Mass Spectrometer (MS) (LCQ Fleet Ion trap, Thermoscientific, Massachusettes, USA). Mass analysis involved injection of 25 µl of the sample at 200 µl/min flow rate into the ion source. Sheath gas flow rate of 30, auxillary gas flow rate of 5 at a spray voltage of 4.5 KV and capillary temperature of 350°C was used for ionizing the sample. The ion-trap detector was set in positive mode with a mass/ charge range of 500-2000. Qual browser, Thermo Xcalibur software was used analysis and Pro-mass software (Thermoscientific) was used for reconstructed the mass spectrum. The fractions which showed pure protein mass were freeze dried.

The freeze dried fusion protein was dissolved in 50 mM Tris-HCl, 150 mM NaCl, 6 M urea pH 8 and desalted using 50 mM Tris-HCl pH 8 buffer using a Hiprep 26/10 desalting column (26 mm X 100 mm). The desalted fusion protein was cleaved using recombinantly expressed and purified TEV protease in the ratio 40:1 (fusion protein:TEV) in 50 mM Tris-HCl containing 0.5 mM EDTA pH 8, overnight at 4ºC.

The predicted pI of KNP is 10.67 while the corresponding pI of the fusion protein and tag were 6.82 and 5.79 respectively. Hence, the difference in their pIs was exploited to purify the cleaved protein from the tag and uncut fusion protein. Cation exchange chromatography (CIEX) was performed with 50 mM Tris-HCl pH 8 as buffer A and 50 mM Tris-HCl, 500 mM NaCl pH 8 as buffer B, on a Hi-Trap-Sulfopropyl (SP)-Sepharose column (34 µm, 16 X 25 mm). Further the cleaved protein peak was purified to homogeneity using RP-HPLC

with Jupiter C18 column (5 µm, 300 Å, 250 mm X 10 mm) with buffer A- 0.05 % FA and buffer B- 0.05% FA with 100% Acetonitrile on a linear gradient of 20-40% B. Purified protein peak was checked on ESI-MS for its purity and freeze dried. The protein was reconstituted in phosphate buffer saline and quantified by absorbance at 280 nm before the assay.

2.2.7. Cloning, expression and purification of ΔHelix and R&H

Two truncations of KNP were designed based on the predicted structure of KNP. Full length KNP lacking the putative helix segment, ΔHelix (Residues 1-34) and a fusion of ring and helix, R&H (residues 1-22 with residues 39-60) were designed. DNA fragments encoding ΔHelix and R&H were obtained using specific primers designed to amplify the required segment out of DNA encoding KNP. Strategies of cloning, expression and purification involved same procedure as described above.

2.2.8. Synthesis of ANP, Ring and Helix

Peptides were synthesized using manual 9-fluorenylmethoxycarbonyl (Fmoc)-solid phase peptide synthesis. All amino acids used were Fmoc-L-(amino acid)-OH derivatives, with some residues containing side-chain protection groups. The side-chain protected amino acids used were: Arg(Pbf), Asn(Trt), Asp(OtBu), Cys(Trt), Gln(Trt), Glu(OtBu), His(Trt), Ser(tBu), Thr(tBu), and Tyr(tBu).

ANP was synthesized using Tyr-preloaded Wang resin, Helix using Novasyn TGA resin and Ring using Novasyn TGR resin. Synthesis scale was set to 0.2 mmol and the appropriate quantity of resin was swollen in DMF. After washing the resin with DMF, an iterative procedure of coupling-deprotection-

coupling was carried out from C-terminal residue of the peptide to N-terminus. Coupling involved activation of 5 times excess of Fmoc-Amino acid derivatives using 4.9 times HATU and 10 times DIPEA in a reaction performed in the ratio 2:1 DMF: NMP. Following coupling, resin was washed with DMF and deprotection of the F-moc group using 20% (v/v) piperidine in DMF was done.

After the completion of synthesis, the resin was washed thrice with DMF-DCM-methanol and dried. The peptides were cleaved from the resin using TFA:EDT:TIS:water (94:2.5:1:2.5) and precipitated using ice cold 1,2 diethyl ether. The crude peptides were purified using Jupiter C18 column (5 µm, 300 Å 10 X 250 mm) using a linear gradient with buffer A-0.1 % Trifluroacetic acid (TFA) and Buffer B- 0.1% TFA with 80% acetonitrile, on Akta purifier system (GE Healthcare). The purity and homogeneity of the peptides were assessed using ESI-MS and pure fractions were freeze fried.

ANP was subjected to air oxidation in 100 mM Tris-HCl pH 8 with 10% acetonitrile while Ring was oxidized using 100 mM Tris-HCl pH 8, 20% DMSO and 10% Acetonitrile at final peptide concentration of 0.5 mg/ml. The oxidized peptides were purified by RP-HPLC and the mass of the peptides determined by ESI-MS.

2.9. Vasorelaxation assay

Male Sprague Dawley (SD) rats (10 weeks old) were euthanized and the descending thoracic aorta was isolated and flushed with physiological solution (Krebs Buffer: 118 mM NaCl, 4.7 mM KCl, 1.2 mM KH_2PO_4, 1.2 mM $MgSO_4$, 1.25 mM $CaCl_2$, 25 mM $NaHCO_3$, 11 mM glucose, pH 7.4). The fat tissues and connective tissues on aorta were removed, cut into 2-3 mm rings

and mounted under 2.5 g tension into the organ bath chamber using two stainless steel hooks. The aortic strips were fixed to MLT0201/RAD Force transducer (AD Instruments). The tissues were equilibrated in chambers at 37℃ containing carbogenated (95% O_2 and 5% CO_2) Krebs buffer for an hour. The presence of endothelium in the aortic strip was checked by pre-contracting the tissue with 300 nM phenylephrine (PE) and relaxing with 10 µM Acetylcholine (ACh). The aortic rings were pre-contracted with 100 nM PE and a cumulative dose response for different peptides/ protein was obtained. Further, the aorta was denuded of endothelium by rubbing the inner surface of the aortic ring with a cotton bud and then pre-contracted with 100 nM PE to construct the cumulative dose-response of the protein/peptides. The efficiency of removal was confirmed by no relaxation response to Ach treatment.

To study the effect of different inhibitors, the tissue was incubated with individual inhibitors including 100 µM L-NAME (L- arginine methyl ester hydrochloride, inhibitor of NO synthesis), 10 µM Indomethacin (cycloxygenase 1 and 2 inhibitor) or 20 µM ODQ (1H-[1,2,4]oxadiazolo[4,3-a]quinoxalin-1-one, soluble guanylyl cyclase inhibitor) for 20 min prior to pre-contraction of tissue. The inhibition was confirmed by attenuated relaxation on Ach treatment. To understand the role of hyperpolarization in mediating KNP signalling, tissues were pre-contracted with 40 mM KCl. The pre-contracted tissue in the presence of a particular inhibitor was used to assess the activity of 300 nM of either ANP/KNP. The relaxation response of different peptides was assessed on three independent tissues. Data are represented as mean ± SEM.

Contraction response of aortic strips with 100 nM PE is considered 0% relaxation. Subsequent relaxation of the aortic strips is in response to different concentrations of the peptide is represented as percentage relaxation. Statistical analysis of the relaxation curves was done using one-way ANOVA with one-tail student t-test and significance was accepted for a P-value < 0.05.

2.2.10. Measurement of Mean arterial pressure and urine volume

Experiments were performed on male Sprague Dawley (SD) rats (220-300 g) in accordance with protocol 041/12 approved by the Institutional Animal Care & Use Committee (IACUC), NUS. Rats were anesthetized with 60-70 mg/kg Pentobarbital (IP) and placed on heating pad at 37°C to maintain body temperature. Urinary bladder catheterization was performed as illustrated in (Robinson *et al.*, 2012) with certain modifications as described. A midline incision was made to expose the urinary bladder. The bladder was retracted and an 18 G needle was used to puncture the bladder neck. A 5 cm long PE 50 catheter was cut at one end to have a pointed and elliptical end, which was introduced into the bladder through the puncture. A purse-string suture was placed in the bladder surface at the site of entry of the catheter to secure it. 0.9% saline was injected into the bladder through the catheter to check if the bladder was leaking.

Subsequently, a left oblique groin incision was made to expose the femoral artery and vein which were isolated and cannulated. After the surgery 1 ml of 0.2% BSA containing saline was injected intravenous to compensate for surgical loss. A fluid filled physiological pressure transducer (MLT 844, AD Instruments) filled with 50 IU/ml heparinized saline was connected to the

femoral artery catheter, while saline containing 0.2% BSA was infused through the catheter inserted into femoral vein at 2 ml/h for equilibration period of 20 min. Mean Arterial Pressure (MAP), heart rate and urine volumes were measured continuously. The experiment begun with a control periods (C-10 min) followed by 2 experimental periods (E1 and E2, 5 min each) during which 0.2 nmol/kg/min ANP or 2 nmol/kg/min KNP or Ring or Helix or ΔHelix in 0.2% BSA saline was infused. The animal was left to recover for 40 min (R1-R4, four recovery periods of 10 min each) during which 0.2% BSA saline was infused. Each peptide was assessed for its bioactivity in five independent trials and the statistical analysis was performed between different time points of ANP and KNP related peptides using one-way student t-test and a P-value < 0.05 was considered to be significant.

2.2.11. Cell culture

CHO-K1 cells were maintained in high-glucose Dulbeco's modified eagle's medium (DMEM) supplemented with 10% fetal bovine serum (FBS), 100 U/ml penicillin and 100 µg/ml streptomycin and 2 mM glutamine in a humidified incubator at 37°C with 5% CO_2. The cells were sub-cultured by trypsinization every three days. The cells were counted using a Bio-rad TC20^{TM} automated cell counter.

2.2.12. NPR-A and NPR-B plasmid preparation

Plasmids encoding NPR-A and NPR-B were generously gifted by Dr. Ruey-Bing Yang (Academia Sinica) and Prof. Micheala Kuhn (University of Wurzburg). The plasmids were transformed into JM109 as described previously. A single colony of the transformant was inoculated in 100 ml of

LB broth containing 100 µg/ml ampicillin and was grown at 37°C, 200 rpm for 22-24 h. The cells were harvested by spinning at 5,000 g for 20 min and the plasmids were extracted using Pure yield™ plasmid maxiprep kit (Promega) using manufacturer's protocol. The DNA concentration was evaluated using nanodrop as described previously.

2.2.13. Transfection of CHO-K1 cells

$1X10^5$ cells were seeded per well in a 24- well plate. The cells were allowed to growth for 20-22 h before transfection. The used media was aspirated from the wells and replenished with 400 µl of DMEM containing 10% FBS without any antibiotics. Each well was provided with 0.8 µg plasmid diluted in 50 µl of serum free DMEM media. Two µl of lipofectamine™ 2000 was diluted in 50 µl of serum free DMEM media was added. Diluted DNA and transfection reagent were mixed and incubated at room temperature for 10-15 min. The DNA- lipofectamine mixture (100 µl/ well) was directly added to the cells within 30 min. The cells were incubated with the DNA-lipid complex for 6 h at 37°C with 5% CO_2. After 6 h the media containing DNA and lipofectamine was aspirated and replaced with DMEM containing 10% FBS and antibiotics. These cells were incubated at 37°C with 5% CO_2 for 16- 20 h before it is treatment with the peptides.

2.2.14. Whole cell cGMP elevation assay

CHO-K1 cells transfected with either NPR-A/ NPR-B/ empty-vector pCMV4.0 were used. Post transfection, the media was aspirated and the cells were washed with 500 µl of PBS. The cells were incubated for 30min after the addition of 150 µl of 0.5 mM IBMX containing vascular growth media.

Meanwhile peptides were reconstituted in 4X concentrations. After 30 min of incubation, 50 µl of peptide solution was added to the cells followed by further incubated for 30 min at 37°C with 5% CO2. Subsequently peptide containing basal media was removed and 150 µl of 0.1 M HCl was added and incubated at room temperature for 30 min with shaking at 50 rpm. The cell lysates were collected and assayed for cGMP levels using Enzo life sciences cGMP ELISA kit, as per the manufacturer's protocol. Total protein content of the cell lysates of a few wells was determined by BCA (bichinchonic acid) assay and this value was used to normalize across different 24 well plates used. Three independent trials for each peptide was done and the statistical comparison between ANP or CNP and KNP related peptides was performed using one-tail ANOVA with t-test and curves with a P-value <0.05 was considered as significant difference.

2.3. Results

2.3.1 Sequence and structural analysis of KNP

The transcriptome of *B. flaviceps* revealed the transcript which encodes 148-residue precursor protein (Figure 2.1). *B. flaviceps* is an uncommon snake which is hard to obtain and difficult to keep in captivity. Further, venom yields per milking are low. Therefore, we were unable to identify the size of the mature KNP protein in the venom. There are three dibasic processing sites in the precursor protein. Processing at the second dibasic site at position 87 leads to 5-residue N-terminal segment ahead of the conserved 17-membered NP ring; such short N-terminal extensions are found in all known NPs (Figure 1.8). Processing at the third dibasic site at position 113 leads to two-residue C-terminal tail; such short tails have not found in elapid NPs and hence, we assumed that the processing may not occur at this site. Therefore, we hypothesized that mature KNP is 60-residue long with a 38-residue tail. The C-terminal tail did not show similarity to any protein in the database and interestingly, the last 21 residues showed propensity to form α- helix (Figure 2.1). Despite the presumption, we also tested the functions of the shorter version of KNP with a short two-residue tail (see below). Because of the unique structural features, we were interested in understanding the functional properties of KNP.

Precursor KNP

MVGPSRLAGGGLLLLLLALLPLALDGKPAPPPQALPKDPAAASAAERIMRALLPDSKSSR
PATDRMVHPEHQAGGGDTRRLQEP**KK**GLLISCFDRRIDRISHTSDMGCRH**RK**DPPRAPP
AAPSAAPLAVTWLIRDLRADSKQSRAA

Mature KNP

GLLISCFDRRIDRISHTSDMGCRHRKDPPRAPPAAPSAAPLAVTWLIRDLRADSKQSRAA

Predicted secondary structure

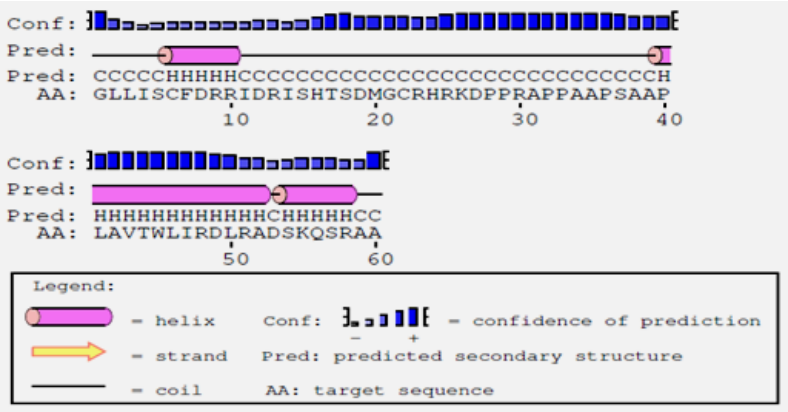

Figure 2.1. Sequence and structural analysis of KNP
Precursor KNP was identified from the transcriptome of the venom gland of *Bungarus flaviceps*. It encoded a 148-residues protein along with a signal peptide (sequence represented in **bold**). The possible maturation sites in the proteins are dibasic residues (indicated in **red** bold letters). The mature protein was assumed to be 60 residues protein with both Cys residues in a disulphide bond. The secondary structure prediction using PSI-PRED, showed that the last 21 amino acid residues of KNP tail had propensity to form an α-helix.

2.3.2 Heterologous expression and purification of KNP

As there was no natural venom source, we recombinantly expressed and purified KNP. Mature protein was heterologously expressed in *E. coli* as Trx-His-fusion protein (Figure 2.2). This protein was obtained from the insoluble fraction. Following a 2 M urea wash, the protein pellet was solubilized protein in 8 M urea containing buffer and was further purified by reversed phase high

performance liquid chromatography (RP-HPLC), and the purity of the protein was assessed using ESI-ion trap mass spectrometry. Fusion protein showed 23734.9 ± 1.9 Da which matched with the calculated mass. The fusion protein was cut by recombinant TEV protease and purified by cation exchange chromatography (CIEX) followed by RP-HPLC. The protein peak showed mass of 6602.3 ± 0.9 Da which corresponded to the calculated mass of the oxidized KNP. Thus completely oxidized KNP was obtained and was used to assess its function.

2.3.3 Purification of ANP

ANP was synthesized by manual Fmoc-based peptide synthesis. The cleaved and purified peptide showed mass of 3082.0 ± 0.5 Da which was corresponding reduced mass of the peptide. It was folded by air-oxidation and the peptide after folding showed mass of 3080.6 ± 0.5 Da indicating the formation of the disulphide bond (Figure 2.3).

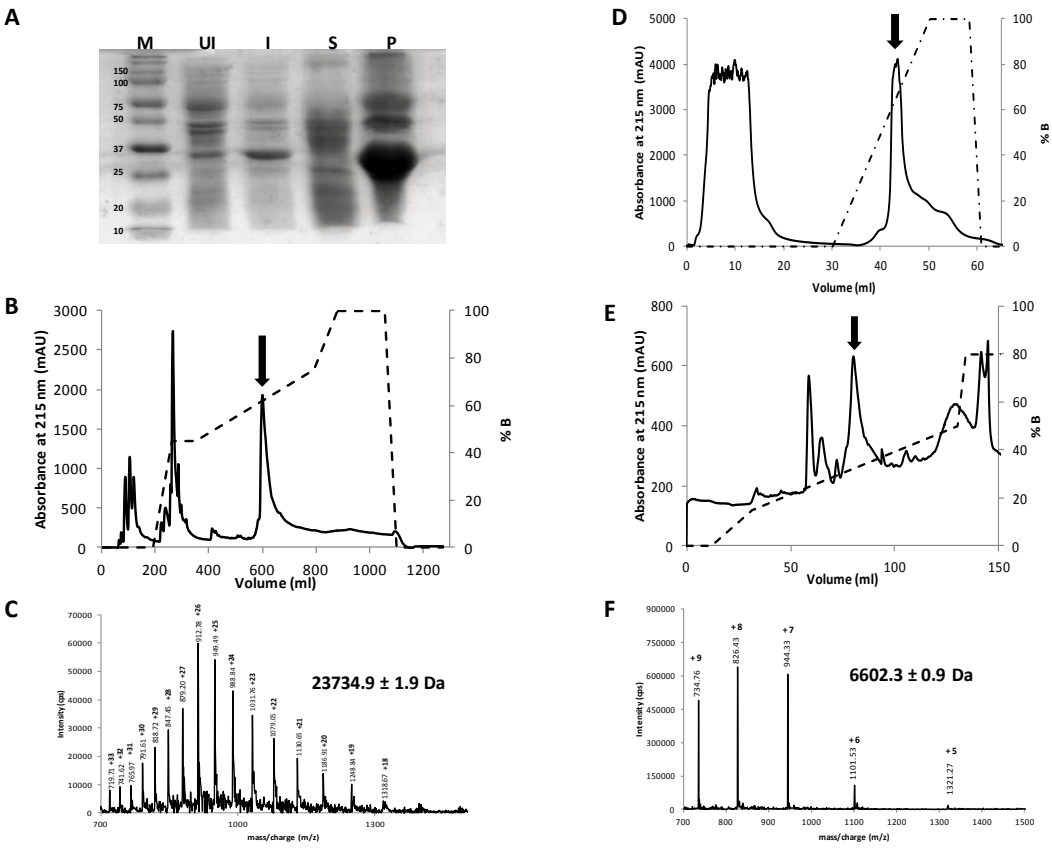

Figure 2.2. Heterologous expression and purification of KNP

A: A 15 % SDS-PAGE analysis shows the expression of trx-KNP fusion protein in insoluble fraction. M- Precision Plus protein^{TM} Dual color standard, UI- Uninduced *E. coli* whole cell lysate, I- Induced *E. coli* whole cell lysate, S- Supernatant containing soluble protein after cell lysis, P- Pellet containing insoluble proteins. **B**: The trx-fusion protein was purified by reversed-phase high performance liquid chromatography using 0.05% formic acid (FA) as buffer-A and 100% Acn with 0.05% FA as buffer-B. The separation was performed on Jupiter C18 column (5µm, 300 Å 250 X 21.2 mm) with a linear gradient of 40- 70% B. The arrow indicates the protein of interest. **C**: Mass of the protein peak indicated by the arrow in panel B was determined by ESI Ion-Trap mass spectrometry. Peaks obtained were reconstructed to obtain a mass of 23734.9 ± 1.9 Da which corresponded to the mass of trx-KNP fusion protein. Pure fractions of the protein were freeze dried. **D**: The freeze dried fusion protein was dissolved in 50 mM Tris-HCl, 6 M urea pH 8 buffer. This protein was desalted with 50 mM Tris-HCl pH 8. TEV protease cleavage reaction was set with protein obtained at a ratio 1:40 (TEV: protein) at 4°C for 16-20 h. Cleaved protein, tag and uncut fusion protein were separated using cation exchange chromatography using 50 mM Tris-HCl pH 8 as buffer-A and 50 mM Tris-HCl, 500 mM NaCl pH 8 as buffer-B. The chromatographic separation was performed using Hi-Trap-Sulfopropyl (SP)-Sepharose column (34 µm, 16 X 25 mm) with a linear gradient of 0-100% B. The arrow indicates the protein peak which was subsequently purified. **E**: Peak indicated in panel D was run on RP-HPLC using Jupiter C18 column (5 µm, 300 Å ,250 X 10 mm) with 0.05% FA as buffer-A and 100% Acn with 0.05% FA as buffer-B on a linear gradient of 15- 50% B. Arrow indicates is the protein of interest. **F**: Mass of the protein indicated from panel E was determined by ESI-ion trap mass spectrometer. The reconstructed mass of the mass spectrum indicated a protein of mass 6602.3 ± 0.9 Da, which corresponded to the calculated mass of oxidized KNP.

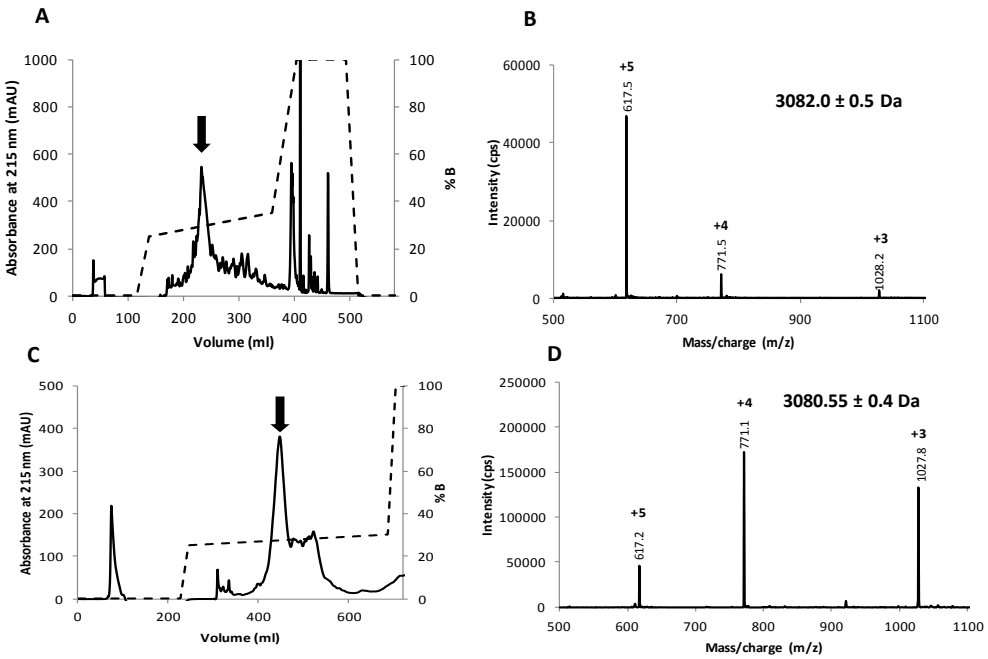

Figure 2.3. Purification of ANP

A- ANP was synthesized by F-moc based manual SPPS and purified by RP-HPLC. Crude mixture of reduced peptides were separated on Jupiter C18column (5µm, 300 Å, 250 X 21.2 mm) using 0.1% TFA as buffer A and 0.1% TFA with 80% Acn as buffer B. A linear gradient 20- 30% B was used to obtain the purified peptide. Arrow indicates the peptide peak of interest. **B**- Mass of the peptide indicated in panel A was determined by ESI-ion trap mass spectrometer. The reconstructed mass spectrum indicated a protein of mass 3082.0 ± 0.5 Da, which corresponded to reduced mass of ANP. **C**- Purified ANP was folded in 100 mM Tris-HCl pH8 containing 10% Acn for 24 h. This folding mixture was purified by RP-HPLC using Jupiter C18 column (5µm, 300 Å, 250 X21.2 mm) using a linear gradient of 20- 30% B (0.1% TFA as buffer A and 0.1% TFA with 80% Acn as buffer B). Arrow indicates the peptide peak of interest. **D**- Mass of the peptide indicated in panel C was determined by ESI-ion trap mass spectrometer. The reconstructed mass spectrum indicated a protein of mass 3080.6 ± 0.4 Da, which was 2 Da lesser than the mass of ANP before folding, suggesting the formation of disulphide linkage.

2.3.4 Ability of KNP and ANP to relax pre-contracted aortic strip

ANP and KNP induced vasorelaxation in the pre-contracted rat aortic strips (Figure 2.4). ANP induced a dose-dependent vasorelaxation with an EC_{50} of 16.3 ± 5.4 nM was comparable to EC_{50} values reported in the literature (Fiscus *et al.*, 1985). KNP also induced a dose-dependent vasorelaxation, but with ~13-fold lower potency (EC_{50} 230.6 ± 37.2 nM) (Figure 2.4 B). ANP caused a quick vasodilatory response at ≥ 10 nM, while KNP induced slow relaxation for all the concentrations tested (Figure 2.4 A). We also examined the effects of KNP on vasorelaxation in endothelium-denuded aortic strips. ANP induced equipotent vasorelaxation with an EC_{50} of 23.4 ± 7.8 nM, as NPRs are expressed in both endothelium as well as vascular smooth muscle (Lowe *et al.*, 1989). Interestingly, the activity of KNP was significantly (P-value: 0.0043) reduced when endothelium was denuded (Figure 2.4 C). Thus, KNP mediates endothelium-dependent vasodilatory response, which is not NPR NPR-dependent. These results suggest that KNP induces vasodilation through a different mechanism.

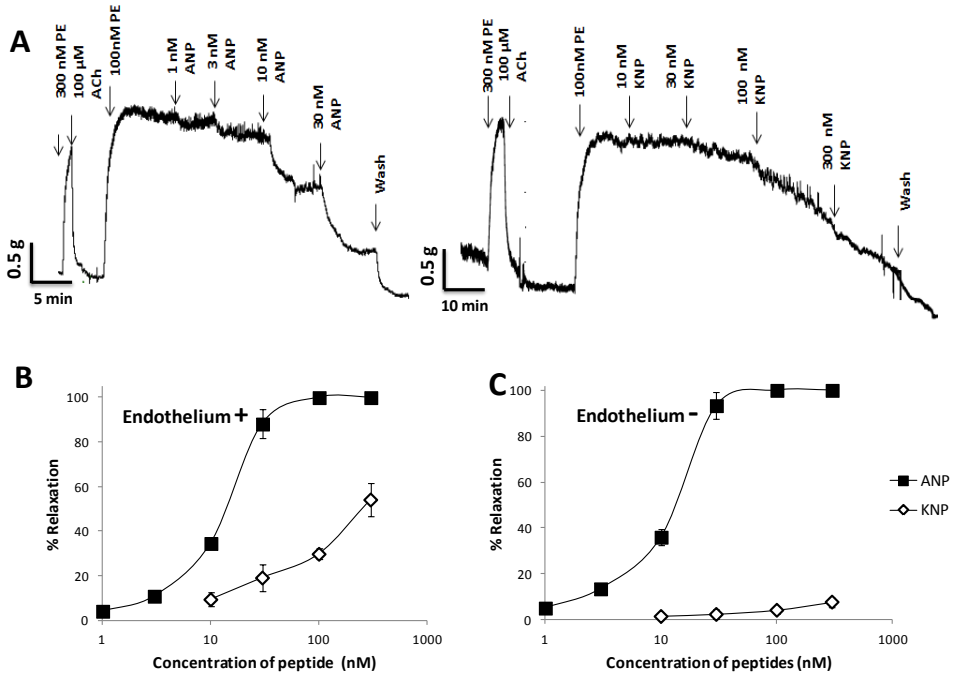

Figure 2.4. KNP mediates endothelium dependent vasorelaxation

A- Data Acquisition of aortic strip relaxation- Thoracic aorta was isolated from 10 weeks old SD rats and cut into 2-3 mm rings which were mounted at 2 g tension resting tension in an organ bath. The tissue was equilibrated for an hour following which the viability of the tissue was assessed by pre-contracting it with 300 nM PE and relaxation in response to 10 µM Ach was indicative of presence of endothelium. The tissue was washed and allowed to rest before pre-contracting it again with 100 nM PE. A cumulative dose response of ANP (left) and KNP (right) are shown as a representation. Each peptide was tested on three independent aortic strips. **B**- Cumulative dose response of ANP and KNP on pre-contracted aortic strip with intact endothelium: Aortic rings were pre-contracted with 100 nM PE. After the stabilization of response to PE, cumulative dose response is assessed. The tissue is incubated with each concentration for 10 min before the additive dosage was given. The data are represented as mean ± SEM and the P-value is 0.005.**C**- Cumulative dose response of ANP and KNP in pre-contracted aortic strip with denuded endothelium: The inner lining of the aortic strip was rubbed with cotton bud to remove endothelium. The absence of endothelium was check with the response to 10 µM Ach after the pre-contraction with 300 nM PE. Tissues which showed no response to Ach were used to assess the dose response. Data represented as mean ± SEM and the P-value is 0.004.

2.3.5 Effect of KNP and ANP on mean arterial pressure (MAP), pulse pressure (PP), heart rate and urine output

We examined the effects of KNP on blood pressure, heart rate and urine output in experimental animals (Figure 2.5). ANP and KNP were intravenously infused into two groups of anesthetized rats for 10 min. The baseline MAP of the animals used were 114.5 ± 2.4 mmHg. In comparison to control animals (0.2% BSA saline infused n = 5) infusion of ANP (0.2 nmol/kg/min in 0.2% BSA saline n = 5) induced 6.5 ± 0.9 mmHg drop in MAP at the end of the infusion period which dropped reaching 8.5 ± 0.5 mmHg during the first 10 min recovery. By the end of 30 min the MAP was restored to the baseline. A 10-fold higher dosage was chosen for KNP based on the difference in activity on the aortic strip. KNP (2 nmol/kg/min in 0.2% BSA saline n = 5) showed a similar reduction in MAP at the end of the infusion period (6.1 ± 3 mmHg) (Figure 2.6 A). MAP continued to drop further reaching a difference of 11.9 ± 1.9 mmHg after the second recovery period. Although the MAP of animals infused with KNP started recovering, it did not recover back to the baseline within the experimental recovery period (40 min); at the end of 40 min, MAP was 10 ± 3 mmHg below the baseline (Figure 2.6 A). Thus, KNP induced a sustained drop in MAP compared to ANP.

ANP caused a steep drop in pulse pressure (PP), calculated as the difference of systolic BP and diastolic BP (Baseline PP: 47.4 ± 2.4 mmHg), by 7.2 ± 0.9 mmHg during infusion. PP began to restore back to baseline by the end of the experiment (Figure 2.6 B). In the case of KNP, although there was a milder drop in PP (3.7 ± 1 mmHg), it did not restore back during recovery period. PP

is dependent on stroke volume and compliance of arteries. ANP is shown to reduce venous return of blood to the heart, which decreases stroke volume (Sasaki *et al.*, 1985). In the case of KNP, change in systolic BP was comparable to ANP, while decrease in diastolic BP was more profound (ANP: 6.5 ± 1 mm Hg, KNP: 11.1 ± 1.8 mmHg). Due to similar differences in systolic and diastolic BP, the net PP was not greatly altered for KNP (Figure 2.7).

Baseline heart rates of the animals were 371.9 ± 10.9 BPM. When ANP was infused, the heart rate was reduced by 39.9 ± 23.6 BPM during infusion which further dropped to a difference of 58.1 ± 19 BPM within the first recovery period (Figure 2.6 C)(Kubo *et al.*, 1990; Shapiro *et al.*, 1986). The reduced heart rate recovered back to baseline within the next 30 min. In the case of animals infused with KNP, the reduction in heart rate was not as profound (10.6 ± 21 BPM). But during the recovery period, heart rate persistently dropped reaching a difference of 42.1 ± 16 BPM at the end of experimental period (Figure 2.6 C).

In the same experimental animals, urine was collected throughout the experimental period by bladder catheterization. The baseline urine flow rate was 3.7 ± 0.5 µl/min. ANP showed marked diuresis with an increased flow rate of 8.8 ± 1.4 µl/min. The urine flow rate returned back to baseline within 20 min of recovery. Similar changes in renal output were observed previously

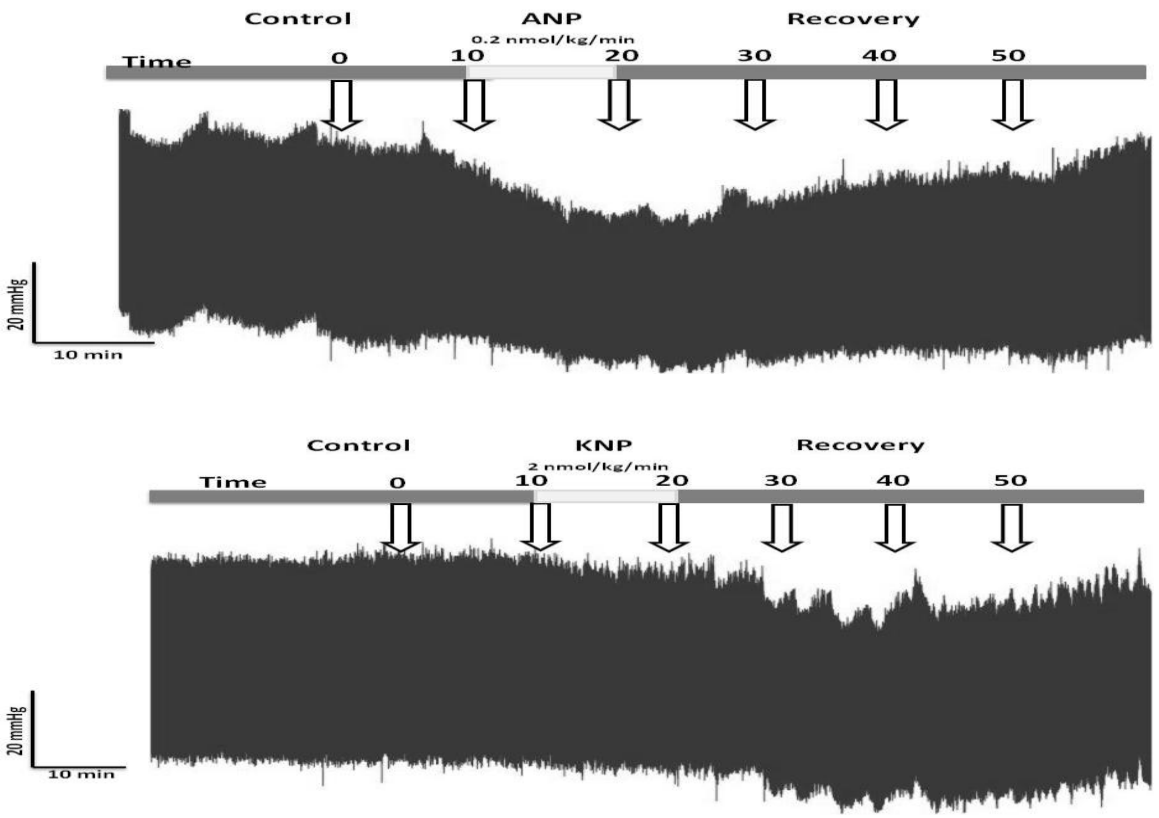

Figure 2.5. Data acquisition for blood pressure measurement

Femoral vein and artery, urinary blabber catheterization was performed for rats anesthetized with sodium pentobarbital. A fluid- filled pressure transducer was inserted into femoral artery and infusion saline/ peptide was given through a syringe pump at a constant flow rate of 2 ml/h through femoral vein. Urine was collected over a period of 10 min. After the completion of surgery the animals were equilibrated for 20 min and the end of which the time is assumed to be t = 0. Following a control period of 10 min, ANP (0.2 nmol/kg/min) or KNP (2 nmol/kg/min) was infused for 10 min. Subsequently, the animals were let to recover for 40 min. During control and recovery periods, 0.2% BSA saline was infused. Blood pressure/ heart rate/ urine flow rate value at t = 0 was assumed as baseline. Average values over a time period of 10 min is used for calculation. (ANP: n = 5, KNP: n = 5)

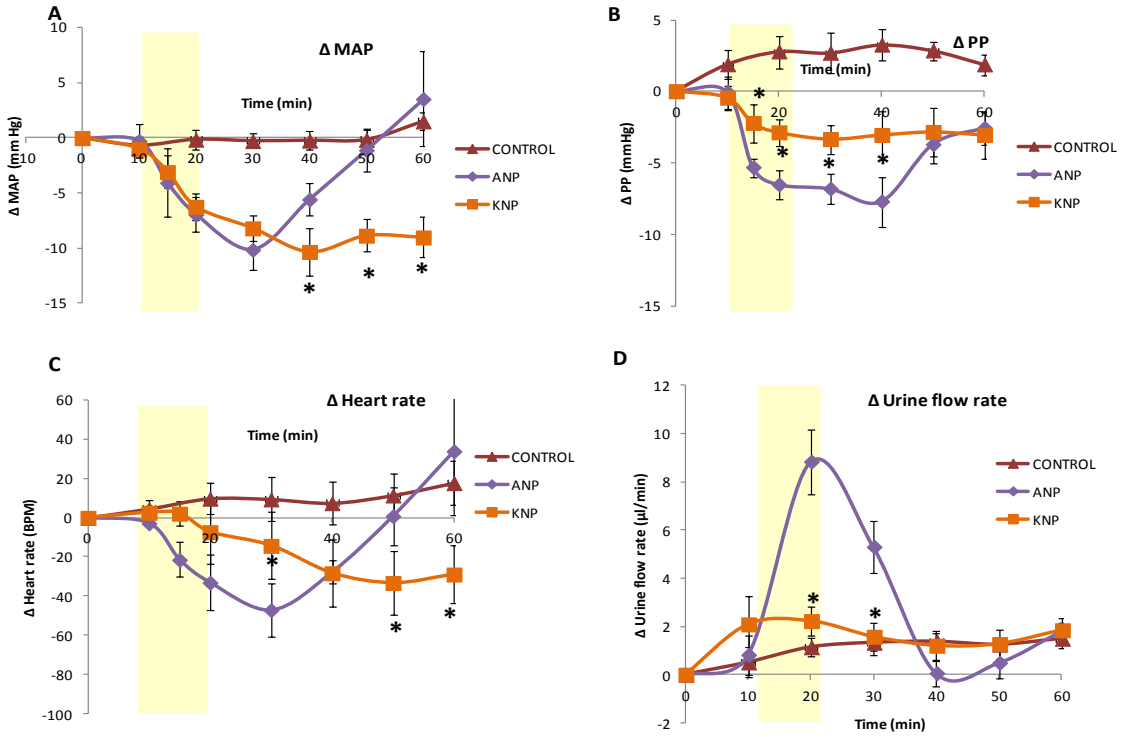

Figure 2.6. KNP causes a prolonged reduction in MAP, PP and heart rate with no renal effects

A: Mean arterial pressure (MAP) was calculated as (⅓ systolic pressure + ⅔ diastolic pressure). Change in MAP with reference to the baseline was plotted against time. **B**: Pulse pressure (PP) was calculated as difference between systolic and diastolic pressure. Change in PP with reference to the baseline was plotted against time. **C**: Heart rate (HR) was calculated as number of beats per minute. Change in HR with reference to baseline was plotted against time. **D**: Urine output was represented as volume of urine collected per minute. Change in urine flow rate with reference to the baseline was plotted against time. Each group of peptide and control were tested on five independent animals and the data are represented as mean ± SEM. Statistical analysis between ANP and KNP were performed using one way student t-test and the data points which were significantly different (P-value < 0.05) are represented using *.

(Frolov *et al.*, 1989). In contrast, the infusion of KNP showed only a minor increase in urine flow rate (2 ± 1.2 µl/min) which was sustained all throughout the experimental period (Figure 2.6 D).

These results indicate that KNP influences blood pressure, heart rate and renal output differently than ANP and further supports on contention that KNP exerts its biological effects through a distinct mechanism.

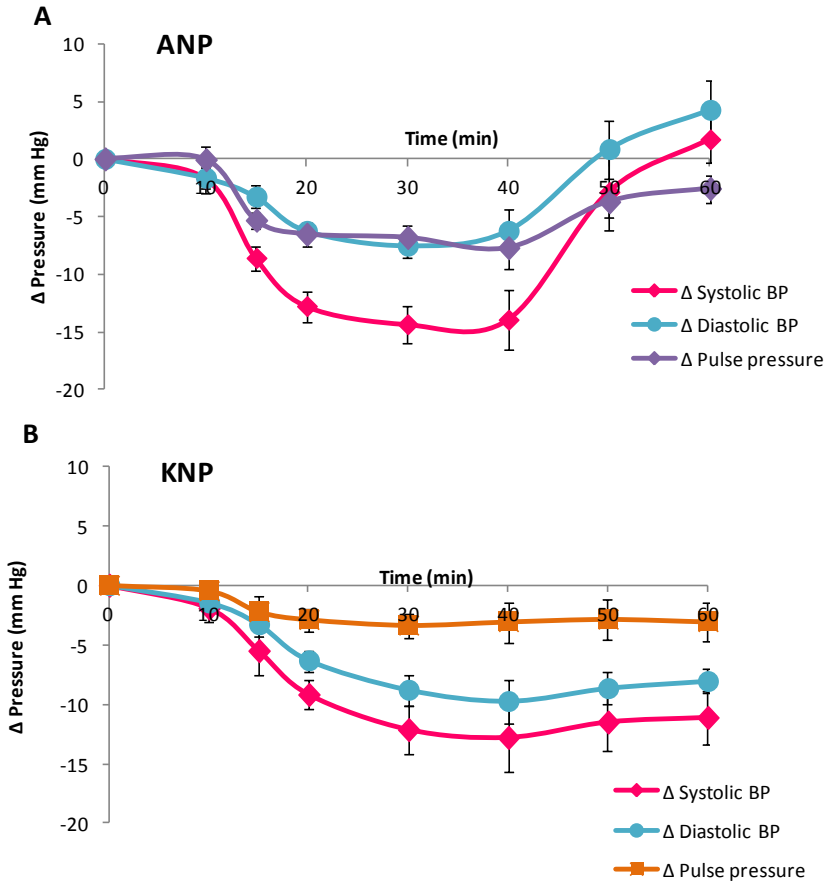

Figure 2.7. KNP causes a profound change in diastolic pressure
Change in systolic, diastolic and PP with reference to baseline was plotted against time for animals infused with **A**- ANP (n = 5) and **B**- KNP (n = 5). Data are represented as mean ± SEM.

2.3.6. Design and Synthesis of KNP mutants

To understand the structure-function relationships and the role of distinct regions in KNP, we designed several truncated and deletion mutants (Figure 2.8). We designed two fragments of KNP, C-terminal α-helix (Helix, residues 35-60) and the entire KNP without this α-helix (ΔHelix, residues 1-34). We also designed a conserved 17-membered ring with two C-terminal residues (Ring, residues 1-24) to help understand the bioactivity of the NP ring and a fusion of the ring with helix (R&H fusion of residues1-22 with residues 39-60). Ring and Helix were manually synthesized by SPPS, while ΔHelix and R&H were cloned from the full length KNP and heterologously expressed and purified. The masses of Ring, Helix, ΔHelix and R&H peptides assessed using ESI–MS matched the theoretical masses (Table 2.1).

Table 2.1. List of observed and theoretical mass of KNP deletion mutants

Construct	Observed mass (Da)	Theoretical mass (Da)
KNP	6602.3 ± 0.9	6602.5*
ANP	3080.6 ± 0.4	3080.2*
Ring	2768.7 ± 0.7	2769.1*
Helix	2765.1 ± 1.0	2765.7
ΔHelix	3855.6 ± 1.2	3855.8*
R&H	5052.5 ± 0.6	5052.4*

*Oxidized mass of the peptides are indicated by **

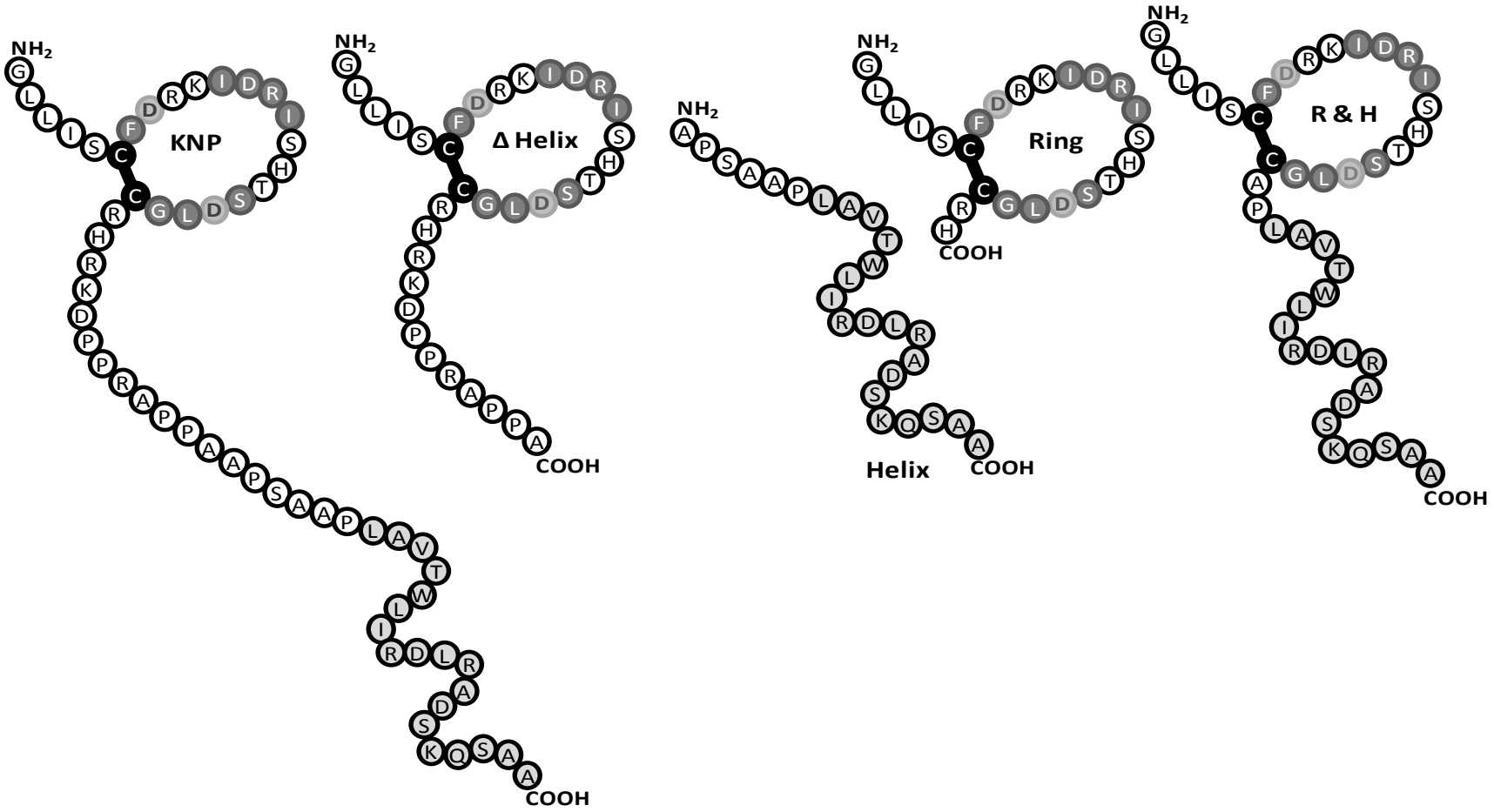

Figure 2.8. Schematic representations of KNP and its deletion mutants

The deletion mutants of KNP were designed based on the predicted structure and the processing sites of KNP.
Δ Helix: Last 26 residues of KNP which had the putative helical segment was deleted to mimic other known elapid NPs
Helix: Last 26 residues of the C-terminal tail of KNP
Ring: Ring of KNP with 2 residue tail was designed to mimic mammalian NPs
R&H: Ring was fused with putative helical segment

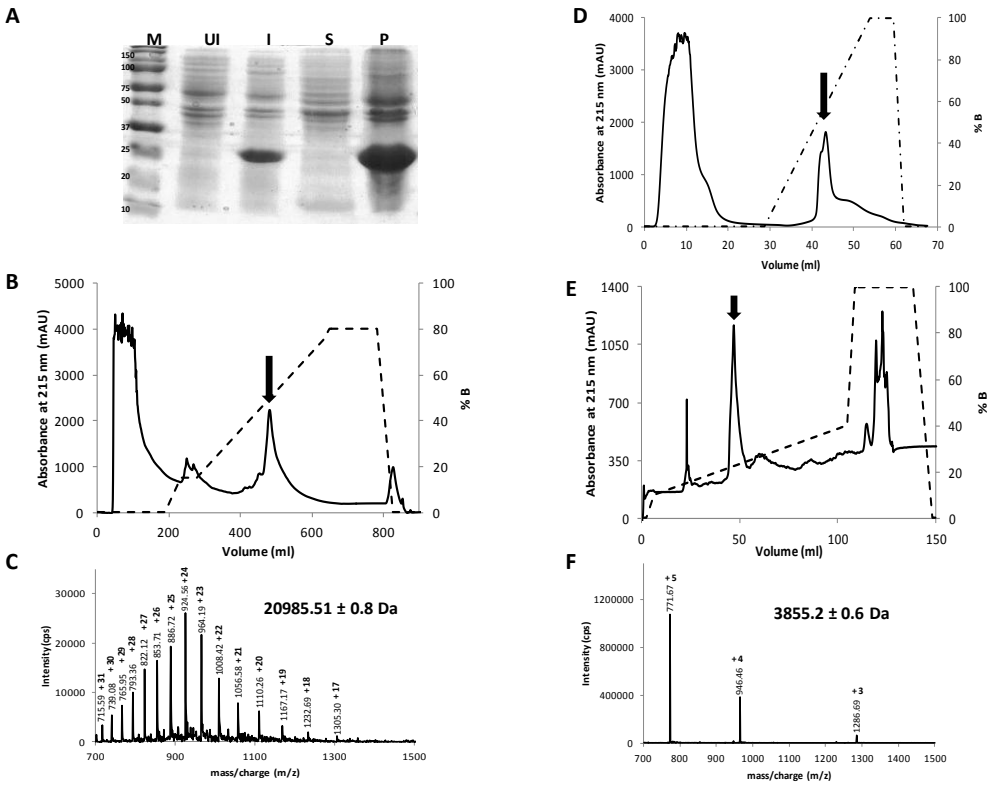

Figure 2.9. Heterologous expression and purification of ΔHelix

A: A 15 % SDS-PAGE analysis shows the expression of trx-ΔHelix fusion protein in insoluble fraction. M- Precision Plus protein™ Dual color standard, UI- Uninduced *E. coli* whole cell lysate, I- Induced *E. coli* whole cell lysate, S- Supernatant containing soluble protein after cell lysis, P- Pellet containing insoluble proteins. **B**: The trx-fusion protein was purified by reversed-phase high performance liquid chromatography using 0.05% formic acid (FA) as buffer-A and 100% Acn with 0.05% FA as buffer-B. The separation was performed on Jupiter C18 column (5µm, 300 Å 250 X 21.2 mm) with a linear gradient of 40- 70% B. The arrow indicates the protein of interest. **C**: Mass of the protein peak indicated by the arrow in panel B was determined by ESI Ion-Trap mass spectrometry. Peaks obtained were reconstructed to obtain a mass of 20985.51 ± 0.8 Da which corresponded to the mass of trx- ΔHelix fusion protein. Pure fractions of the protein were freeze dried. **D**: The freeze dried fusion protein was dissolved in 50 mM Tris-HCl, 6 M urea pH 8 buffer. This protein was desalted with 50 mM Tris-HCl pH 8. TEV protease cleavage reaction was set with protein obtained at a ratio 1:40 (TEV: protein) at 4°C for 16-20 h. Cleaved protein, tag and uncut fusion protein were separated using cation exchange chromatography using 50 mM Tris-HCl pH 8 as buffer-A and 50 mM Tris-HCl, 500 mM NaCl pH 8 as buffer-B. The chromatographic separation was performed using Hi-Trap-Sulfopropyl (SP)-Sepharose column (34 µm, 16 X 25 mm) with a linear gradient of 0-100% B. The arrow indicates the protein peak which was subsequently purified. **E**: Peak indicated in panel D was run on RP-HPLC using Jupiter C18 column (5 µm, 300 Å ,250 X 10 mm) with 0.05% FA as buffer-A and 100% Acn with 0.05% FA as buffer-B on a linear gradient of 15- 50% B. Arrow indicates is the protein of interest. **F**: Mass of the protein indicated from panel E was determined by ESI-ion trap mass spectrometer. The reconstructed mass of the mass spectrum indicated a protein of mass 3855.6 ± 1.2 Da, which corresponded to the calculated mass of oxidized Δ Helix.

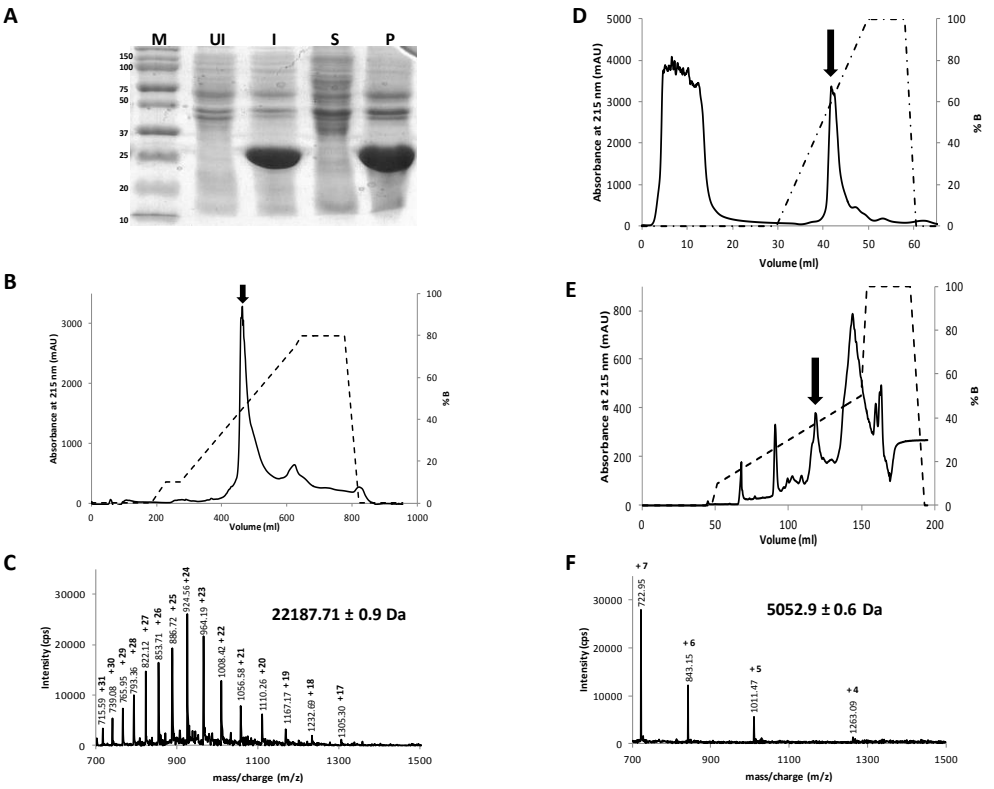

Figure 2.10. Heterologous expression and purification of R&H

A: A 15 % SDS-PAGE analysis shows the expression of trx-R&H fusion protein in insoluble fraction. M- Precision Plus protein^{TM} Dual color standard, UI- Uninduced *E. coli* whole cell lysate, I- Induced *E. coli* whole cell lysate, S- Supernatant containing soluble protein after cell lysis, P- Pellet containing insoluble proteins. **B**: The trx-fusion protein was purified by reversed-phase high performance liquid chromatography using 0.05% formic acid (FA) as buffer-A and 100% Acn with 0.05% FA as buffer-B. The separation was performed on Jupiter C18 column (5µm, 300 Å 250 X 21.2 mm) with a linear gradient of 40- 70% B. The arrow indicates the protein of interest. **C**: Mass of the protein peak indicated by the arrow in panel B was determined by ESI Ion-Trap mass spectrometry. Peaks obtained were reconstructed to obtain a mass of 22187.7 ± 0.9 Da which corresponded to the mass of trx-R&H fusion protein. Pure fractions of the protein were freeze dried. **D**: The freeze dried fusion protein was dissolved in 50 mM Tris-HCl, 6 M urea pH 8 buffer. This protein was desalted with 50 mM Tris-HCl pH 8. TEV protease cleavage reaction was set with protein obtained at a ratio 1:40 (TEV: protein) at 4°C for 16-20 h. Cleaved protein, tag and uncut fusion protein were separated using cation exchange chromatography using 50 mM Tris-HCl pH 8 as buffer-A and 50 mM Tris-HCl, 500 mM NaCl pH 8 as buffer-B. The chromatographic separation was performed using Hi-Trap-Sulfopropyl (SP)-Sepharose column (34 µm, 16 X 25 mm) with a linear gradient of 0-100% B. The arrow indicates the protein peak which was subsequently purified. **E**: Peak indicated in panel D was run on RP-HPLC using Jupiter C18 column (5 µm, 300 Å ,250 X 10 mm) with 0.05% FA as buffer-A and 100% Acn with 0.05% FA as buffer-B on a linear gradient of 15- 50% B. Arrow indicates is the protein of interest. **F**: Mass of the protein indicated from panel E was determined by ESI-ion trap mass spectrometer. The reconstructed mass of the mass spectrum indicated a protein of mass 5052.9 ± 0.6 Da, which corresponded to the calculated mass of oxidized R&H.

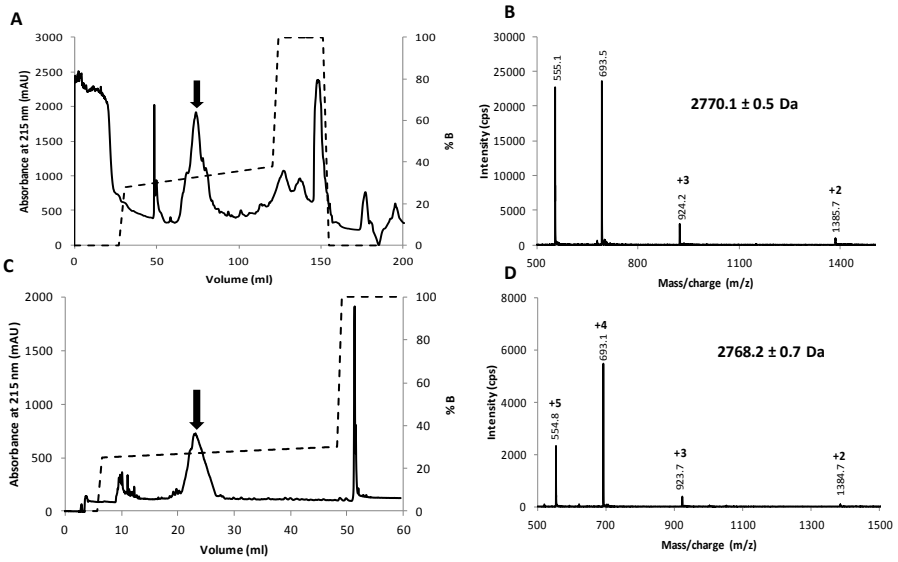

Figure 2.11. Purification and oxidation of Ring

A- Ring was synthesized by F-moc based manual SPPS and purified by RP-HPLC. Crude mixture of reduced peptides were separated on Jupiter C18column (5µm, 300 Å, 250 X 21.2 mm) using 0.1% TFA as buffer A and 0.1% TFA with 80% Acn as buffer B. A linear gradient 20- 30% B was used to obtain the purified peptide. Arrow indicates the peptide peak of interest. **B**- Mass of the peptide indicated in panel A was determined by ESI-ion trap mass spectrometer. The reconstructed mass spectrum indicated a protein of mass 2770.1 ± 0.5 Da, which corresponded to reduced mass of Ring. **C**- Purified Ring was folded in 100 mM Tris-HCl pH8 containing 10% Acn for 24 h. This folding mixture was purified by RP-HPLC using Jupiter C18 column (5µm, 300 Å, 250 X21.2 mm) using a linear gradient of 20- 30% B (0.1% TFA as buffer A and 0.1% TFA with 80% Acn as buffer B). Arrow indicates the peptide peak of interest. **D**- Mass of the peptide indicated in panel C was determined by ESI-ion trap mass spectrometer. The reconstructed mass spectrum indicated a protein of mass 2768.2 ± 0.7 Da, which was 2 Da lesser than the mass of Ring before folding, suggesting the formation of disulphide linkage

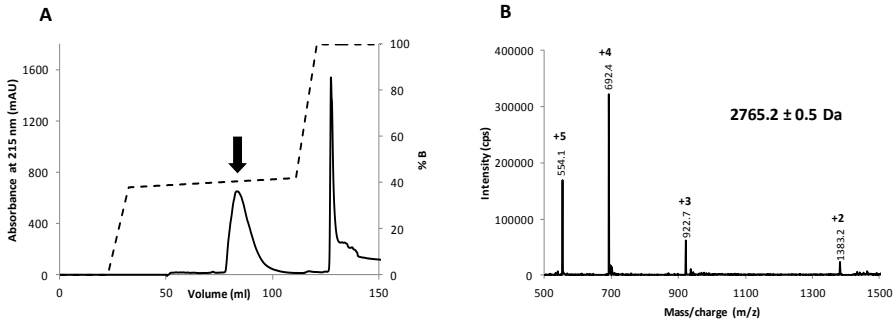

Figure 2.12. Purification of Helix

A- Helix was synthesized by F-moc based manual SPPS and purified by RP-HPLC. Crude mixture of peptides were separated on Jupiter C18 column (5µm, 300 Å, 250 X 10 mm) using 0.1% TFA as buffer A and 0.1% TFA with 80% Acn as buffer B. A linear gradient 20- 40% B was used to obtain the purified peptide. Arrow indicates the position of elution of Helix. **B**- Mass of the protein indicated in panel A was determined by ESI-ion trap mass spectrometer. The reconstructed indicated a protein of mass 2765.2 ± 0.5 Da, which corresponded to calculated mass of Helix.

2.3.7. Vasodilatory properties of KNP deletion mutants

The truncated segments of KNP were assessed for their ability to relax pre-contracted aortic strip (Figure 2.13). The EC_{50} values of the different mutants are listed in table 2.2. The Ring evoked equipotent relaxation in aortic strips with and without endothelium (P-value: 0.33 no significant difference). Although Ring's ability to relax was equivalent to full length KNP (P-value: 0.25 no significant difference), it elicited an endothelium independent relaxation similar to a classical NP.

Table 2.2. EC50 of ANP, KNP and KNP mutants for inducing vasorelaxation

Construct	EC_{50} (nM) ± SEM	
	Endothelium +	Endothelium -
ANP	16.3 ± 5.4	23.4 ± 7.8
KNP	230.6 ± 37.2	-
Ring	228.6 ± 43.1	279.5 ± 47.2
Helix	326.7 ± 64.3	-
R&H	267.13 ± 45.7	-
ΔHelix	> 1000	> 1000

ΔHelix with the putative helical segment deleted had much lowered potency to induce relaxation compared to KNP (P-value: 0.0002), but it showed equivalent response in both the population of aortic strips. Helix and R&H showed vasorelaxation ability in strips with endothelium with equivalent potency as KNP (P-value: 0.25) which was significantly reduced on removing endothelium (P-value of helix with and without endothelium: 0.015, P-value R&H of with and without endothelium: 0.02). These results suggest that C-terminal putative helix forming region of KNP contributes to its entire activity, despite the presence of a functional ring. The putative helical segment seems

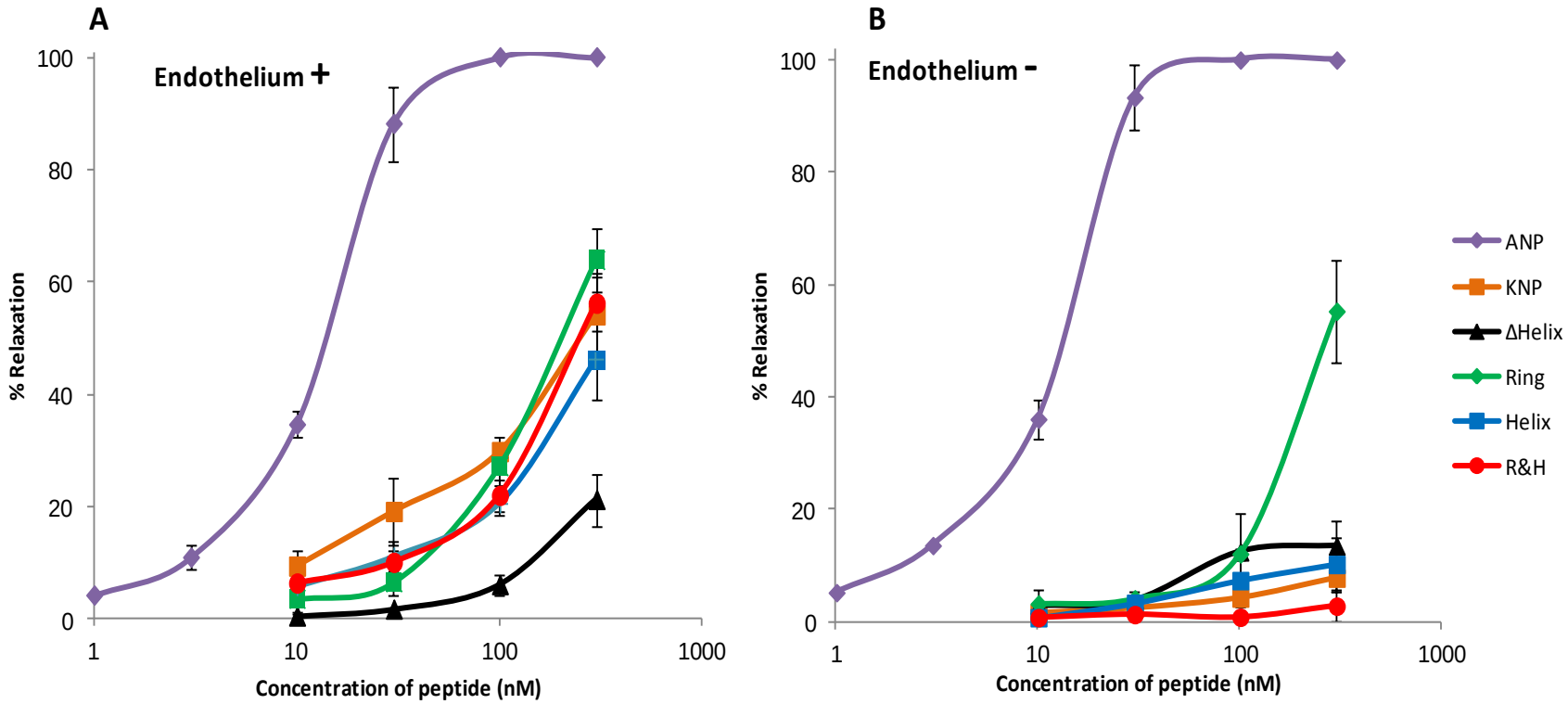

Figure 2.13. Helix mediates the vasodilatory effects of KNP

A- Cumulative dose response of KNP deletion mutants in endothelium intact aortic strips- Aortic strip was pre-contracted with 100 nM PE and the dose response of different peptides have been evaluated. **B-** Cumulative dose response of KNP deletion mutants in endothelium denuded aortic strips- strip was pre-contracted with 100 nM PE and the dose response of different peptides have been evaluated.
Every data point is an average of three independent trials for each concentration of the peptide and is represented as mean ± SEM. Statistical analysis was performed between the dose-response curve using one-way ANOVA.

to redirect the ring of KNP away from NPR, which is evidently shown by the modulated activity of KNP and R&H in the presence and absence of endothelium.

2.3.8. Activation of NPR-A and NPR-B by KNP and its mutants

To understand the ability of the KNP and its mutants to activate NPR-A and NPR-B, cells endogenous lacking these receptors (CHO-K1) were transfected with plasmids encoding rat NPR-A and NPR-B separately. The abilities of KNP and its deletion mutants to induce signal transduction and evoke cGMP response in these cells were measured and compared with those of ANP on NPR-A and CNP on NPR-B.

On cells expressing NPR-A, ANP evoked a dose-dependent cGMP response (Figure 2.14 A). Ring elicited a 10-fold less potency compared to ANP. Interestingly, C-terminal extensions in KNP, ΔHelix and R&H led to further loss in cGMP response. Helix did not cause any elevation of cGMP indicating that it does not interact with NPR-A. These observations were in agreement to the vasodilatory properties of these peptides.

On cells expressing NPR-B, CNP evoked highly potent cGMP response. However, as expected because of the presence of C-terminal residues, KNP and its deletion mutants were not able to evoke any cGMP response in cells expressing NPR-B (Figure 2.14 B).

These results show that Ring is a specific ligand to NPR-A, but with a lower potency compared to ANP and the presence of the C-terminal tail redirects the ring away from NPR-A.

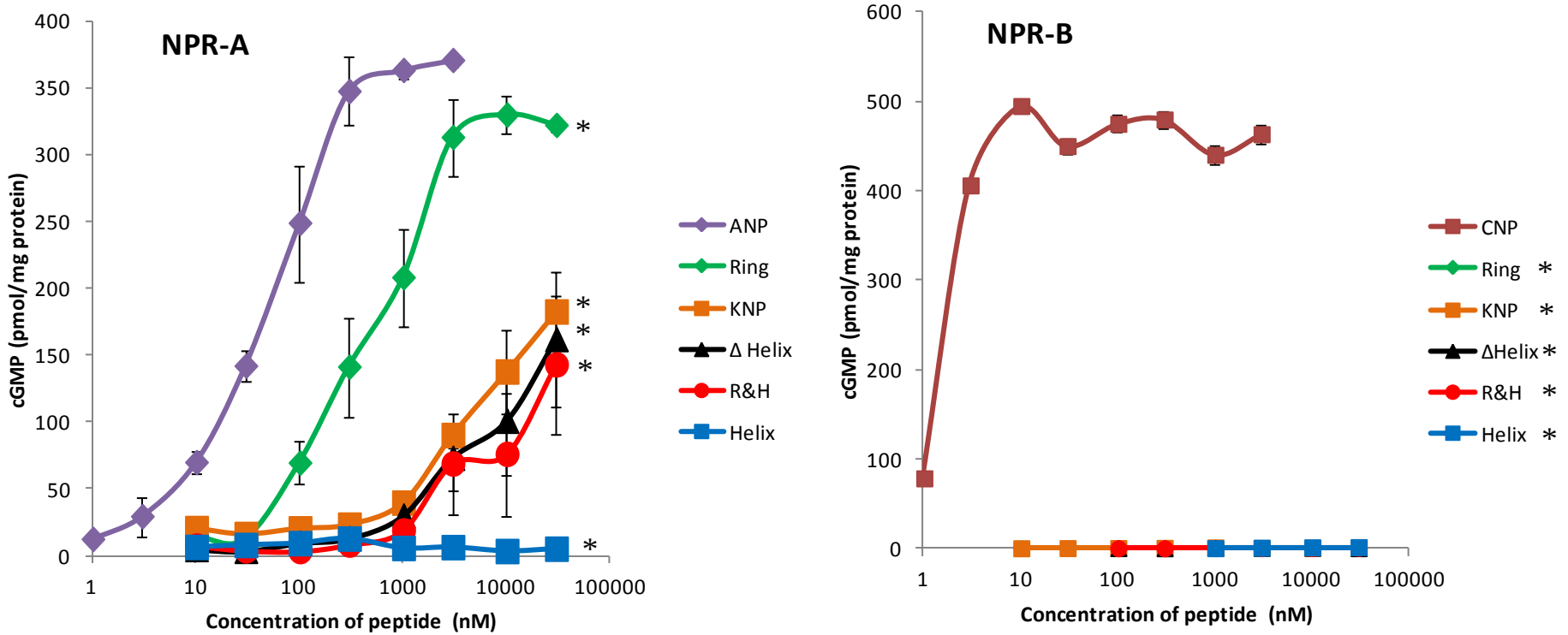

Figure 2.14. C-terminal tail of KNP redirects the ring away from NPR

A- Dose dependent cGMP response of ANP, Ring, KNP, Δ Helix, R&H, Helix were evaluated on CHO-K1 cells transfected with plasmid encoding NPR-A. **B**- Dose dependent cGMP response of CNP, Ring, KNP, Δ Helix, R&H, Helix were evaluated on CHO-K1 cells transfected with plasmid encoding NPR-B. Data points of 3 independent trials have been plotted as mean ±SEM. Statistically analysis has been performed using one-way ANOVA using one way t-test for comparing the different dose response curves with ANP or CNP. * represents curves with a P-value < 0.01

2.3.9. Downstream activators of KNP signaling

As KNP and Helix require endothelium to function, we examined the role of various intermediates involved in endothelium-mediated vasorelaxation. Endothelial cells respond to different vasoactive factors by synthesizing nitric oxide (NO), prostacyclins and factor that stimulate hyperpolarization of smooth muscle (Mitchell *et al.*, 2008) (Figure 2.15 A). These factors diffuse from endothelium to the vascular smooth muscle to arouse cGMP/cAMP levels to mediate vasorelaxation (Ignarro, 1989). In a NPR mediated signaling, the cGMP is aroused by the GC domain linked to the receptor. Hence, the above mentioned vasoactive factors have negligible role in NP-NPR-signaling. Therefore, we used specific inhibitors namely L-NAME for Nitric oxide synthase (NOS), indomethacin for cycloxgenase 1 and 2 (COX), ODQ for soluble guanylyl cyclase (sGC) and KCl-induced pre-contraction to subdue the hyperpolarization process (Figure 2.15 A), to investigate the role of the endothelium-derived vasoactive factors in KNP signaling.

ANP's ability to relax the pre-contracted aortic strip was unmodulated in the presence of any of the inhibitors (Figure 2.15 B). With KCl-pre-contracted strips there was a slight decrease in the activity. Similar to ANP, Ring also had no influence of L-NAME, ODQ and indomethacin on its activity, but lost about 30% of its activity which pre-contracted with KCl. Thus, Ring acts similar to classical NPs and does not require any endothelial factors to cause vasodilation. A NPR-mediated vasodilation involves cGMP-dependent activation PKG which phosphorylates (a) myosin light chain and (b) opens big conductance potassium channel leading to hyperpolarization (Alioua *et al.*,

1998). These two processes cause the smooth muscle relaxation. Thus, the activity of ANP and Ring are lowered when KCl was used for pre-contraction.

KNP's activity was completely abrogated in the presence of L-NAME. NO either activates COX or diffuses to vascular smooth muscle and activates soluble guanylyl cyclase (sGC) (Stankevicius *et al.*, 2003) (Figure 2.15 A). The inhibition of COX-1 and COX-2 by indomethacin and that of sGC by ODQ leads to 60% and 90% loss of KNP's activity, respectively. Similarly, inhibition by L-NAME and ODQ completely abolished the ability of Helix to cause vasodilation, while COX inhibition by indomethacin resulted in 70% reduction in its activity. These results indicate that NO plays a key role in KNP-induced vasorelaxation. KNP evoked 25% relaxation in KCl-contracted aortic strips; this is 50% lower when compared to PE-contracted strips. Helix failed to evoke relaxation of KCl-contracted aortic strip. These results can be explained in two alternate ways: (a) hyperpolarization plays an important role in KNP signaling, but not in Helix signaling; and (b) high salt concentration breaks the interaction of Helix with its receptor. The second possibility is supported by high density of positively (4) and negatively (2) residues in 26 residues. In this scenario, high salt would also interfere with binding of C-terminal helix to its receptor and the observed partial activity could be due to the binding of the KNP ring. However, further studies are required to clarify the role of hyperpolarization.

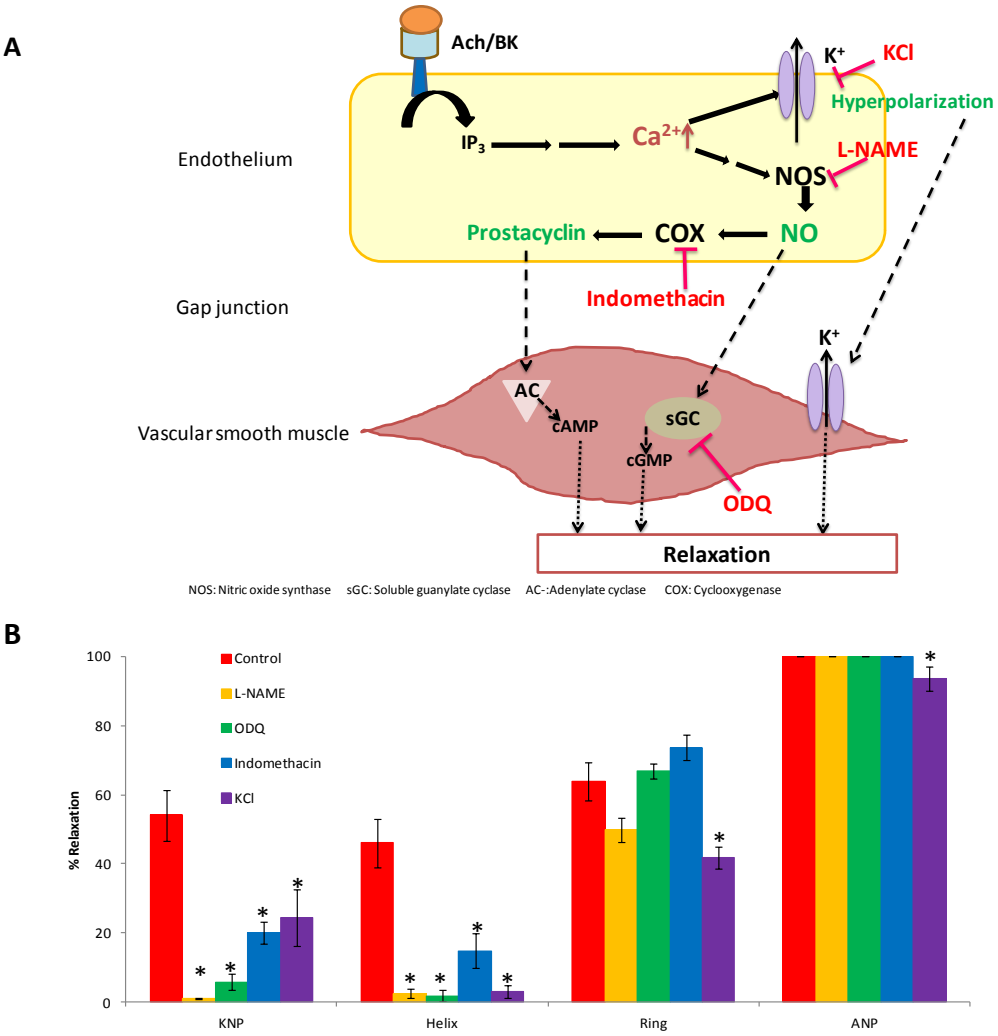

Figure 2.15. KNP requires NO, prostacyclin and hyperpolarization factor for vasodilation

A- Schematic representation of endothelium dependent vasorelaxation pathway
In response to agonist s such as Acetylchloline/ Bradykinin, receptor mediated activation of Phospholipase C produces IP3 and DAG as secondary messengers. IP3 causes the intracellular Ca^{2+} to increase which through certain downstream targets activates nitric oxise synthase (NOS). Intracellular Ca^{2+} increase opens Ca^{2+}activated K^{+} channels to cause hyperpolarization. Activation of NOS, stimulates production of nitric oxide (NO).Subsequently, NO binds to heme-core of cycloxygenase (COX) and diffuses to smooth muscle to activate soluble guanylyl cyclase (sGC) thereby increasing cGMP. COX produces prostacyclins, which diffuses to smooth muscle to elevate cAMP levels. K+ ions from the endothelium cells open the K+ channels of smooth muscle, thus causing hyperpolarization. NO, Prostacyclin and Hyperpolarization factors are common intermediates identified in endothelium dependent vasodilation (Sautebin *et al.*, 1995), (Busse *et al.*, 2002) **B**- Role of nitric oxide, prostacyclin and hyperpolarization factor in mediating KNP mediated vasorelaxation. The indicated inhibitors (L-NAME: 100 µM, Indomethacin: 10 µM, ODQ: 20 µM) were incubated with aortic strip for 20 min prior to pre-contraction. Subsequently, the tissue was pre-contracted with 100 nM PE and the response of 300 nM of the peptides was tested. KCl (40 mM) was used for pre-contraction of the tissue and the response for 300 nM of ANP/KNP/ Ring/ Helix was recorded. Each data point is an average of three independent trials and is represented as mean ± SEM. The statistical analysis using one-tail student t-test has been performed to compare the significance of the response between control aortic strips and inhibitor treated aortic strips for each peptide. * represents the response with a P-value < 0.01.

2.3.10. In-vivo effect of KNP truncations on MAP, PP, heart rate and urine output

To understand the contribution of different pharmacophores of KNP to its in-vivo activity, Ring, ΔHelix and Helix (2 nmol/kg/min) were intravenous infused in experimental rats. Ring decreased MAP by 10.7 ± 2.5 mmHg during infusion which recovered back within the experimental period while ΔHelix and Helix caused a mild drop (4.3 ± 1.4 mmHg and 4.7 ± 1.1 mmHg) during infusion period which was sustained during the recovery period (Figure 2.16 A). Alteration in MAP profile of Ring was similar to that of ANP (P-value > 0.05; no significant difference) while the additive effect of Helix and ΔHelix seemed to reflect KNP's profile.

Ring and ΔHelix caused a meek reduction in heart rate (22.2 ± 12 BPM) which quickly returned back to baseline in case of ring while was sustained in case of ΔHelix (Figure 2.16 B). Heart rate remained unperturbed in animals infused with Helix similar to control. Although Ring and ΔHelix had lowered potencies, the overall heart rate profile of Ring matched that of ANP while ΔHelix was similar to KNP.

Ring reduced PP to similar extent as that of KNP (4.5 ± 1 mmHg) but restored within 20 min after the infusion was stopped (Figure 2.16 C). ΔHelix and Helix showed a mild decrease (2 ± 1.3 mmHg) which restored back in case of ΔHelix while sustained in case of Helix. Like the heart rate profile, Ring evoked similar changes in PP like ANP with lesser effects (at t =30, 40, 50 and 60 min, P-value < 0.05 compared to ANP) while Helix caused comparable effects to that of KNP (P-value > 0.05, no significant difference).

None of the KNP truncation had influence on urine volume like the full length molecule (Figure 2.16 D). Thus, the overall effect on hemodynamic parameters evoked by the Ring was like a classical NP while both the pharmacophores seems to contribute to KNP's function.

.

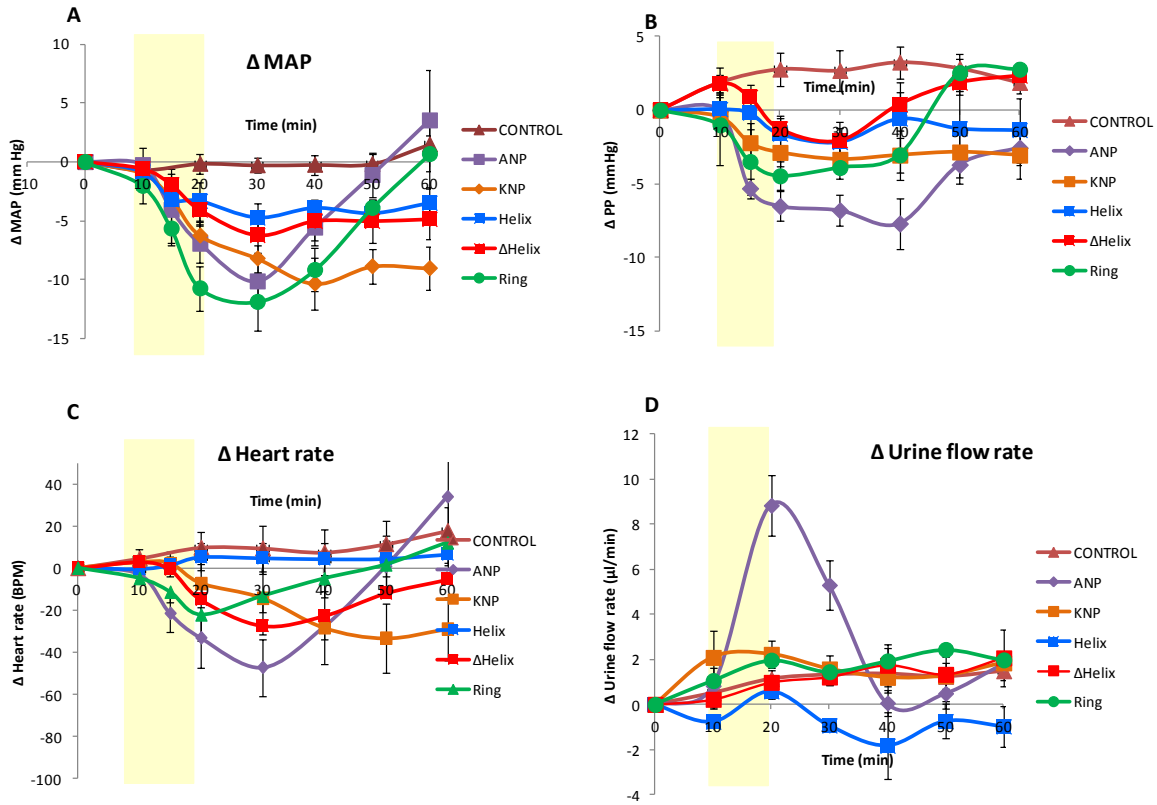

Figure 2.16. Ring reduces MAP, PP and heart rate like ANP with no renal effects while ring and helix contribute to KNP's function

A: Mean arterial pressure (MAP) was calculated as (⅓ systolic pressure + ⅔ diastolic pressure). Change in MAP with reference to baseline was plotted against time. **B**: Pulse pressure (PP) was calculated as difference between systolic and diastolic pressure. Change in PP with reference to baseline was plotted against time. **C**: Heart rate (HR) was calculated as number of beats per minute. Change in HR with reference to baseline was plotted against time. **D**: Urine output was represented as volume of urine collected per minute. Change in urine flow rate is plotted against time. Every data point is an average of five independent trials and represented as mean ± SEM. The statistically analysis for the comparison of ANP with the different KNP truncations was performed using one-way student t-test and P-value < 0.05 is considered significant.

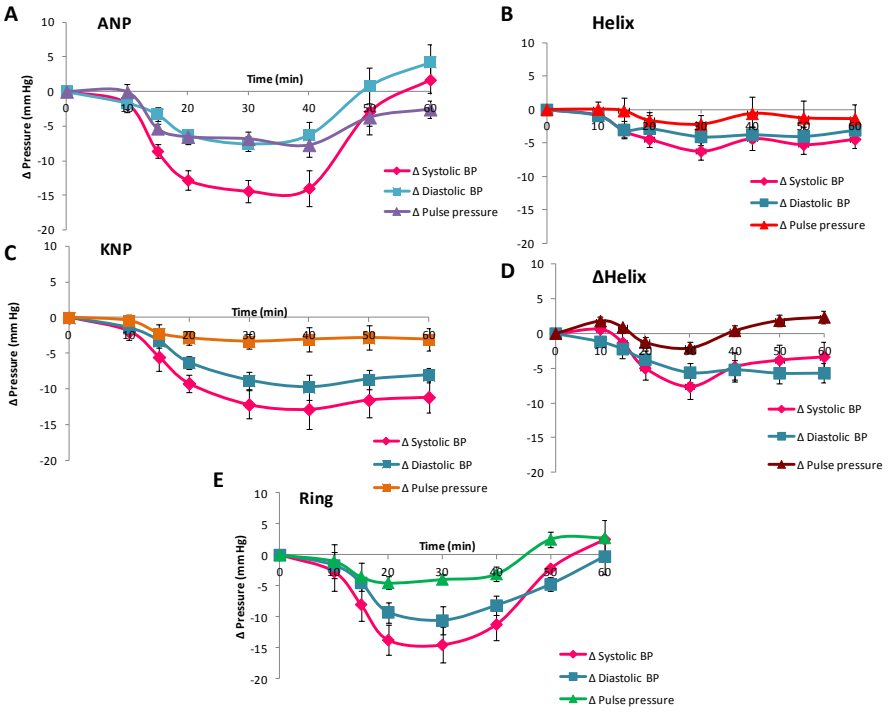

Figure 2.17. Changes in systolic and diastolic pressure induced by KNP truncations

Change in systolic, diastolic and PP with reference to baseline was plotted against time for animals infused with **A**- ANP, **B**- Helix, **C**- KNP, **D**- ΔHelix and **E**- Ring. Each peptide was tested in five independent animals. Data are represented as mean ± SEM.

2.4. Discussion

Natriuretic peptides are present in venom. Like mammalian NPs, venom NPs are synthesized as precursors and processed to their active form. These mature counterparts have the conserved 17-residue ring with variable C-terminal extensions. Despite their overall structural similarity, NPs from reptilian venom have distinct biological activity compared to mammalian NPs (Section 1.9). Though this has been attributed to subtle changes in the sequence, no previous reports on structure-activity relationship of venom NPs have been described.

This study focuses on the mode of action and structure-activity of KNP, a novel NP from *Bungarus flaviceps (Siang et al., 2010).* The precursor encoding KNP was found from the transcriptome analysis of venom gland of *B.flaviceps*, which encoded for a 147 amino acid residues long precursor with a signal peptide. The precursor was speculated to be processed at position 87 after dibasic (KK) residue by a common prehormone processing enzyme Kexin (Rockwell *et al.*, 2002), to produce the mature KNP (60 amino acid residues). Mature KNP has 5 residues in the N-terminal segment, 17-residue ring and 38 residues long C- terminal tail. This tail has no similarity to any sequence known and is predicted to have the ability to have an α-helical structure, which is not reported for any other NP. Ring of KNP has all the evolutionarily conserved residues except D residues at position 8 and 19, which are G residues in all known NPs. In ANP, F8 and R14 within the ring, N24 and R27 in the tail, are pivotal for receptor binding. KNP has F7, R13 and R26 in equivalent positions (Bovy, 1990; He *et al.*, 2001; Li *et al.*, 1995). Hence, with these structural features one may speculate, KNP with a long C-terminal tail might interact with NPR-A with lower affinity due to the steric hindrance that the tail might impose.

In contrast to the assumption, KNP evoked aortic strip relaxation in an endothelium dependent manner or otherwise NPR-A independent mechanism, unlike ANP (Winquist *et al.*, 1984). Thus, initial characterization of KNP showed it was a weak vasodilator compared to ANP which required endothelium derived vasoactive factors to exert this action.

Previous studies have shown that infusion of supraphysiological doses of ANP results in marked reduction of BP (Kleinert *et al.*, 1986). This lowering of BP

is due to decreased, stroke volume, heart rate, peripheral resistance and increased excretion of water. Our experiments on effect of KNP on vascular and renal parameters suggest that KNP does not seem to follow the paradigm of NPs. It was evident that KNP infusion resulted in reduction in cardiac output as it lessened heart rate. But KNP seems to affect these parameters in a sustained manner in contrast to the prompt recovery seen in the case of ANP. Further, KNP did not have any significant renal effect which was a striking difference between the two peptides.

To understand the differences between KNP and ANP, a structure-based activity assessment gave some insight to this non-classical activity. KNP ring functioned as a classical NP, with 10 fold lower potency compared to ANP. The lower activity of Ring could be attributed to two important features of the ring. The two D substitution in place of G at positions 8 and 19 and the lack of C-terminal NSFRY sequence similar to ANP. The crystal structure of ANP with NPR-A indicates that G residues (9, 20) at equivalent positions fall in the vicinity of E169A and E169B of the receptor (Figure 3.10). On replacement of this G with D as in case of Ring might cause an electrostatic repulsion, which could result in lower potency. Further, receptor binding studies have shown that ANP loses its affinity to NPR-A on deletion of the C-terminal extension. This fact is supported by the information from the crystal structure. Residues N24, S25, F26 and R27 of the C-terminal extension of ANP form a β-sheet with Q186 B and F188 B of the receptor along with a hydrogen bond between N24 of ANP with E187 B. KNP ring lacks these interactions with two basic residues as its tail. These structural changes may explain the lower potency of Ring.

Interestingly, Helix relaxed aortic strip in an endothelium dependent manner with comparable activity to that of full length. This showed that KNP has two pharmacologically active segments, which induced vasorelaxation by distinct mechanisms. Although both the segments have equipotent activity comparable to that of full length, putative helical segment of the tail seemed to contribute to the action of KNP. The vasorelaxant ability of R&H was in agreement with that observed for KNP. The presence of the helical segment attributed function to R&H as well as KNP in an endothelium dependent manner. Further, Δ Helix showed much lower aortic strip dilation abilities compared to full length which was not influenced by endothelium.

Similar observations were obtained when intracellular cGMP levels were measured in response to activation NPR-A by different ligands. Ring elicited a 10 fold lower activity compared to ANP. In comparison to ANP, KNP, Δ Helix and R&H showed a 300 fold lower potency in elevating cGMP levels in the cells. This showed that the presence of any segment of tail of KNP lower the binding ability of the ring. In other words, tail segment of KNP was redirecting the otherwise functional ring away from the NPR. These results were conclusive to show that despite the presence of a functional NP ring, KNP lacks classical NP like functions due to its C-terminal tail.

In an investigation to obtain insights into the molecular players of KNP evoked vasorelaxation, endothelium derived vasoactive factors namely NO, prostacyclin and hyperpolarization seem to influence KNP's vasodilatory properties. KNP and Helix did have alteration in their vasodilatory properties in the presence of different inhibitors. Although all three factors seem to influence the activity of the peptides, inhibition of NO production lead to

complete loss of function. Hence, looking at the possible mechanisms through which NOS is activated might lead us to understand the exact molecular target. Endothelial NOS is activated by pathways that increase intracellular calcium. This increase in Ca^{2+} is dependent either on IP3 and DAG or Gq protein when different receptors are activated (Furchgott, 1984). Further, direct potassium channel openers have shown to increase intracellular calcium (Busse *et al.,* 2002; Sheng *et al.,* 2009; Strobaek *et al.,* 2004). Hence, sequential inhibition of phospholipase C (enzyme that produces IP3 and DAG), Gq protein activation, different classes of potassium channel (Calcium activated-, voltage gated-, ATP dependent- potassium channels)(Busse *et al.*, 2002) and monitoring the vasodilatory properties of Helix and KNP will further narrow down the possible molecular target through which these peptides function.

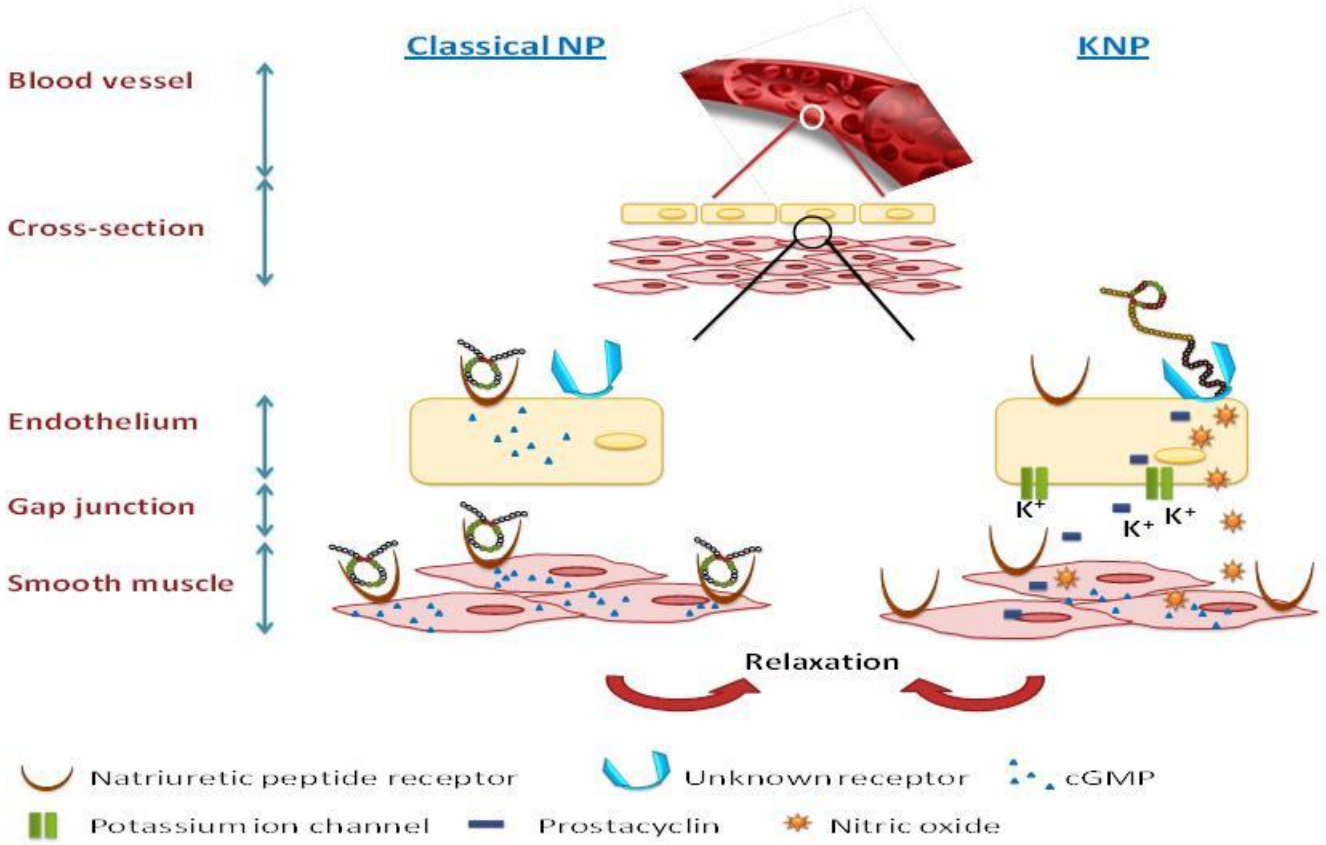

Figure 2.18. Proposed mechanism of action of KNP

A non- classical NP like KNP binds to an unknown receptor or ion channel on endothelium using to tail to evoke NO, prostacyclin and potassium ion mediated hyperpolarization. These factors cause the relaxation of the underlying vascular smooth muscle. KNP functions through its tail despite the presence of the functional ring.

Thus with this study we have been able to propose a mechanism of action of KNP. A classical NP like ANP will bind to NPR on both endothelium and vascular smooth muscle to elevate cGMP to cause vasodilation. While KNP, a non-classical NP, binds to a unknown target receptor or ion- channel on endothelial cells and produces NO, prostacyclin and K^+ hyperpolarization to cause relaxation of the underlying smooth muscle cells using its tail, despite the presence of a functional ring. Thus, KNP's tail wags its ring (Figure 2.18).

In-vivo the activity of KNP seems to be the contribution of both the pharmacophores. It may be speculated that KNP may be proteolytically cleaved to produce both the functional segments and hence an additive effect of both the segments is observed as KNP's activity. Further, the presence of a long tail may increase the PK of KNP.

Although the present experiments does not confirm the processing of KNP, it is evident that one particular segment of KNP does not contribute to its entire activity. Further, neither KNP nor its truncations had any renal effects. Despite being able to bind to NPR-A like ANP, Ring did not cause diuresis which was an intriguing observation. In the past, alternately spliced variant of BNP was shown to have renal effects while lacking vascular functions (Pan *et al.*, 2009). The presence of the D residues in place of conserved G at positions 3 and 14 of the ring may alter the conformational plasticity of the receptor which dictates the physiological response. Thus, we speculate that the conformational changes for the receptor activation may be altered in the case of Ring which dictates the tissue specific response.

CHAPTER 3

The ring of resistance- KNP ring is resistant to degradation

Chapter 3: The ring of resistance- KNP ring is resistant to degradation

3.1. Introduction

Natriuretic peptides are involved in regulating key physiological functions and hence an appropriate level of the peptides has to be sustained in circulation so as to exhibit necessary activity. Release and clearance of NPs play major roles in regulating plasma concentrations of NPs. Physiological stimuli such as atrial wall stretch increases NP levels in the blood stream and multiple clearance mechanisms render the peptide inactive. Among the various processes involved in degradation of NPs; receptor mediated internalization and proteolytic hydrolysis of the peptides have major roles.

NPR-C is involved in active clearance of NPs by receptor mediated endocytosis and degradation. It is a promiscuous receptor that binds to all three mammalian NPs with relative affinities ranked as CNP=ANP > BNP. The crystal structure of the three NPs with NPR-C shows that the receptor provides a rigid molecular interface for ligand binding. The lack of conformational plasticity in the receptor binding pocket renders the NPs to adopt different receptor bound conformations to overcome the entropic penalties. Due to the different local shape the NPs take up when they are bound to the receptor, they utilize different interaction surface on NPR-C (He *et al.*, 2006). Further C-terminal residues of ANP and BNP in complex with NPR-C seem to be more solvent accessible compared their NPR-A bound conformation (Ogawa *et al.*, 2004). It may be inferred for these facts that, NPR-C provides a fixed volume binding pocket, which accommodates the ring

residues of all NPs. Hence, the residues of NP ring play key role in altering the affinities of the peptide to NPR-C.

The second major route of clearance of NPs are by proteolytic degradation by neutral endopeptidase (NEP), a zinc- dependent membrane bound mettaloprotease. It cuts at the N-terminus of hydrophobic residue which is C1-F2 bond in case of NPs, rendering in disruption of the ring structure. Hydrolysis potency of the NPs in-vitro may be ranked as CNP = ANP > BNP, which is ascribed to their structural difference. Present studies show that size of NP is a factor that attributes NEP resistance. Peptides with long N- terminus and C-terminus tails are less prone to hydrolysis. It is thought that NP with longer tails cannot be accommodated within the binding pocket due to spatial constraints the tail would impose. In accordance with this theory, peptides with long tails like urodilatin and DNP have higher resistance to degradation compared to BNP. Thus, the residues in the N-terminus and C-terminus of a NP influence its susceptibility to NEP, but there is no knowledge about the contribution of residues within the ring of NP.

With the understanding that the molecule of our interest, KNP had a varied biological effect compared to other NPs, we wanted to understand the stability of this peptide to degradation. With the prior knowledge, we predicted that KNP with the longest tail among the NPs known may have high resistance to proteolysis. Further the Ring of KNP has substitutions in position 3 and 14 where a conserved G is replaced by D. Apart from these changes the Ring has more polar residues in comparison to ANP. With these differences in sequence of Ring, we hypothesized that Ring KNP might have higher resistance to hydrolysis. Hence, our study focused on understanding the half life of KNP

and its Ring. The experiments were designed to look the overall in-vitro degradation of KNP and its ring by both NEP and NPR-C.

3.2. Materials and Methods

3.2.1. Materials

Most the materials used in the experiments are as described in chapter 2. Apart from thelready mentioned chemicals, Recombinant NEP (Sino biological, Shangai, China) and KNP mutants rings (Genescript Corporation, NY, USA)

3.2.2. Synthesis of KNP, ANP, Ring, Ring mutants and K-ANP

KNP was recombinantly expressed and purified as described in Chapter 2. Ring and ANP were synthesized using F-moc based manual SPPS and purified as described in Chapter 2.

3.2.3. Degradation of NPs with recombinant purified NEP

10 µM of respective NPs or mutant NPs were mixed with of 1 µg/µl BSA in 50 mM HEPES buffer containing 150 mM NaCl, 5 mM $MgCl_2$ at pH 7.4. A peptide aliquot was withdrawn before the addition of NEP, and this served as zero time point. The peptide mixture was pre-incubated at 37°C for 5 min before the addition of NEP. Recombinant NEP dissolved in 50 mM HEPES, 150 mM NaCl, 5 mM $MgCl_2$, pH 7.4 at 0.1 µg/µl concentration and stored at -30°C until used for assay. An aliquot of the enzyme was thawed on ice and 2 µl NEP per 50 µl reaction volume was added to bring the final concentration of NEP to 4 ng/µl and a time chase experiment was conducted. At time points 5 min, 15 min, 30 min (90 min and 150 min for KNP), an aliquot (100 µl) of the NEP-NP mixture was withdrawn and the reaction was terminated by the

addition of 2 µl of 1 M HCl to every 100 µl of reaction mixture. After the complete time chase experiment was completed, 51 µl from each time point was used for degradation profiling by LC-MS and rest 51 µl was used for in-vitro half-life determination.

3.2.4. Degradation profiling by LC-MS

The aliquot of NP-NEP mixture that was sampled from every time point was neutralized with 1 µl of 1 M NaOH. Following the neutralization, NEP-NP mixture was reduced using 100 mM DTT (final concentration) and the final volume was increased to 100 µl. The samples were run on reversed-chromatography followed by ESI-ion trap mass spectrometer to analyze the degradation products. 70 µl of the samples were injected and the separation was performed on Thermo scientific Hypersil Gold column (C18, 3 µm, 2.1 X 30 mm) using 0.1% FA as buffer A and 0.1% FA with 80% Acn as buffer B. The methodology began with sample injection followed by column wash for 5 min (flow rate 200 µl/min). During wash, elute from the column was redirected to waste. Following the wash, a simple gradient 0-50 % B in 30 min was used to separate the fragments of the NPs generated during degradation. During the gradient, elute from the column was linked to ESI source which was set which following parameters for elute to ionize: Sweep gas flow rate: 30 ARB, Auxillary gas flow rate: 5 ARB, Spray voltage: 4.5 kV, Capillary temperature: 350°C, Capillary voltage: 9 V. The ion-trap detector was set in the positive mode with mass/charge range 500-2000. The total ion count generated over the entire gradient was analyzed to determine the degradation pattern. The mass spectrum was reconstructed using Pro-mass X-calibur software to obtain the mass of the peptide fragment. Using Expasy- protparam

tool, the possible peptide fragment molecular weights were calculated, which aided the identification of the exact lytic bond. Five independent trials have been performed for each peptide to confirm the degradation pattern.

3.2.5. Cell culture and transfection

The cells were grown and transfected by the procedure described in chapter 2.

3.2.6. Ability of Ring mutants to activate NPR-A

The method performed is as described in chapter 2.

3.2.7. In-vitro half life determination

The peptide aliquots were neutralized with 1 µl of 1 M NaOH. Peptide final concentration equal to 100 nM ANP, 1 µM Ring, 300 nM GRG, 1 µM K-ANP and 2 µM DRG from the NEP-NP mixture were incubated with the cells transfected with NPR-A. Prior to treatment with peptides, the transfected cells were washed with PBS and treated with 150 µl of 0.5 mM IBMX containing basal vascular growth media without FBS for 30 min. The peptide aliquots from different time point were added to pre- incubated cells to a final concentration as indicated and further incubated at 37°C in 5% carbon-di-oxide atmosphere for 30 min. After the incubation, the peptide containing media was aspirated and 150 µl of 0.1 M HCl was added to the cells. The plates were incubated with shaking at 50 rpm at room temperature for 30 min. The cell lysates were collected and assayed for intracellular cGMP levels using Enzo life science cGMP ELISA kit. Manufacturer's protocol was followed to perform the assay. The whole cell protein concentration was measured by BCA assay to normalize the obtained cGMP response.

3.2.8. cGMP response in cells co-transfected with NPR-A and NPR-C

Transfection procedure was same as prescribed in chapter 2, but changes in changes in DNA concentration. NPR-A and NPR-C plasmid were taken in 1:2 ratio. Per well 0.5 µg of NPR-A and 1 µg NPR-C plasmids were transfected using 2.5 µl lipofectamine 2000^{TM}. In control population of cells, 0.5 µg of NPR-A and 1 µg empty pCMV-4 vector was transfected.

The cGMP response to ANP and Ring were evaluated in both populations of cells.

3.3. Results

3.3.1. Stability of KNP and ANP to NEP mediated proteolysis

Previous studies have shown that NPs with long C- or N- terminal extensions were resistant to NEP mediated proteolytic digestion. Hence, we wanted to evaluate if KNP with the longest C-terminal tail among the known NPs was resistant to hydrolysis. ANP was used as the control for the experiment. The peptides incubated for different time points were reduced and separated on liquid chromatography linked to mass spectrometer to analyze the degradation product. Further, peak area of the maximum intense ion of the peptide was used for determining the relative amount of peptide remaining at a time point. ANP was markedly degraded within 5 min incubation. The degradation products showed similar profile as previously reported. The lytic bonds were assessed based on the molecular weight. This was in accordance with a study that identified the cleavages sites as C1-F2, R5-M6, R8-I9, G10-A11 and G14-L15 (Vanneste *et al.*, 1988) with C1-F2 being the first bond to be cleaved. In contrast incubation of KNP with NEP did not show any difference in the ion count all through the experimental time point (150 min) and no degradation products were detected. This experiment showed that KNP was completely resistant to hydrolysis by NEP for at least 150 min.

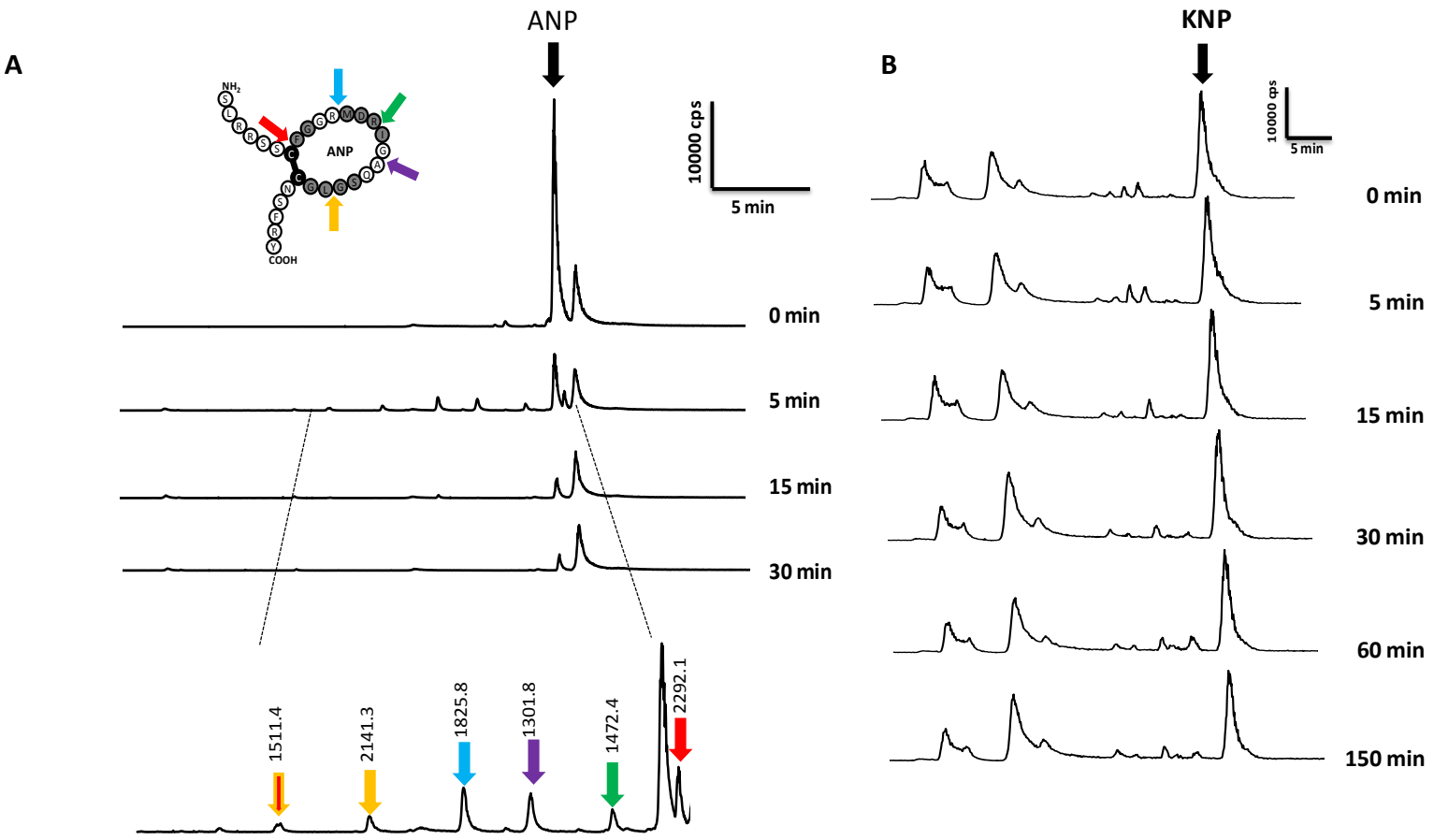

Figure 3.1. KNP is resistant to degradation
LC-MS degradation profiling of **A-** ANP and **B-** KNP is as shown. The peptides were incubated with purified NEP for indicated amount of time and profiled on LC-MS. The colored arrowed locate the lytic bond on the peptide. KNP did not degrade up to 150 min.

3.3.2. Sequence analysis of Ring

KNP was resistant to NEP hydrolysis. Although previous studies would suggest that the length of C-terminal tail of KNP would confer resistance to NEP, we wanted to look at the influence of residues within the ring of KNP to hydrolysis. The sequence of Ring was compared to the NPs about which the susceptibility to hydrolysis is previously known, namely; ANP, BNP, CNP and DNP. Apart from the residues which are conserved between the NPs, Ring has two D residues at position 3 and 14 that have replaced normally conserved G's in ANP, BNP and CNP. Other residues within the Ring are common to either BNP or DNP. It is also interesting to note that at positions 10, 11, 12 and 14, Ring had polar residues while other NPs have a combination of polar and hydrophobic residues. As mentioned in the introduction, NEP cleaves peptide bonds at the N-terminus of hydrophobic residues. Hence, we hypothesized that the Ring of KNP might have higher resistance to degradation than the ring structures of other NPs. Moreover, Ring had only two residues in its C-terminal tail, second shortest, next to CNP. Hence, it would serve as a good model to look at the influence of residues within the ring on hydrolysis of NPs.

```
                  1  3 4          12 14  17
CNP     -GLSKGCFGLKLDRIGSMSGLGC-----------------
ANP     -LRRSSCFGGRMDRIGAQSGLGCNSFRY------------
DNP     EVKYDPCFGHKIDRINHVSNLGCPSLRDPRPRPNAPSTSA
Ring    -GLLISCFDRRIDRISHTSDMGCRH---------------
BNP     MVQGSGCFGRKMDRISSSSGLGCKVLRRH-----------
```

Figure 3.2. Ring of KNP is a chimera of BNP and DNP ring with unique substitutions

Sequence of NPs whose degradation ability is previously studied was aligned. Yellow residues are conserved in all NPs. Pink residues are common between Ring and BNP. Grey residues are common between Ring and DNP. Blue residues are unique to Ring.

3.3.3. Degradation pattern of Ring vs ANP

It is of interest to note that Ring had 5 residues in the N-terminus and 2 residues in C-terminus which are shorter compared to ANP (6 residues in N-terminal and 5 residues in C-terminus). The stability of Ring was assessed by incubating the peptide with NEP for the indicated periods. Using LC coupled with MS, the cleavage pattern and the relative quantities of uncleaved peptides were compared with those of ANP. The degradation pattern of Ring was similar to that of ANP. Cleavage sites within the ring were mapped to be C1-F2, R5-I6, and R9-I10. But no cleavage was detected between D14-L15. Although the lytic bonds were similar, we observed that C1-F2 might not be the only peptide bond to be cleaved as the reaction begins. The degradation pattern showed the presence of peptides with mass 1225.3 Da and 1563.3 Da which corresponded to N-terminal and C-terminal peptide segments when R8-I9 bond was cleaved. This observation suggested that R8-I9 was cleaved in equal proportion as C1-F2 as the reaction began. In the cleavage pattern of ANP the masses of all the peptide fragments showed that they were derived after the NP was cleaved at C1-F2. This observation suggested that NEP has difficulty recognizing the conserved lytic bond C1-F2 of Ring as the reaction begins, although it is cleaved eventually.

Further, Ring seemingly degraded slowly compared to ANP. The intensity of the parent ion of Ring (indicated by the black arrow in Figure 3.3.B) disappeared in a delayed fashion in comparison to ANP.

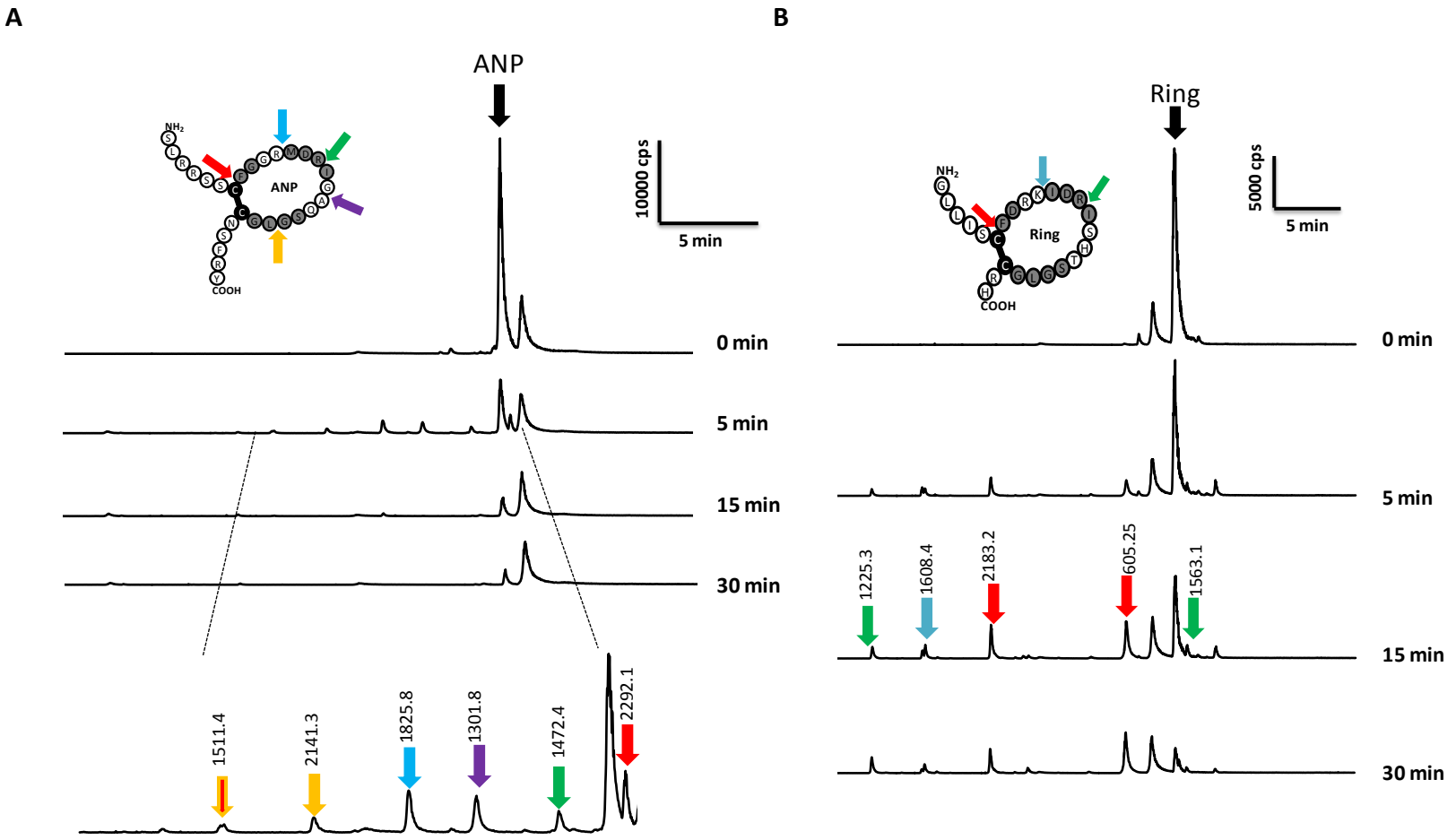

Figure 3.3. Ring degrades slower but at similar positions compared to ANP

LC-MS profiling of degradation products of **A-** ANP and **B-** Ring is as shown. The parent ion indicated by the black arrow, reduces slower in case of Ring. The lytic bonds are similar between ANP and Ring. Arrows of the same color in Ring degradation profile indicates same positions with mass of the two fragments

3.3.4. In- vitro half life of ANP and Ring

Since, the degradation of Ring seemed slower than ANP, the in-vitro half life of these peptides were evaluated based on its activity. To assess its activity, peptides treated with NEP for indicated amount of time were tested for their ability to evoke cGMP response in CHO-K1 expressing NPR-A. ANP showed a marked decrease in its activity by 5 min. The half- life of ANP was about 1.8 min. This value matched with the previously reported values for ANP (Stephenson and Kenny, 1987). Ring on the other hand showed an extended half-life of 12 min (Figure 3.4). This remarkable increase in half-life (about 6.5 times higher than ANP) suggested that residues within the ring of KNP had great influence on the degradation of the peptide.

The results obtained so far show that Ring of KNP has increased resistance to hydrolysis and is not cleaved in the same manner as ANP although the lytic bonds were similar. Hence, based on the previously described model for NEP hydrolysis (Chapter 1, section 1.7.2), we hypothesized that the presence of D3, R4 apart from D7, R8 might mislead the peptide into an improper orientation within the binding pocket. Since the peptide is cleaved at the conserved position as ANP, it is evident that the peptide can place itself in the right position but it requires more time to do so. It could be postulated that the presence of two DR sites of the Ring of KNP places the peptide in two different spatial orientations which are in equilibrium (Figure 3.5). The process of switching the conformation delays the metabolism of the ring. Further we observe that Ring was not hydrolyzed at position D14-L15 as ANP, which suggested that D residue at position 14 had some influence on

hydrolysis. Hence, we wanted to understand if D3, R4, D14 have influence on hydrolysis. To investigate this hypothesis we designed mutant Rings of KNP.

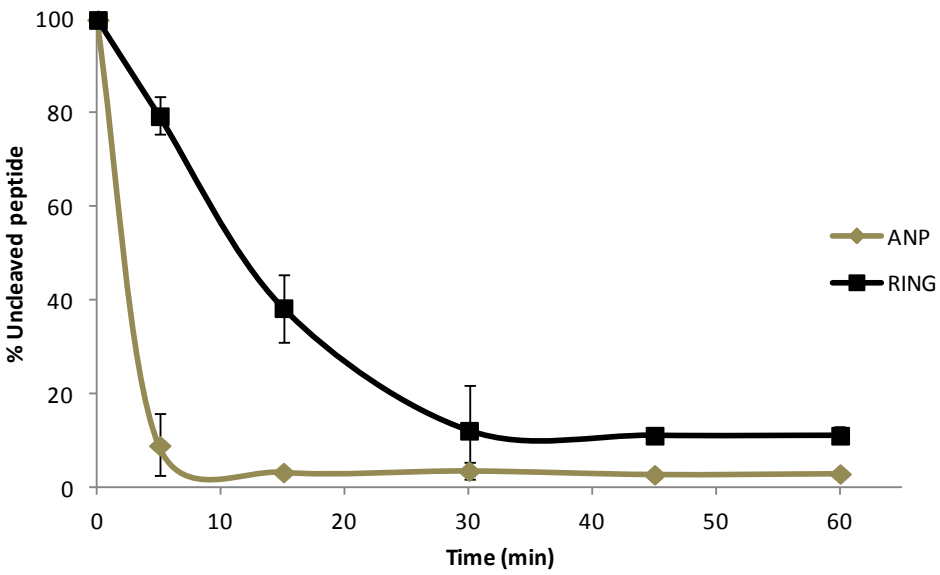

Figure 3.4. Ring has 6.5 fold higher half-life compared to ANP
Peptides incubated with NEP for the indicated time points were treated with cells transfected with NPR-A. The relative cGMP produced during different time points were calculated with t = 0 as the baseline (100%). The half-life of ANP was calculated to be 1.8 min and that of Ring was 12 min.
Each data point is an average on 3 independent trials and is represented as mean ± SEM

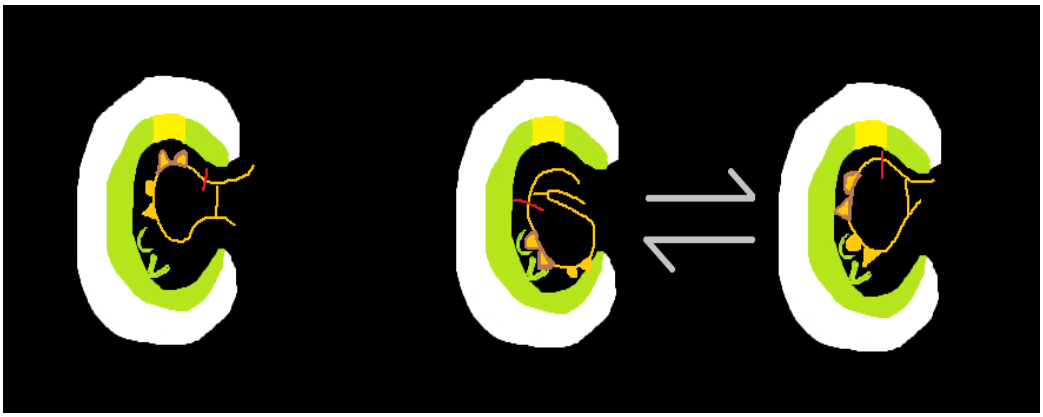

Figure 3.5. Hypothetical model for degradation of Ring
The presence two DR sites on the sequence of Ring misguides the peptide to orient the lytic bond in a wrong position. Thus, the peptide has to switch its conformation to be hydrolyzed. This process delays the metabolism of the Ring. Red line indicates the position of C1-F2 bond.

3.3.5. Design of Ring mutants

Mutant rings with D3, R4 and D14 sequentially replaced by G as in the case of ANP. Ring mutant GRG, with both D3 and D14 would typically resemble BNP ring without C-terminal tail. Mutant DGD had R4 replaced by G. Third mutant had D14 replaced by G, called DRG. Finally G residue at 3, 4 and 14 of ANP ring was replaced with D, R and D. This peptide was called K-ANP. These mutants were designed to understand the influences of residues within the ring on hydrolysis.

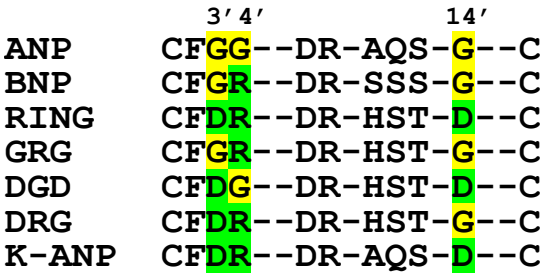

Figure 3.6. Design of Ring mutants
Residues at positions 3, 4 and 14 of Ring were sequentially swapped with the residue of ANP at that particular position to generate the mutants.

3.3.6. Degradation profile of Ring mutants

Similar to Ring and ANP, the degradation pattern and susceptibility were determined by profiling the degradation products on LC-MS. The lytic bonds were similar to that of Ring. Complete N-terminal and C-terminal peptide fragments of R8-I9 cleavage were absent in GRG and DGD, while these peptides were detected for DRG. This observation suggested that the presence D3 and R4 residue in the ring influenced the orientation of C1-F2 peptide bond in the active pocket of NEP. K-ANP showed similar cleavage pattern like ANP but was cleaved at an uncommon location between R4-R5. Cleavage

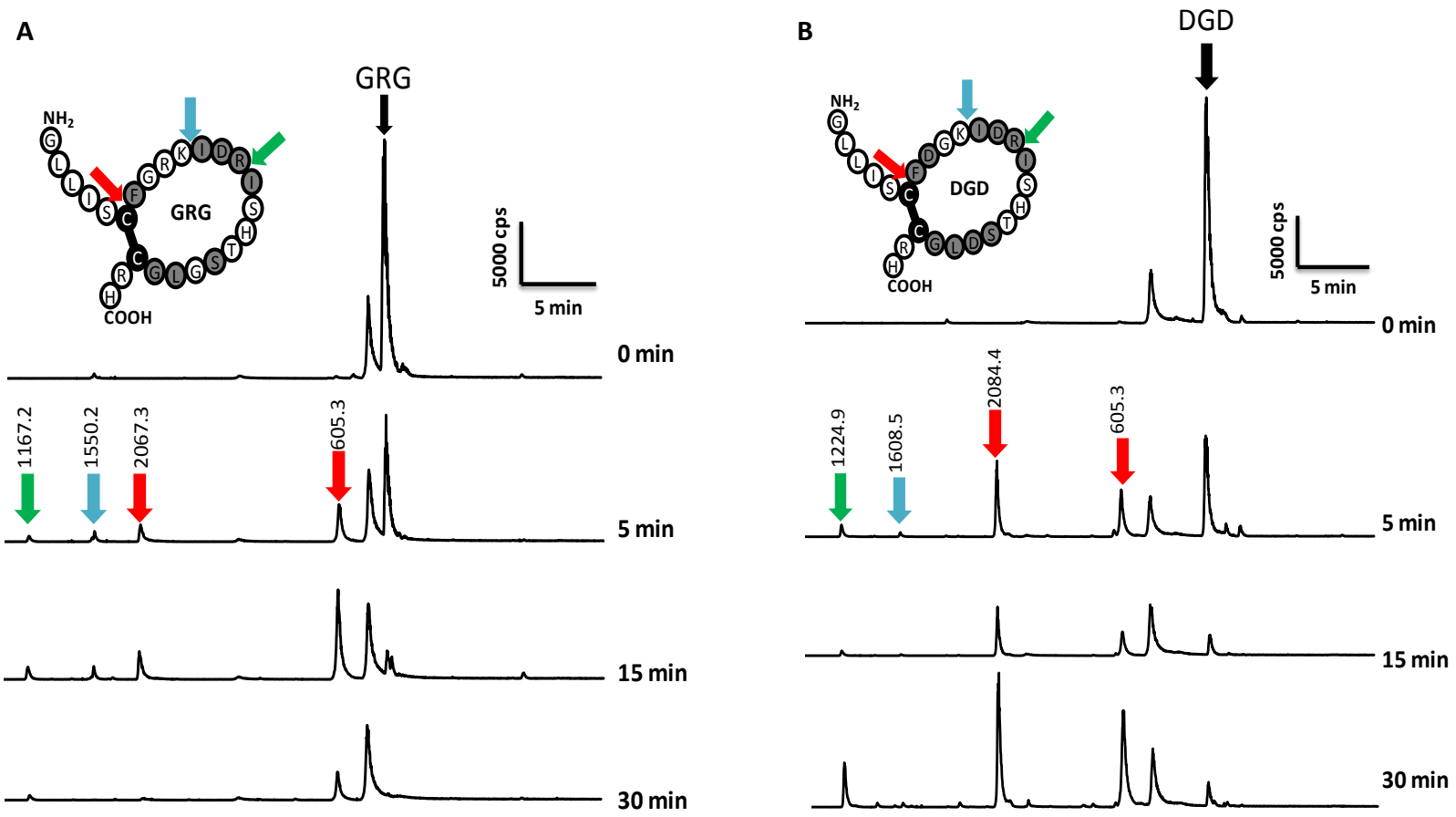

Figure 3.7. Degradation profile of GRG and DGD Ring mutants

LC-MS profiling of degradation products of **A-** GRG and **B-** DGD is as shown. The lytic bonds of both the peptides are similar to Ring but the rate of disappearance of the parent ion (indicated by black arrow) is faster than Ring. Same arrow color in Ring degradation profile indicates same positions with mass of the two fragments

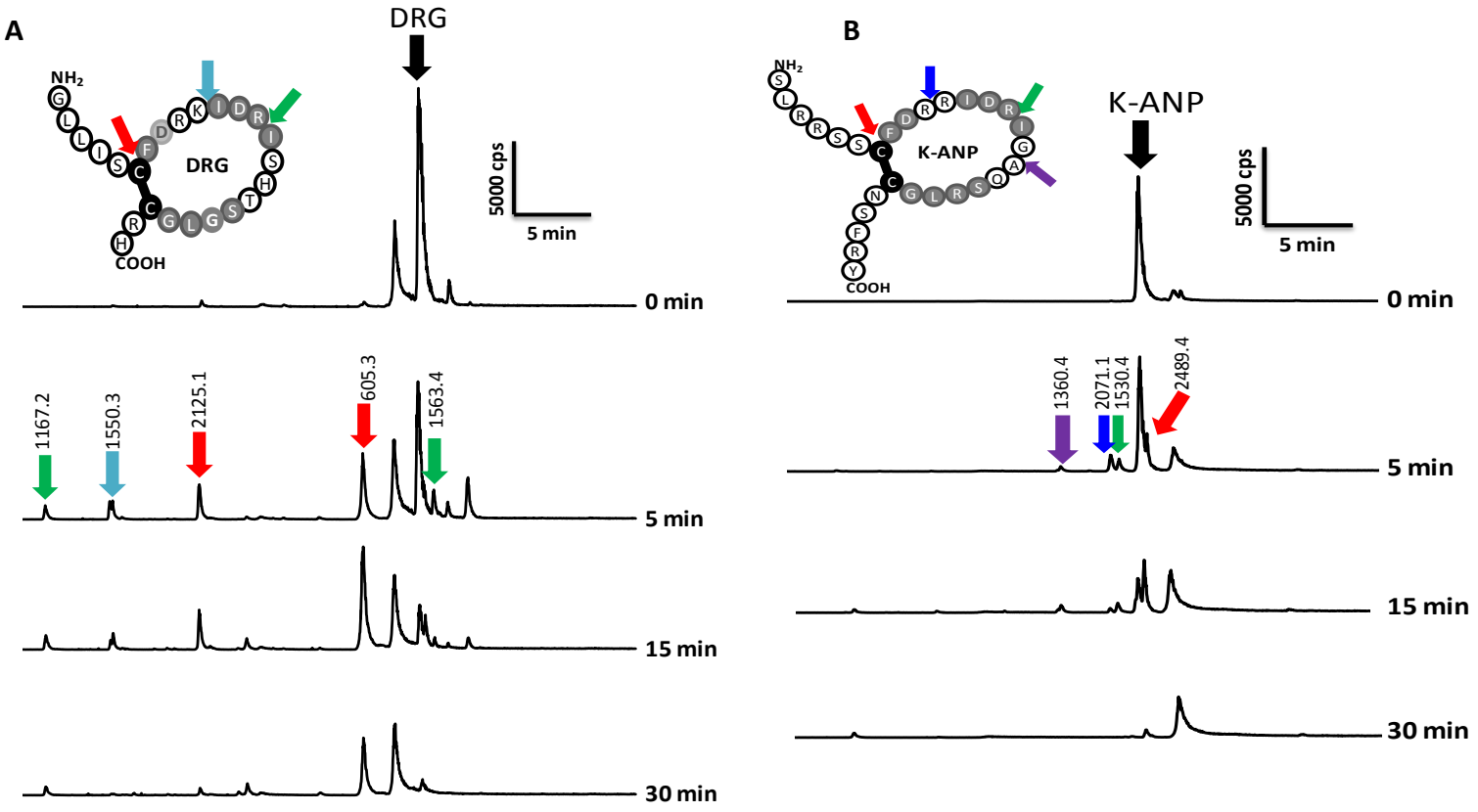

Figure 3.8. Degradation profile of DRG and K-ANP

LC-MS profiling of degradation products of **A-** DRG and **B-** K-ANP is as shown. The lytic bonds of both the peptides are similar to Ring but the rate of disappearance of the parent ion (indicated by black arrow) is faster than Ring. Same arrow color in Ring degradation profile indicates same positions with mass of the two fragments

at R5-I6 was not detected for K-ANP. Further, there was no hydrolysis detected between D14-L15 for all the mutants.

GRG seemed to degrade faster like ANP in comparison to Ring. While DRG, DGD and K-ANP seemed have an intermediate degradation rate between GRG and Ring. These results evidently suggested that D3 and R4 residues influence the spatial orientation of the peptide in NEP binding pocket which renders its cleavage at uncommon sites, thereby delaying metabolism. Since the degradation profiling suggested that the residues under consideration altered the rate of hydrolysis, we assessed the in-vitro half-lives of the mutants.

3.3.7. Ability of Ring mutants to bind to NPR-A

In order to evaluate the in-vitro half life of Ring mutants, the potency of these mutants to evoke cGMP response in NPR-A transfected CHO-K1 cells was required. The concentration to be tested for determining the half-life was chosen based on the potency of the peptide.

GRG showed an increased ability to activate NPR-A compared to Ring. This peptide's potency could be considered equivalent to that of BNP (Kambayashi *et al.*, 1990; Nakao *et al.*, 1991). DGD mutant lost its ability to evoke cGMP response by ~ 30 fold compared to native ring. The capabilities of GRG and DGD to activate NPR-A suggests that certain molecular interaction with the receptor is enhanced in the absence of both D residues, while the presence of R9 orients the peptide in a position that prevents this unfavorable interaction. The ability of DRG to induce cGMP response was lesser compared to Ring, while the activity was significantly improved compared to DGD. This

observation could be explained with the crystal structure of ANP with NPR-A. G3 and G14 residues are in the vicinity of E169A and E169 B of receptor at a distance of 5.7 Å and 4.4 Å respectively (Figure 3.10). Thus replacement of G with D might introduce electrostatic repulsion in these locations. However, the presence of R9 residue seems to improve the interaction with the receptor. Further K-ANP, which has ring with substitution at positions G3, G4 and G14 with D, R and D showed equivalent potency as that of Ring, which was 10 fold lower compared to ANP. This observation confirmed the fact that despite the presence of C-terminal tail of ANP, K-ANP did not elicit equipotent response as ANP, which is attributed to D3, R4 and D14.

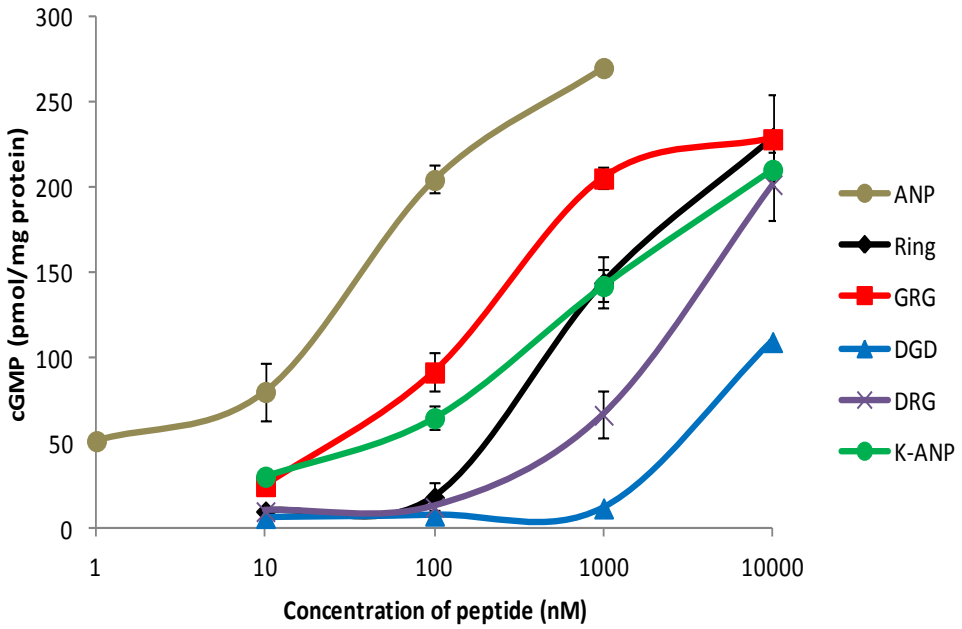

Figure 3.9. D3, R4, D14 within the Ring influences NPR-A activation
Ring mutants were evaluated for the amount of cGMP produced when treated with NPR-A transfected CHO-K1 cells. Each data point is an average of 3 independent trials represented as mean ± SEM.

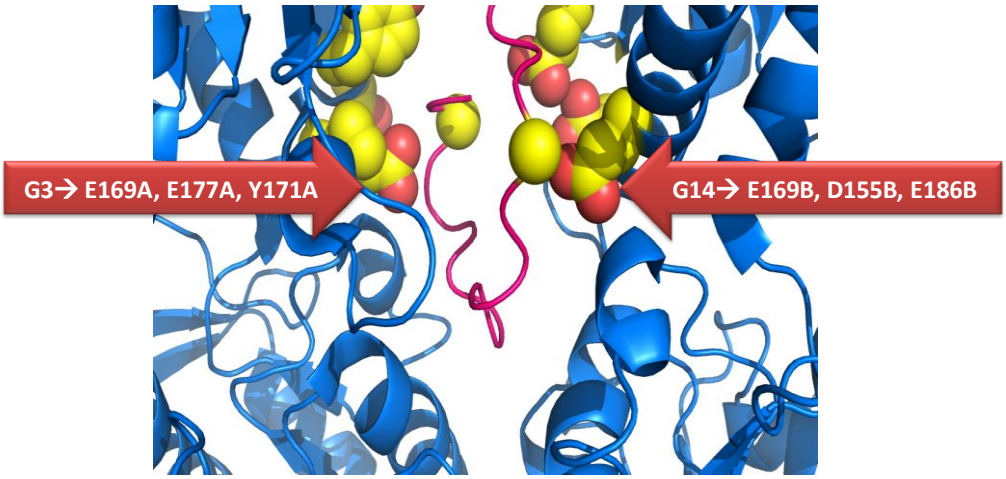

Figure 3.10. D3 and D14 within the ring may cause electrostatic repulsion on NPR-A binding
Crystal structure of ANP- NPR-A shows that G3 and G14 are in the vicinity of E169 residue of the receptor. Replacement of G to D might cause electrostatic repulsion.

3.3.8. In-vitro half life of Ring mutants

GRG mutant showed similar half-life as ANP, suggesting both the D residues have influence on degradation. The half life of DGD was not evaluated owing to its low potency. DRG Ring was more prone to hydrolysis compared to native Ring, but had 3 times higher resistance compared to ANP. Further, K-ANP showed 4 fold increased half-life by compared to ANP. These results suggested that residues within the ring of a NP played crucial role in influencing their hydrolysis. The residues D3, R4 and D13 seem to confer resistance to the peptide. These results also support our hypothesis that the presence of two DR sites places the peptide in two different conformations within the binding pockets, which delays its metabolism. Although further modeling is required to understand the placement of the D14 in the active site, one may observe that this residue as well plays important role in decreasing the peptide's sensitivity to degradation.

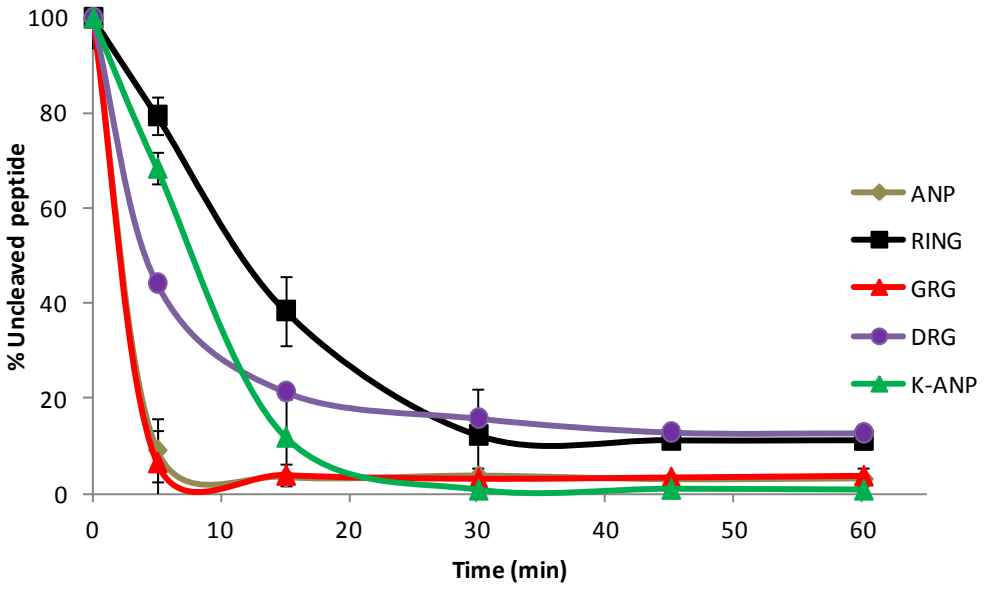

Figure 3.11. D3, R4, D14 residues influence the half-life of NP ring
Peptides incubated with NEP for the indicated time points were treated with cells transfected with NPR-A.
Each data point is an average on 3 independent trials and is represented as mean ± SEM.

3.3.9. Ability of Ring to evoke cGMP response in the presence of NPR-C

NPR-C is a promiscuous receptor which binds to all NPs. The relative difference in affinity of the NPs to NPR-C is attributed to the side chains of amino acid residues within the ring. Among the different interaction sites on NPR-C available for NP binding, the pocket that accommodates residue 12 of NP ring seems to contribute to the lack of selectivity of this receptor. Position 12 of the ring is occupied by either a hydrophobic residue or a polar residues among different NPs (M in CNP, Q in ANP, V in DNP and S in BNP), which fit in the same binding pocket. This pocket of NPR-C is composed of hydrophobic residues F119, Y126, A96, A116 and F170 (Figure 3.12). Thus, interaction of a hydrophobic residue is more favored. KNP Ring has T in position 12 (polar residue) which is a bulkier substitution compared to S of

BNP. Moreover, two D residues (3 and 14) substitution to G have larger side chains to be accommodated.. Thus the hypothesis was NPR-C a receptor with rigid ligand interaction interface conformation and Ring of KNP with bulkier substitution in its sequence compared to other known NPs, might have less NPR-C binding ability.

To test this hypothesis, CHO-K1 cells were co-transfected with NPR-A: NPR-C in the ratio 1:2. The cGMP response of these cells on treatment with ANP or Ring was compared to cells which were transfected with NPR-A: pCMV4 empty vector (1:2). The dose dependent cGMP response of ANP in population of cells which are expressing both NPR-A and NPR-C was 100 fold lower compared to the population of cells with equivalent expression of only NPR-A. While Ring showed a difference of 10 fold lower ability to evoke cGMP in the presence of NPR-C. This was a preliminary experiment conducted and will be repeated. The data is the average value of two independent trials. However, this preliminary data suggests that Ring has lower NPR-C binding ability compared to NPR-A.

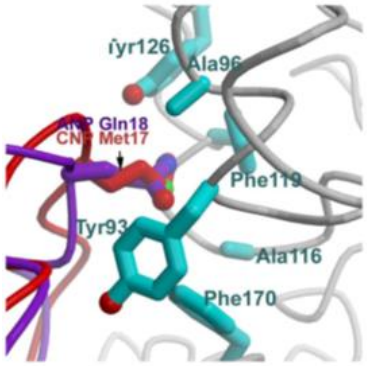

Figure 3.12. Binding pocket of residue 12 of NP with NPR-C
The binding pocket is composed of hydrophobic residues which accommodates both polar and non-polar side chains of residues in position 12 of NP ring.

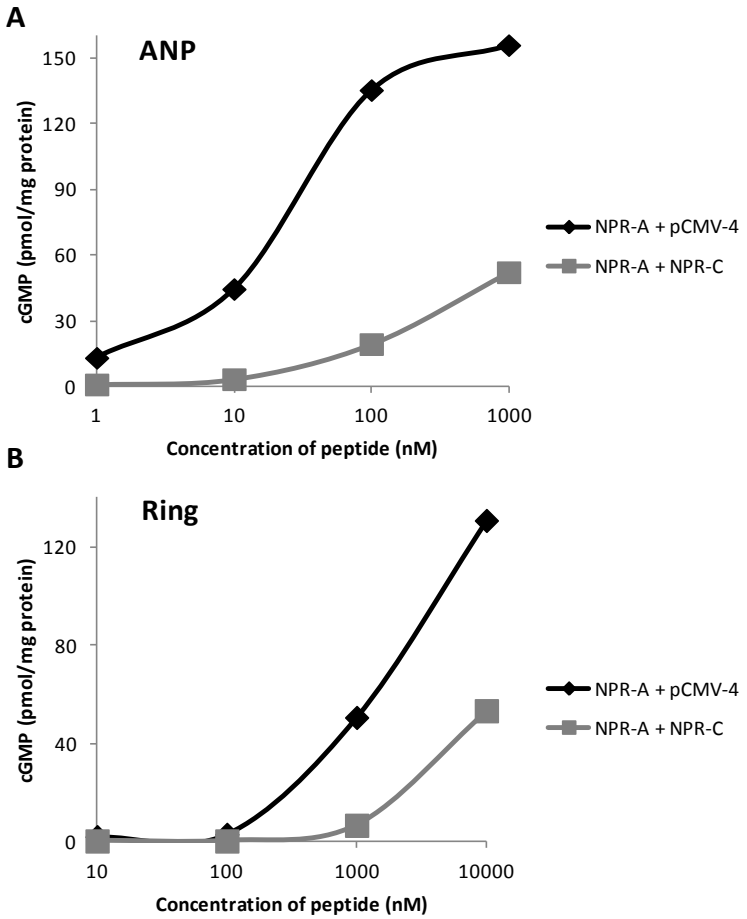

Figure 3.13. Ring has lower ability to bind to NPR-C
Preliminary results of the ability of the peptides to evoke cGMP response in cells expressing both NPR-A and NPR-C are as shown. **A-** ANP, **B**- Ring.The data points represent average value of two independent trials.

3.4. Discussion

Rapid degradation of NPs, necessitate higher dose infusions to harness their therapeutic potential. Previous studies have shown the size of a NP as an indicative factor of its susceptibility to degradation. Increasing the lengths of N- and C-terminal extensions of NPs increases half-life (Dickey and Potter, 2011). The primary processes involved in the degradation are protease mediated hydrolysis and receptor- mediated endocytosis.

The protease involved in NP metabolism is NEP, an ubiquitous enzyme which is involved in degradation of a number of vasoactive peptide hormones such as angiotensin II, endothelin, vasopressin and many others. Inhibition of NEP in-vivo has resulted in increased plasma levels of NPs, suggesting its influential role in the degradation of NPs (Wegner *et al.*, 1995). Previous studies have shown that the susceptibility of NPs to hydrolysis is proportional to the decreasing lengths of C- and N- termini extensions. A recent study by Pankow *et al.*, has proposed a model illustrating the mechanism of NEP mediated hydrolysis by docking NP into the active site of NEP. This model has exemplified the possible role on longer N- and C- termini tails of NPs in conferring resistance to hydrolysis. The authors suggest that the resistant NPs with longer extensions have difficulty to slip into interior cavity of the enzyme which does not allow them to orient correctly. In correlation with the known information, KNP was completely resistant to NEP mediated hydrolysis until 150 min (experimental period of the study).

However, no information about the influence of residues within the ring upon degradability of NP has been previously reported. Our investigation on the vulnerability of Ring (only Ring of KNP) to degradation has resulted in

insights about the influence of residues within the NP ring. Ring of KNP showed a 6.5 fold increase in half-life compared to ANP despite its shorter C-terminal extension. Although the degradation pattern was similar, the residues within the Ring altered the preferred peptide bond for cleavage. This observation led us hypothesize that the orientation of KNP ring within the pocket of NEP is misguided in the presence of two DR residues within the sequence.

The creation of Ring mutants were D3, R4, D14 in KNP Ring have been sequentially replaced by G to mimic ANP, aided in the understanding the influence of these residues on NPR-A activation and NEP hydrolysis. The replacement of R4 to G while retaining both D residues, rendered the peptide to lose 30 fold activity when compared to native Ring, while replacement of both D residues to G while retaining R4 increased its ability to activate NPR-A. From the NPR-A- ANP complex crystal structure it was evident that G3 and G20 were in the vicinity of E169A and E169B of the receptor. These facts suggested that R4 of Ring aided the placement of both the D residues away from their actual pockets which are negatively charged. This observation was further strengthened as the incorporation of D3, R4 and D20 into ANP ring (K-ANP) resulted in 10 fold loss in its ability to activate NPR-A similar to Ring in comparison to ANP.

The degradability of these mutant Rings implied that D3, R4 and D20 have crucial roles in conferring resistance to degradation. K-ANP showed an increased half-life 4 times longer than ANP, which further elucidated the role of these residues. We observe that inclusion of D, R, and D extended the half-life of ANP but not as long as Ring, which could be attributed to other

residues within the ring. A sequence comparison between different NPs show that position 10, 11, 12 and 13 of KNP- Ring was occupied by polar residues which are probably not recognized by NEP which cleaves a hydrophobic residue. BNP has polar residues in all these positions while ANP, CNP and DNP have a combination of polar and hydrophobic residues. Among these residues position 12 of the NP ring is variable position. This position is occupied Q in ANP, S in BNP, V in DNP, M in CNP while T in Ring. Thus evaluating the role of the residue at position 12 could potentially increase the half-life of NPs. Thus, the investigation of residues within the Ring of KNP has shed light on possible role of residues within the ring to confer resistance.

Following the study on NEP mediated hydrolysis of Ring, we concluded a preliminary study conducted on the preference of Ring to bind to the clearance receptor. Structural studies on NPR-C show that the receptor offers a rigid scaffold for ligand interaction. The peptides adopt their local structure to fit into a fixed volume available in the binding pocket. Our groundwork experiment which assessed the cGMP response of ANP and Ring in cells expressing both NPR-A and NPR-C was indicative that Ring of KNP had lower ability to bind to NPR-C in comparison to ANP. This may be attributed to the bulky amino acid replacements in Ring of KNP compared to ANP which would require larger volume for accommodation into the NPR-C binding pocket.

Thus far, all known previous studies have shown that longer the N- and C-termini extension of NP better is its resistance to hydrolysis. Our study has extrapolated the information known about the structural requirements of a NP to have increased stability. With Ring of KNP as the model, we have

demonstrated that residues within the ring of NP have influential role in conferring higher stability to both the processes of degradation that are equally involved in the clearance of NPs. Further incorporation of the identified residues into ANP ring, improved its stability, which puts forward the possibility of creating the “ring of resistance”.

CHAPTER 4

Lessons from KNP

Chapter 4: Lessons from KNP

4.1. Conclusions

This thesis focuses on the mechanisms of action and clearance of a unique NP-like peptide; KNP which was initially identified from the partial cDNA library *Bungarus flaviceps* venom gland. KNP is composed of 60 amino acid residues protein with a 5 residue N-terminal extension, 17- residue conserved NP ring and 38 residue long C-terminal tail. Sequence and structural analysis of KNP showed that the C-terminal tail has a unique sequence which does not match with any known sequences in the non-redundant database. Also the last 21 residues of the C-terminal tail has propensity to form an α- helix, a distinctive feature not known in any other NPs. Ring of KNP had two substitutions at position 3 and 14 where a conserved G residue was replaced by D. These differences in the sequence and structure of KNP are pivotal in modulating KNP bioactivity.

To elucidate the mechanism of action of KNP, this protein was recombinantly expressed in *E.coli* and purified by various chromatographic methods. KNP was tested for its activity using in-vivo, ex-vivo and in-vitro assays. KNP was able to relax aortic strips with intact endothelium with lower potency compared to ANP, but had no significant relaxant effect on aortic strips which were denuded of endothelium. This finding established that KNP acts via an NPR-independent mechanism to elicit vasorelaxation.

In anesthetized rats, infusion of ANP or KNP dropped blood pressure, but in distinctly different patterns. ANP caused a quick drop in blood pressure which recovered in a short time. In contrast, KNP caused a continuous drop in blood pressure which persisted throughout the experimental period. Further animals

infused with ANP showed remarkable diuresis while there was no renal response to KNP. These results conclusively showed that KNP was a non-classical NP.

Different deletion and truncation mutants of KNP were designed based on its predicted structure to understand its non- canonical activity. Ring of KNP behaved exactly like a classical NP with lower potency while the putative Helix exhibits an identical response to KNP (i.e. equivalent potency) on endothelium-denuded and intact aortic strips. Further deletion of the putative helical segment from KNP diminished its activity significantly.

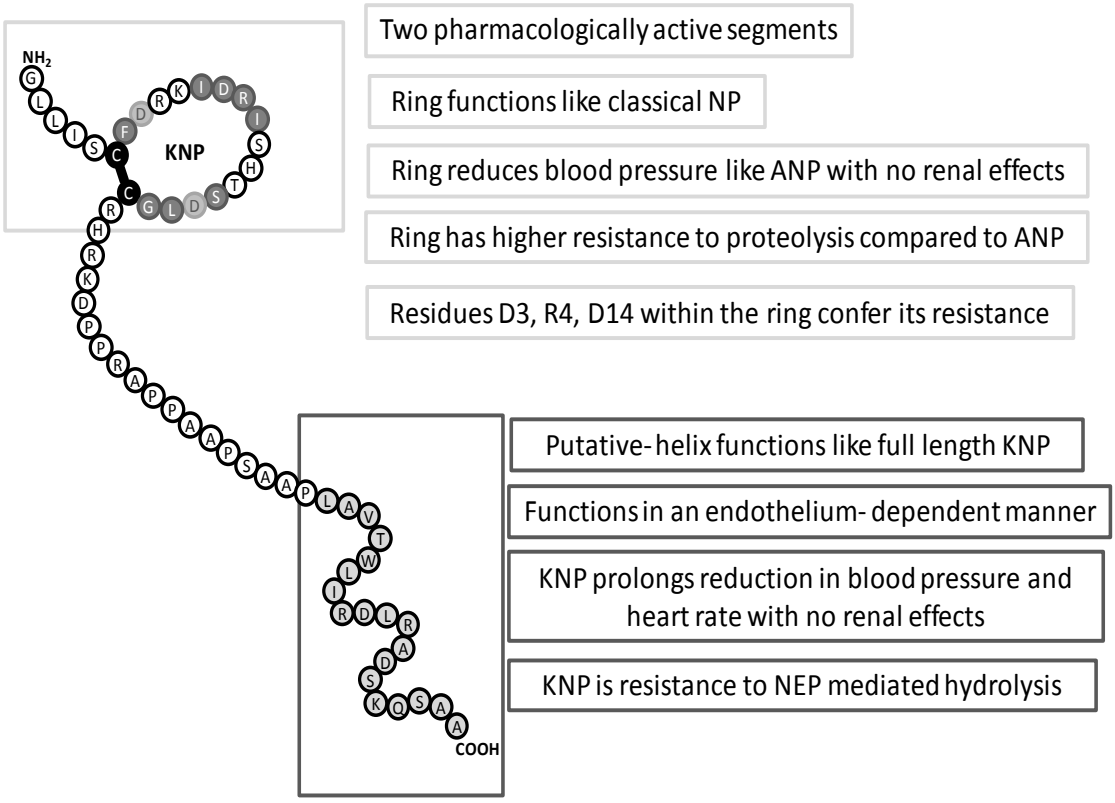

Figure 4.1. KNP- A non-classical NP

These observations demonstrated that KNP has two pharmacologically active segments namely; ring and helix. Helix contributed to the activity of KNP. Further on cells expressing NPR-A, Ring was able to produce a dose-dependent cGMP response. But the ability of the ring to bind to NPR-A was significantly lost in the presence of the C-terminal tail of KNP. Thus, the C-terminal tail of KNP seemed to confer its biological action while redirecting its ring away from the NPR.

Using specific inhibitors for endothelium dependent vasorelaxation pathway, nitric oxide, prostacyclin and hyperpolarization factor were shown to be necessary to mediate KNP and helix signaling. From these observations, KNP can be classified as a non-classical NP, which functions via its C-terminal tail to evoke endothelium-dependent vasorelaxation despite the presence of a potentially functional NP- ring.

Although in-vitro and ex-vivo establish the role of C-terminal tail in conferring the entire function to KNP, infusion of different truncations of KNP in experimental rats, showed that the in-vivo activity of KNP may be a combination effect of both the pharmacophores.

Following the characterization of biological action of KNP, its resistance to degradation was evaluated. KNP had a remarkable resistance to degradation (> 150 min) when incubated with NEP, a major enzyme involved in the clearance of NPs. The Ring of KNP had two substitutions of evolutionarily conserved residue (G at position 3 and 14 were replaced by D). Ring showed an increased half-life which was 6.5 times greater compared to ANP. Sequential mutations of selected residues with the Ring of KNP to G showed that D3, R4 and D14 were key residues which conferred resistance to Ring degradation.

Studies prior to this have main focused on improving half-life of NPs by increasing their size by addition of longer N-terminal and C-terminal tails. This study pinpoints the importance of residues within the ring of NPs to influence degradation. Further, as a proof of concept, incorporation of D3, R4 and D13 in the ring of ANP demonstrated that the half-life of mutant K-ANP increased to 4 times higher than ANP.

Thus, the studies described in this thesis presents several interesting observations contributing to the understanding of NPs and open up avenues for further research on KNP and the NEP resistant Ring of KNP.

4.2. Future Perspectives

4.2.1. Immediate prospects

The first part of the study encompassed in this thesis describes the bioassay-determined actions KNP while the second part illustrates KNP's resistance to degradation. There are important further questions to be addressed in both the sections as follows:

4.2.1.1. Identification of the molecular target of Helix

As seen from the results described, Helix of KNP has no sequence similarity to any known peptides. We know that Helix requires NO, prostacyclin and hyperpolarization factors to cause vasodilation. It is evident that Helix is a NO stimulator. Hence, to identify the molecular target, the vasodilatory response of Helix may be evaluated in the presence of different inhibitors upstream of the identified mediators such as phospholipase C inhibitors, Gq protein inhibitors, potassium channel inhibitors.

4.2.1.2. In-vivo half-life of K-ANP

Through in-vitro experiments, K-ANP has been shown to have a longer half-life, although its potency is lowered compared to ANP. From a therapeutic perspective, ANP is associated in potent hypotension and short half- life. ANP with D3, R4 and D14 incorporated in the ring, called K-ANP is a less potent NP with longer half-life, pharmacologically desired characteristics. Hence, would be of great interest to look at in-vivo activity of K-ANP.

4.2.2. Big Picture

In spite of high activation of NP system during heart failure, the increased levels of circulating ANP and BNP are inadequate to counter the neurohormonal activation which leads to high sodium retention and congestion (Lee and Burnett, 2007a). Nevertheless, further elevating the circulating levels of ANP or BNP by intravenous infusion has bioactivity and reduces cardiac load, plasma renin levels together with increased natriuresis and diuresis. The discovery of different NPs from endogenous (alternately spliced BNP, familial mutation in ANP) and exogenous source (snake venom) has aided the creation of chimeric NPs which have potentially improved pharmacological characteristics. In order to gain insight into the therapeutic potential of a NP, there is necessity to evaluate its pharmacodynamic properties in larger animal models (Both normal and with heart failure).

4.2.2.1 Influence of KNP on hemodynamic parameters in larger animal models

To understand the therapeutic potential of KNP, its effect of hemodynamic s and renal parameters has to be evaluated in larger animal models. Pharmacodynamics of a number of NPs have been assessed in both dogs and

sheep models. Hence, similar dosages of KNP may be evaluated in both anesthetized and conscious healthy animals. Further, KNP can be evaluated on animal models with heart failure. These models may help predict the efficiency of KNP in human heart failure.

4.2.2.2. Development of NEP resistant NP

The second part of this thesis has increased understanding of the role of residues within the NP ring in conferring resistance to hydrolysis. Further research is necessary to identify other potential residues within the ring which influence the peptide's degradability. Incorporation of these residues in NP will result in increased half-life of the peptide which would lessen the necessary dosage of NP infusions and potentially increase the pharmacological efficacy of NPs in patients with hypertension.

4.2.2.3. Metabolism of KNP in-vivo

The present findings show that both the pharmacophore seems to be contributing to the in-vivo activity of KNP. Further, in-vitro and ex-vivo experiments have conclusively shown the presence of the tail prevents the ring from binding to NPR. Hence, one probable explanation to these observations is the metabolism of KNP in-vivo. KNP might be proteolytically cleaved which renders both the segments to function. Hence, in-vivo cleavage products to KNP can be assessed using mass-spectrometric analysis of plasma samples collected at various time points after injecting KNP into rats.

Bibliography

Abassi, Z.A., Golomb, E., Agbaria, R., Roller, P.P., Tate, J., and Keiser, H.R. (1994). Hydrolysis of iodine labelled urodilatin and ANP by recombinant neutral endopeptidase EC. 3.4.24.11. British journal of pharmacology *113*, 204-208.

Abraham, W.T., Adams, K.F., Fonarow, G.C., Costanzo, M.R., Berkowitz, R.L., LeJemtel, T.H., Cheng, M.L., Wynne, J., and Invest, A.S.A.C. (2005). In-hospital mortality in patients with acute decompensated heart failure requiring intravenous vasoactive medications - An analysis from the Acute Decompensated Heart Failure National Registry (ADHERE). Journal of the American College of Cardiology *46*, 57-64.

Ahluwalia, A., MacAllister, R.J., and Hobbs, A.J. (2004). Vascular actions of natriuretic peptides. Cyclic GMP-dependent and -independent mechanisms. Basic research in cardiology *99*, 83-89.

Alioua, A., Tanaka, Y., Wallner, M., Hofmann, F., Ruth, P., Meera, P., and Toro, L. (1998). The large conductance, voltage-dependent, and calcium-sensitive K+ channel, Hslo, is a target of cGMP-dependent protein kinase phosphorylation in vivo. The Journal of biological chemistry *273*, 32950-32956.

Amininasab, M., Elmi, M.M., Endlich, N., Endlich, K., Parekh, N., Naderi-Manesh, H., Schaller, J., Mostafavi, H., Sattler, M., Sarbolouki, M.N., *et al.* (2004). Functional and structural characterization of a novel member of the natriuretic family of peptides from the venom of Pseudocerastes persicus. FEBS letters *557*, 104-108.

Anand-Srivastava, M.B. (2005). Natriuretic peptide receptor-C signaling and regulation. Peptides *26*, 1044-1059.

Anand-Srivastava, M.B., Sairam, M.R., and Cantin, M. (1990). Ring-deleted analogs of atrial natriuretic factor inhibit adenylate cyclase/cAMP system. Possible coupling of clearance atrial natriuretic factor receptors to adenylate cyclase/cAMP signal transduction system. The Journal of biological chemistry *265*, 8566-8572.

Anand-Srivastava, M.B., Sehl, P.D., and Lowe, D.G. (1996). Cytoplasmic domain of natriuretic peptide receptor-C inhibits adenylyl cyclase. Involvement of a pertussis toxin-sensitive G protein. The Journal of biological chemistry *271*, 19324-19329.

Anwaruddin, S., Lloyd-Jones, D.M., Baggish, A., Chen, A., Krauser, D., Tung, R., Chae, C., and Januzzi, J.L., Jr. (2006). Renal function, congestive heart failure, and amino-terminal pro-brain natriuretic peptide measurement: results from the ProBNP Investigation of Dyspnea in the Emergency Department (PRIDE) Study. Journal of the American College of Cardiology *47*, 91-97.

Barbouche, R., Marrakchi, N., Mansuelle, P., Krifi, M., Fenouillet, E., Rochat, H., and el Ayeb, M. (1996). Novel anti-platelet aggregation polypeptides from Vipera lebetina venom: isolation and characterization. FEBS letters *392*, 6-10.

Barletta, G., Lazzeri, C., Vecchiarino, S., Del Bene, R., Messeri, G., Dello Sbarba, A., Mannelli, M., and La Villa, G. (1998). Low-dose C-type natriuretic peptide does not affect cardiac and renal function in humans. Hypertension *31*, 802-808.

Bazaa, A., Marrakchi, N., El Ayeb, M., Sanz, L., and Calvete, J.J. (2005). Snake venomics: comparative analysis of the venom proteomes of the Tunisian snakes Cerastes cerastes, Cerastes vipera and Macrovipera lebetina. Proteomics *5*, 4223-4235.

Beavo, J.A. (1995). Cyclic nucleotide phosphodiesterases: functional implications of multiple isoforms. Physiological reviews *75*, 725-748.

Bennett, B.D., Bennett, G.L., Vitangcol, R.V., Jewett, J.R., Burnier, J., Henzel, W., and Lowe, D.G. (1991). Extracellular domain-IgG fusion proteins for three human natriuretic peptide receptors. Hormone pharmacology and application to solid phase screening of synthetic peptide antisera. The Journal of biological chemistry *266*, 23060-23067.

Bettencourt, P., Azevedo, A., Pimenta, J., Frioes, F., Ferreira, S., and Ferreira, A. (2004). N-terminal-pro-brain natriuretic peptide predicts outcome after hospital discharge in heart failure patients. Circulation *110*, 2168-2174.

Bovy, P.R. (1990). Structure activity in the atrial natriuretic peptide (ANP) family. Medicinal research reviews *10*, 115-142.

Brandt, R.R., Mattingly, M.T., Clavell, A.L., Barclay, P.L., and Burnett, J.C., Jr. (1997). Neutral endopeptidase regulates C-type natriuretic peptide metabolism but does not potentiate its bioactivity in vivo. Hypertension *30*, 184-190.

Brenner, B.M., Ballermann, B.J., Gunning, M.E., and Zeidel, M.L. (1990). Diverse biological actions of atrial natriuretic peptide. Physiological reviews *70*, 665-699.

Breuhaus, B.A., Saneii, H.H., Brandt, M.A., and Chimoskey, J.E. (1985). Atriopeptin II lowers cardiac output in conscious sheep. The American journal of physiology *249*, R776-780.

Brockhoff, C., Warnholtz, A., and Munzel, T. (2000). [Atrial natriuretic peptides: diagnostic and therapeutic potential]. Therapeutische Umschau Revue therapeutique *57*, 305-312.

Brunner-La Rocca, H.P., Kaye, D.M., Woods, R.L., Hastings, J., and Esler, M.D. (2001). Effects of intravenous brain natriuretic peptide on regional sympathetic activity in patients with chronic heart failure as compared with healthy control subjects. Journal of the American College of Cardiology *37*, 1221-1227.

Burnett, J.C., Jr., Granger, J.P., and Opgenorth, T.J. (1984). Effects of synthetic atrial natriuretic factor on renal function and renin release. The American journal of physiology *247*, F863-866.

Burnett, J.C., Jr., Kao, P.C., Hu, D.C., Heser, D.W., Heublein, D., Granger, J.P., Opgenorth, T.J., and Reeder, G.S. (1986). Atrial natriuretic peptide elevation in congestive heart failure in the human. Science *231*, 1145-1147.

Burrell, L.M., Lambert, H.J., and Baylis, P.H. (1991). Effect of atrial natriuretic peptide on thirst and arginine vasopressin release in humans. The American journal of physiology *260*, R475-479.

Busse, R., Edwards, G., Feletou, M., Fleming, I., Vanhoutte, P.M., and Weston, A.H. (2002). EDHF: bringing the concepts together. Trends in pharmacological sciences *23*, 374-380.

Cao, L., and Gardner, D.G. (1995). Natriuretic peptides inhibit DNA synthesis in cardiac fibroblasts. Hypertension *25*, 227-234.

Carvajal, J.A., Germain, A.M., Huidobro-Toro, J.P., and Weiner, C.P. (2000). Molecular mechanism of cGMP-mediated smooth muscle relaxation. Journal of cellular physiology *184*, 409-420.

Cataliotti, A., Boerrigter, G., Costello-Boerrigter, L.C., Schirger, J.A., Tsuruda, T., Heublein, D.M., Chen, H.H., Malatino, L.S., and Burnett, J.C., Jr. (2004). Brain natriuretic peptide enhances renal actions of furosemide and suppresses furosemide-induced aldosterone activation in experimental heart failure. Circulation *109*, 1680-1685.

Chang, M.S., Lowe, D.G., Lewis, M., Hellmiss, R., Chen, E., and Goeddel, D.V. (1989). Differential activation by atrial and brain natriuretic peptides of two different receptor guanylate cyclases. Nature *341*, 68-72.

Charles, C.J., Espiner, E.A., Nicholls, M.G., Richards, A.M., Yandle, T.G., Protter, A., and Kosoglou, T. (1996). Clearance receptors and endopeptidase 24.11: equal role in natriuretic peptide metabolism in conscious sheep. The American journal of physiology *271*, R373-380.

Chartier, L., Schiffrin, E., Thibault, G., and Garcia, R. (1984). Atrial natriuretic factor inhibits the stimulation of aldosterone secretion by angiotensin II, ACTH and potassium in vitro and angiotensin II-induced steroidogenesis in vivo. Endocrinology *115*, 2026-2028.

Chen, H.H., Grantham, J.A., Schirger, J.A., Jougasaki, M., Redfield, M.M., and Burnett, J.C., Jr. (2000). Subcutaneous administration of brain natriuretic peptide in experimental heart failure. Journal of the American College of Cardiology *36*, 1706-1712.

Cheung, B. (1994). Measurement of plasma brain natriuretic peptide in heart failure. Lancet *343*, 858.

Chobanian, A.V., Bakris, G.L., Black, H.R., Cushman, W.C., Green, L.A., Izzo, J.L., Jr., Jones, D.W., Materson, B.J., Oparil, S., Wright, J.T., Jr., *et al.* (2003). The Seventh Report of the Joint National Committee on Prevention, Detection, Evaluation, and Treatment of High Blood Pressure: the JNC 7 report. JAMA : the journal of the American Medical Association *289*, 2560-2572.

Chusho, H., Tamura, N., Ogawa, Y., Yasoda, A., Suda, M., Miyazawa, T., Nakamura, K., Nakao, K., Kurihara, T., Komatsu, Y., *et al.* (2001). Dwarfism and early death in mice lacking C-type natriuretic peptide. Proceedings of the National Academy of Sciences of the United States of America *98*, 4016-4021.

Clerico, A., Iervasi, G., and Pilo, A. (2000). Turnover studies on cardiac natriuretic peptides: methodological, pathophysiological and therapeutical considerations. Current drug metabolism *1*, 85-105.

Cody, R.J., Atlas, S.A., Laragh, J.H., Kubo, S.H., Covit, A.B., Ryman, K.S., Shaknovich, A., Pondolfino, K., Clark, M., Camargo, M.J., *et al.* (1986). Atrial natriuretic factor in normal subjects and heart failure patients. Plasma levels and renal, hormonal, and hemodynamic responses to peptide infusion. The Journal of clinical investigation *78*, 1362-1374.

Cohen, D., Koh, G.Y., Nikonova, L.N., Porter, J.G., and Maack, T. (1996). Molecular determinants of the clearance function of type C receptors of natriuretic peptides. The Journal of biological chemistry *271*, 9863-9869.

Collinson, P.O., Barnes, S.C., Gaze, D.C., Galasko, G., Lahiri, A., and Senior, R. (2004). Analytical performance of the N terminal pro B type natriuretic peptide (NT-proBNP) assay on the Elecsys 1010 and 2010 analysers. European journal of heart failure *6*, 365-368.

Colucci, W.S. (2000). Intravenous nesiritide, a natriuretic peptide, in the treatment of decompensated congestive heart failure (vol 343, pg 246, 2000). New Engl J Med *343*, 1504-1504.

de Boer, R.A., van Veldhuisen, D.J., Gans, R.O., and Gansevoort, R.T. (2003). [Treatment of hypertension: angiotensin-II antagonists potentially better than beta-blockers in the occurrence of cardiovascular and cerebrovascular damage; the LIFE study in perspective]. Nederlands tijdschrift voor geneeskunde *147*, 96-99.

de Bold, A.J. (1985). Atrial natriuretic factor: a hormone produced by the heart. Science *230*, 767-770.

de Bold, A.J., Borenstein, H.B., Veress, A.T., and Sonnenberg, H. (1981). A rapid and potent natriuretic response to intravenous injection of atrial myocardial extract in rats. Life sciences *28*, 89-94.

de Bold, A.J., de Bold, M.L., and Sarda, I.R. (1986). Functional-morphological studies on in vitro cardionatrin release. Journal of hypertension Supplement : official journal of the International Society of Hypertension *4*, S3-7.

Del Bo, A., Le Doux, J.E., and Reis, D.J. (1985). Sympathetic nervous system and control of blood pressure during natural behaviour. Journal of hypertension Supplement : official journal of the International Society of Hypertension *3*, S105-106.

Dickey, D.M., Burnett, J.C., Jr., and Potter, L.R. (2008). Novel bifunctional natriuretic peptides as potential therapeutics. The Journal of biological chemistry *283*, 35003-35009.

Dickey, D.M., and Potter, L.R. (2011). Dendroaspis natriuretic peptide and the designer natriuretic peptide, CD-NP, are resistant to proteolytic inactivation. Journal of molecular and cellular cardiology *51*, 67-71.

Dickey, D.M., Yoder, A.R., and Potter, L.R. (2009). A familial mutation renders atrial natriuretic Peptide resistant to proteolytic degradation. The Journal of biological chemistry *284*, 19196-19202.

Dickstein, K., Vardas, P.E., Auricchio, A., Daubert, J.C., Linde, C., McMurray, J., Ponikowski, P., Priori, S.G., Sutton, R., and van Veldhuisen, D.J. (2010). 2010 Focused Update of ESC Guidelines on device therapy in heart failure: an update of the 2008 ESC Guidelines for the diagnosis and treatment of acute and chronic heart failure and the 2007 ESC guidelines for cardiac and resynchronization therapy. Developed with the special contribution of the Heart Failure Association and the European Heart Rhythm Association. European heart journal *31*, 2677-2687.

Epstein, M., and Calhoun, D.A. (2011). Aldosterone blockers (mineralocorticoid receptor antagonism) and potassium-sparing diuretics. J Clin Hypertens (Greenwich) *13*, 644-648.

Evangelista, J.S., Martins, A.M., Nascimento, N.R., Sousa, C.M., Alves, R.S., Toyama, D.O., Toyama, M.H., Evangelista, J.J., Menezes, D.B., Fonteles, M.C., *et al.* (2008). Renal and vascular effects of the natriuretic peptide isolated from Crotalus durissus cascavella venom. Toxicon : official journal of the International Society on Toxinology *52*, 737-744.

Farris, W., Mansourian, S., Chang, Y., Lindsley, L., Eckman, E.A., Frosch, M.P., Eckman, C.B., Tanzi, R.E., Selkoe, D.J., and Guenette, S. (2003). Insulin-degrading enzyme regulates the levels of insulin, amyloid beta-protein, and the beta-amyloid

precursor protein intracellular domain in vivo. Proceedings of the National Academy of Sciences of the United States of America *100*, 4162-4167.

Fiscus, R.R., Rapoport, R.M., Waldman, S.A., and Murad, F. (1985). Atriopeptin II elevates cyclic GMP, activates cyclic GMP-dependent protein kinase and causes relaxation in rat thoracic aorta. Biochimica et biophysica acta *846*, 179-184.

Florkowski, C.M., Richards, A.M., Espiner, E.A., Yandle, T.G., and Frampton, C. (1994). Renal, endocrine, and hemodynamic interactions of atrial and brain natriuretic peptides in normal men. The American journal of physiology *266*, R1244-1250.

Forssmann, W.G., Richter, R., and Meyer, M. (1998). The endocrine heart and natriuretic peptides: histochemistry, cell biology, and functional aspects of the renal urodilatin system. Histochemistry and cell biology *110*, 335-357.

Frolov, V.A., Kimura, K., Drozdova, G.A., Ishii, M., Sugimoto, T., Matsuo, N., and Ogava, S. (1989). [Effects of atrial natriuretic factor on the cardiovascular system and several parameters of renal excretory function in spontaneously hypertensive rats]. Biulleten' eksperimental'noi biologii i meditsiny *108*, 24-26.

Fry, B.G., Wickramaratana, J.C., Lemme, S., Beuve, A., Garbers, D., Hodgson, W.C., and Alewood, P. (2005). Novel natriuretic peptides from the venom of the inland taipan (Oxyuranus microlepidotus): isolation, chemical and biological characterisation. Biochemical and biophysical research communications *327*, 1011-1015.

Furchgott, R.F. (1984). The Role of Endothelium in the Responses of Vascular Smooth-Muscle to Drugs. Annu Rev Pharmacol *24*, 175-197.

Furuya, M., Yoshida, M., Hayashi, Y., Ohnuma, N., Minamino, N., Kangawa, K., and Matsuo, H. (1991). C-type natriuretic peptide is a growth inhibitor of rat vascular smooth muscle cells. Biochemical and biophysical research communications *177*, 927-931.

Gaffney, P.J., Marsh, N.A., and Talalak, P. (1979). Snake venoms and haemostasis: some suggested mechanisms of action. The Southeast Asian journal of tropical medicine and public health *10*, 258-265.

Gerbes, A.L., and Vollmar, A.M. (1990). Degradation and clearance of atrial natriuretic factors (ANF). Life sciences *47*, 1173-1180.

Gheorghiade, M., Zannad, F., Sopko, G., Klein, L., Pina, I.L., Konstam, M.A., Massie, B.M., Roland, E., Targum, S., Collins, S.P., *et al.* (2005). Acute heart failure syndromes: current state and framework for future research. Circulation *112*, 3958-3968.

Go, A.S., Mozaffarian, D., Roger, V.L., Benjamin, E.J., Berry, J.D., Blaha, M.J., Dai, S., Ford, E.S., Fox, C.S., Franco, S., *et al.* (2014). Heart disease and stroke statistics--2014 update: a report from the American Heart Association. Circulation *129*, e28-e292.

Gustafsson, F., Steensgaard-Hansen, F., Badskjaer, J., Poulsen, A.H., Corell, P., and Hildebrandt, P. (2005). Diagnostic and prognostic performance of N-terminal ProBNP in primary care patients with suspected heart failure. Journal of cardiac failure *11*, S15-20.

Guyenet, P.G. (2006). The sympathetic control of blood pressure. Nature reviews Neuroscience *7*, 335-346.

Hall, J.E., Granger, J.P., do Carmo, J.M., da Silva, A.A., Dubinion, J., George, E., Hamza, S., Speed, J., and Hall, M.E. (2012). Hypertension: physiology and pathophysiology. Comprehensive Physiology *2*, 2393-2442.

Harris, P.J., Cullinan, M., Thomas, D., and Morgan, T.O. (1987a). Digital image capture and analysis for split-drop micropuncture. Pflugers Archiv : European journal of physiology *408*, 615-618.

Harris, P.J., Thomas, D., and Morgan, T.O. (1987b). Atrial natriuretic peptide inhibits angiotensin-stimulated proximal tubular sodium and water reabsorption. Nature *326*, 697-698.

He, X., Chow, D., Martick, M.M., and Garcia, K.C. (2001). Allosteric activation of a spring-loaded natriuretic peptide receptor dimer by hormone. Science *293*, 1657-1662.

He, X.L., Dukkipati, A., and Garcia, K.C. (2006). Structural determinants of natriuretic peptide receptor specificity and degeneracy. Journal of molecular biology *361*, 698-714.

Hirsch, J.R., Skutta, N., and Schlatter, E. (2003). Signaling and distribution of NPR-Bi, the human splice form of the natriuretic peptide receptor type B. American journal of physiology Renal physiology *285*, F370-374.

Hollister, A.S., Rodeheffer, R.J., White, F.J., Potts, J.R., Imada, T., and Inagami, T. (1989). Clearance of atrial natriuretic factor by lung, liver, and kidney in human subjects and the dog. The Journal of clinical investigation *83*, 623-628.

Holmes, S.J., Espiner, E.A., Richards, A.M., Yandle, T.G., and Frampton, C. (1993). Renal, endocrine, and hemodynamic effects of human brain natriuretic peptide in normal man. The Journal of clinical endocrinology and metabolism *76*, 91-96.

Holtwick, R., Gotthardt, M., Skryabin, B., Steinmetz, M., Potthast, R., Zetsche, B., Hammer, R.E., Herz, J., and Kuhn, M. (2002). Smooth muscle-selective deletion of guanylyl cyclase-A prevents the acute but not chronic effects of ANP on blood pressure. Proceedings of the National Academy of Sciences of the United States of America *99*, 7142-7147.

Holtwick, R., van Eickels, M., Skryabin, B.V., Baba, H.A., Bubikat, A., Begrow, F., Schneider, M.D., Garbers, D.L., and Kuhn, M. (2003). Pressure-independent cardiac hypertrophy in mice with cardiomyocyte-restricted inactivation of the atrial natriuretic peptide receptor guanylyl cyclase-A. The Journal of clinical investigation *111*, 1399-1407.

Hu, R.M., Levin, E.R., Pedram, A., and Frank, H.J. (1992). Atrial natriuretic peptide inhibits the production and secretion of endothelin from cultured endothelial cells. Mediation through the C receptor. The Journal of biological chemistry *267*, 17384-17389.

Huo, X., Abe, T., and Misono, K.S. (1999). Ligand binding-dependent limited proteolysis of the atrial natriuretic peptide receptor: juxtamembrane hinge structure essential for transmembrane signal transduction. Biochemistry *38*, 16941-16951.

Ignarro, L.J. (1989). Biological actions and properties of endothelium-derived nitric oxide formed and released from artery and vein. Circulation research *65*, 1-21.

Jaubert, J., Jaubert, F., Martin, N., Washburn, L.L., Lee, B.K., Eicher, E.M., and Guenet, J.L. (1999). Three new allelic mouse mutations that cause skeletal overgrowth involve the natriuretic peptide receptor C gene (Npr3). Proceedings of the National Academy of Sciences of the United States of America *96*, 10278-10283.

John, S.W., Veress, A.T., Honrath, U., Chong, C.K., Peng, L., Smithies, O., and Sonnenberg, H. (1996). Blood pressure and fluid-electrolyte balance in mice with reduced or absent ANP. The American journal of physiology *271*, R109-114.

Johns, D.G., Ao, Z., Heidrich, B.J., Hunsberger, G.E., Graham, T., Payne, L., Elshourbagy, N., Lu, Q., Aiyar, N., and Douglas, S.A. (2007). Dendroaspis natriuretic peptide binds to the natriuretic peptide clearance receptor. Biochemical and biophysical research communications *358*, 145-149.

Johnson, G.R., Arik, L., and Foster, C.J. (1989). Metabolism of 125I-atrial natriuretic factor by vascular smooth muscle cells. Evidence for a peptidase that specifically removes the COOH-terminal tripeptide. The Journal of biological chemistry *264*, 11637-11642.

Johnson, G.R., and Foster, C.J. (1990). Partial characterization of a metalloendopeptidase activity produced by cultured endothelial cells that removes the COOH-terminal tripeptide from 125I-atrial natriuretic factor. Biochemical and biophysical research communications *167*, 110-116.

Kalra, P.R., Clague, J.R., Bolger, A.P., Anker, S.D., Poole-Wilson, P.A., Struthers, A.D., and Coats, A.J. (2003). Myocardial production of C-type natriuretic peptide in chronic heart failure. Circulation *107*, 571-573.

Kambayashi, Y., Nakao, K., Kimura, H., Kawabata, T., Nakamura, M., Inouye, K., Yoshida, N., and Imura, H. (1990). Biological characterization of human brain natriuretic peptide (BNP) and rat BNP: species-specific actions of BNP. Biochemical and biophysical research communications *173*, 599-605.

Kangawa, K., Fukuda, A., and Matsuo, H. (1985). Structural identification of beta- and gamma-human atrial natriuretic polypeptides. Nature *313*, 397-400.

Kangawa, K., and Matsuo, H. (1984). Purification and complete amino acid sequence of alpha-human atrial natriuretic polypeptide (alpha-hANP). Biochemical and biophysical research communications *118*, 131-139.

Kapoun, A.M., Liang, F., O'Young, G., Damm, D.L., Quon, D., White, R.T., Munson, K., Lam, A., Schreiner, G.F., and Protter, A.A. (2004). B-type natriuretic peptide exerts broad functional opposition to transforming growth factor-beta in primary human cardiac fibroblasts: fibrosis, myofibroblast conversion, proliferation, and inflammation. Circulation research *94*, 453-461.

Kasama, S., Toyama, T., Hatori, T., Sumino, H., Kumakura, H., Takayama, Y., Ichikawa, S., Suzuki, T., and Kurabayashi, M. (2006). Comparative effects of valsartan and enalapril on cardiac sympathetic nerve activity and plasma brain natriuretic peptide in patients with congestive heart failure. Heart *92*, 625-630.

Kawakami, H., Sumimoto, T., Hamada, M., Mukai, M., Shigematsu, Y., Matsuoka, H., Abe, M., and Hiwada, K. (1995). Acute effect of glyceryl trinitrate on systolic blood pressure and other hemodynamic variables. Angiology *46*, 151-156.

Kishimoto, I., Dubois, S.K., and Garbers, D.L. (1996). The heart communicates with the kidney exclusively through the guanylyl cyclase-A receptor: acute handling of

sodium and water in response to volume expansion. Proceedings of the National Academy of Sciences of the United States of America *93*, 6215-6219.

Kleinert, H.D., Volpe, M., Odell, G., Marion, D., Atlas, S.A., Camargo, M.J., Laragh, J.H., and Maack, T. (1986). Cardiovascular effects of atrial natriuretic factor in anesthetized and conscious dogs. Hypertension *8*, 312-316.

Koller, K.J., Lowe, D.G., Bennett, G.L., Minamino, N., Kangawa, K., Matsuo, H., and Goeddel, D.V. (1991). Selective activation of the B natriuretic peptide receptor by C-type natriuretic peptide (CNP). Science *252*, 120-123.

Komalavilas, P., and Lincoln, T.M. (1996). Phosphorylation of the inositol 1,4,5-trisphosphate receptor. Cyclic GMP-dependent protein kinase mediates cAMP and cGMP dependent phosphorylation in the intact rat aorta. The Journal of biological chemistry *271*, 21933-21938.

Komatsu, Y., Itoh, H., Suga, S., Igaki, T., Ogawa, Y., Kishimoto, I., Nakagawa, O., Yoshimasa, T., and Nakao, K. (1996). Regulation of secretion and clearance of C-type natriuretic peptide in the interaction of vascular endothelial cells and smooth muscle cells. Journal of hypertension *14*, 585-592.

Kubo, S.H., Rector, T.S., Heifetz, S.M., Sato, H., and Cohn, J.N. (1990). Atrial natriuretic factor attenuates sympathetic reflexes during lower body negative pressure in normal men. Journal of cardiovascular pharmacology *16*, 881-889.

Kurose, H., Inagami, T., and Ui, M. (1987). Participation of adenosine 5'-triphosphate in the activation of membrane-bound guanylate cyclase by the atrial natriuretic factor. FEBS letters *219*, 375-379.

Lachance, D., Garcia, R., Gutkowska, J., Cantin, M., and Thibault, G. (1986). Mechanisms of release of atrial natriuretic factor. I. Effect of several agonists and steroids on its release by atrial minces. Biochemical and biophysical research communications *135*, 1090-1098.

Langenickel, T.H., Buttgereit, J., Pagel-Langenickel, I., Lindner, M., Monti, J., Beuerlein, K., Al-Saadi, N., Plehm, R., Popova, E., Tank, J., *et al.* (2006). Cardiac hypertrophy in transgenic rats expressing a dominant-negative mutant of the natriuretic peptide receptor B. Proceedings of the National Academy of Sciences of the United States of America *103*, 4735-4740.

Lee, C.Y., and Burnett, J.C., Jr. (2007a). Natriuretic peptides and therapeutic applications. Heart failure reviews *12*, 131-142.

Lee, C.Y.W., and Burnett, J.C. (2007b). Natriuretic peptides and therapeutic applications. Heart failure reviews *12*, 131-142.

Lee, C.Y.W., Chen, H.H., Lisy, O., Swan, S., Cannon, C., Lieu, H.D., and Burnett, J.C. (2009). Pharmacodynamics of a Novel Designer Natriuretic Peptide, CD-NP, in a First-in-Human Clinical Trial in Healthy Subjects. Journal of clinical pharmacology *49*, 668-673.

Li, B., Tom, J.Y., Oare, D., Yen, R., Fairbrother, W.J., Wells, J.A., and Cunningham, B.C. (1995). Minimization of a polypeptide hormone. Science *270*, 1657-1660.

Light, D.B., Corbin, J.D., and Stanton, B.A. (1990). Dual ion-channel regulation by cyclic GMP and cyclic GMP-dependent protein kinase. Nature *344*, 336-339.

Lindenfeld, J., Albert, N.M., Boehmer, J.P., Collins, S.P., Ezekowitz, J.A., Givertz, M.M., Katz, S.D., Klapholz, M., Moser, D.K., Rogers, J.G., *et al.* (2010). HFSA 2010 Comprehensive Heart Failure Practice Guideline. Journal of cardiac failure *16*, e1-194.

Lisy, O., Huntley, B.K., McCormick, D.J., Kurlansky, P.A., and Burnett, J.C., Jr. (2008). Design, synthesis, and actions of a novel chimeric natriuretic peptide: CD-NP. Journal of the American College of Cardiology *52*, 60-68.

Lisy, O., Jougasaki, M., Heublein, D.M., Schirger, J.A., Chen, H.H., Wennberg, P.W., and Burnett, J.C. (1999). Renal actions of synthetic dendroaspis natriuretic peptide. Kidney international *56*, 502-508.

Lopez, M.J., Garbers, D.L., and Kuhn, M. (1997). The guanylyl cyclase-deficient mouse defines differential pathways of natriuretic peptide signaling. The Journal of biological chemistry *272*, 23064-23068.

Lowe, D.G., Chang, M.S., Hellmiss, R., Chen, E., Singh, S., Garbers, D.L., and Goeddel, D.V. (1989). Human atrial natriuretic peptide receptor defines a new paradigm for second messenger signal transduction. The EMBO journal *8*, 1377-1384.

Lu, B., Gerard, N.P., Kolakowski, L.F., Jr., Bozza, M., Zurakowski, D., Finco, O., Carroll, M.C., and Gerard, C. (1995). Neutral endopeptidase modulation of septic shock. The Journal of experimental medicine *181*, 2271-2275.

Lubien, E., DeMaria, A., Krishnaswamy, P., Clopton, P., Koon, J., Kazanegra, R., Gardetto, N., Wanner, E., and Maisel, A.S. (2002). Utility of B-natriuretic peptide in detecting diastolic dysfunction: comparison with Doppler velocity recordings. Circulation *105*, 595-601.

Maack, T., Atlas, S.A., Camargo, M.J., and Cogan, M.G. (1986). Renal hemodynamic and natriuretic effects of atrial natriuretic factor. Federation proceedings *45*, 2128-2132.

Maack, T., Suzuki, M., Almeida, F.A., Nussenzveig, D., Scarborough, R.M., McEnroe, G.A., and Lewicki, J.A. (1987). Physiological role of silent receptors of atrial natriuretic factor. Science *238*, 675-678.

MacGregor, G.A., Cappuccio, F.P., and Markandu, N.D. (1987). Sodium intake, high blood pressure, and calcium channel blockers. The American journal of medicine *82*, 16-22.

Manickavasagam, S., Merla, R., Koerner, M.M., Fujise, K., Kunapuli, S., Rosanio, S., and Barbagelata, A. (2009). Management of hypertension in chronic heart failure. Expert review of cardiovascular therapy *7*, 423-433.

Marin-Grez, M., Fleming, J.T., and Steinhausen, M. (1986). Atrial natriuretic peptide causes pre-glomerular vasodilatation and post-glomerular vasoconstriction in rat kidney. Nature *324*, 473-476.

Martin, F.L., Sangaralingham, S.J., Huntley, B.K., McKie, P.M., Ichiki, T., Chen, H.H., Korinek, J., Harders, G.E., and Burnett, J.C., Jr. (2012). CD-NP: a novel engineered dual guanylyl cyclase activator with anti-fibrotic actions in the heart. PloS one *7*, e52422.

Matsuo, H., and Kangawa, K. (1984). Human and rat atrial natriuretic polypeptides (hANP & rANP) purification, structure and biological activity. Clinical and experimental hypertension Part A, Theory and practice *6*, 1717-1722.

Mitchell, J.A., Ali, F., Bailey, L., Moreno, L., and Harrington, L.S. (2008). Role of nitric oxide and prostacyclin as vasoactive hormones released by the endothelium. Experimental physiology *93*, 141-147.

Miyagi, M., and Misono, K.S. (2000). Disulfide bond structure of the atrial natriuretic peptide receptor extracellular domain: conserved disulfide bonds among guanylate cyclase-coupled receptors. Biochimica et biophysica acta *1478*, 30-38.

Miyagi, M., Zhang, X., and Misono, K.S. (2000). Glycosylation sites in the atrial natriuretic peptide receptor: oligosaccharide structures are not required for hormone binding. European journal of biochemistry / FEBS *267*, 5758-5768.

Mukoyama, M., Nakao, K., Hosoda, K., Suga, S., Saito, Y., Ogawa, Y., Shirakami, G., Jougasaki, M., Obata, K., Yasue, H., *et al.* (1991). Brain natriuretic peptide as a novel cardiac hormone in humans. Evidence for an exquisite dual natriuretic peptide system, atrial natriuretic peptide and brain natriuretic peptide. The Journal of clinical investigation *87*, 1402-1412.

Muller, D., Schulze, C., Baumeister, H., Buck, F., and Richter, D. (1992). Rat insulin-degrading enzyme: cleavage pattern of the natriuretic peptide hormones ANP, BNP, and CNP revealed by HPLC and mass spectrometry. Biochemistry *31*, 11138-11143.

Murayama, N., Hayashi, M.A., Ohi, H., Ferreira, L.A., Hermann, V.V., Saito, H., Fujita, Y., Higuchi, S., Fernandes, B.L., Yamane, T., *et al.* (1997). Cloning and sequence analysis of a Bothrops jararaca cDNA encoding a precursor of seven bradykinin-potentiating peptides and a C-type natriuretic peptide. Proceedings of the National Academy of Sciences of the United States of America *94*, 1189-1193.

Nakamura, M., Ichikawa, K., Ito, M., Yamamori, B., Okinaka, T., Isaka, N., Yoshida, Y., Fujita, S., and Nakano, T. (1999). Effects of the phosphorylation of myosin phosphatase by cyclic GMP-dependent protein kinase. Cellular signalling *11*, 671-676.

Nakamura, S., Naruse, M., Naruse, K., Kawana, M., Nishikawa, T., Hosoda, S., Tanaka, I., Yoshimi, T., Yoshihara, I., Inagami, T., *et al.* (1991). Atrial natriuretic peptide and brain natriuretic peptide coexist in the secretory granules of human cardiac myocytes. American journal of hypertension *4*, 909-912.

Nakao, K., Itoh, H., Kambayashi, Y., Hosoda, K., Saito, Y., Yamada, T., Mukoyama, M., Arai, H., Shirakami, G., Suga, S., *et al.* (1990). Rat brain natriuretic peptide. Isolation from rat heart and tissue distribution. Hypertension *15*, 774-778.

Nakao, K., Mukoyama, M., Hosoda, K., Suga, S., Ogawa, Y., Saito, Y., Shirakami, G., Arai, H., Jougasaki, M., and Imura, H. (1991). Biosynthesis, secretion, and receptor selectivity of human brain natriuretic peptide. Canadian journal of physiology and pharmacology *69*, 1500-1506.

Norman, J.A., Little, D., Bolgar, M., and Di Donato, G. (1991). Degradation of brain natriuretic peptide by neutral endopeptidase: species specific sites of proteolysis determined by mass spectrometry. Biochemical and biophysical research communications *175*, 22-30.

Nussenzveig, D.R., Lewicki, J.A., and Maack, T. (1990). Cellular mechanisms of the clearance function of type C receptors of atrial natriuretic factor. The Journal of biological chemistry *265*, 20952-20958.

Ogawa, H., Qiu, Y., Ogata, C.M., and Misono, K.S. (2004). Crystal structure of hormone-bound atrial natriuretic peptide receptor extracellular domain: rotation mechanism for transmembrane signal transduction. The Journal of biological chemistry *279*, 28625-28631.

Ogawa, H., Qiu, Y., Philo, J.S., Arakawa, T., Ogata, C.M., and Misono, K.S. (2010). Reversibly bound chloride in the atrial natriuretic peptide receptor hormone-binding domain: possible allosteric regulation and a conserved structural motif for the chloride-binding site. Protein science : a publication of the Protein Society *19*, 544-557.

Olins, G.M., Patton, D.R., Bovy, P.R., and Mehta, P.P. (1988). A linear analog of atrial natriuretic peptide (ANP) discriminates guanylate cyclase-coupled ANP receptors from non-coupled receptors. The Journal of biological chemistry *263*, 10989-10993.

Oliver, P.M., Fox, J.E., Kim, R., Rockman, H.A., Kim, H.S., Reddick, R.L., Pandey, K.N., Milgram, S.L., Smithies, O., and Maeda, N. (1997). Hypertension, cardiac hypertrophy, and sudden death in mice lacking natriuretic peptide receptor A. Proceedings of the National Academy of Sciences of the United States of America *94*, 14730-14735.

Palmer, S.C., Prickett, T.C., Espiner, E.A., Yandle, T.G., and Richards, A.M. (2009). Regional release and clearance of C-type natriuretic peptides in the human circulation and relation to cardiac function. Hypertension *54*, 612-618.

Pan, S., Chen, H.H., Dickey, D.M., Boerrigter, G., Lee, C., Kleppe, L.S., Hall, J.L., Lerman, A., Redfield, M.M., Potter, L.R., *et al.* (2009). Biodesign of a renal-protective peptide based on alternative splicing of B-type natriuretic peptide. Proceedings of the National Academy of Sciences of the United States of America *106*, 11282-11287.

Pankow, K., Schwiebs, A., Becker, M., Siems, W.E., Krause, G., and Walther, T. (2009). Structural Substrate Conditions Required for Neutral Endopeptidase-Mediated Natriuretic Peptide Degradation. Journal of molecular biology *393*, 496-503.

Pfeifer, A., Aszodi, A., Seidler, U., Ruth, P., Hofmann, F., and Fassler, R. (1996). Intestinal secretory defects and dwarfism in mice lacking cGMP-dependent protein kinase II. Science *274*, 2082-2086.

Pfeifer, A., Klatt, P., Massberg, S., Ny, L., Sausbier, M., Hirneiss, C., Wang, G.X., Korth, M., Aszodi, A., Andersson, K.E., *et al.* (1998). Defective smooth muscle regulation in cGMP kinase I-deficient mice. The EMBO journal *17*, 3045-3051.

Potter, L.R. (2005). Domain analysis of human transmembrane guanylyl cyclase receptors: implications for regulation. Frontiers in bioscience : a journal and virtual library *10*, 1205-1220.

Potter, L.R., Abbey-Hosch, S., and Dickey, D.M. (2006). Natriuretic peptides, their receptors, and cyclic guanosine monophosphate-dependent signaling functions. Endocrine reviews *27*, 47-72.

Potter, L.R., and Garbers, D.L. (1992). Dephosphorylation of the guanylyl cyclase-A receptor causes desensitization. The Journal of biological chemistry *267*, 14531-14534.

Potter, L.R., and Hunter, T. (1998). Phosphorylation of the kinase homology domain is essential for activation of the A-type natriuretic peptide receptor. Molecular and cellular biology *18*, 2164-2172.

Potter, L.R., and Hunter, T. (1999). Identification and characterization of the phosphorylation sites of the guanylyl cyclase-linked natriuretic peptide receptors A and B. Methods *19*, 506-520.

Potter, L.R., Yoder, A.R., Flora, D.R., Antos, L.K., and Dickey, D.M. (2009). Natriuretic peptides: their structures, receptors, physiologic functions and therapeutic applications. Handbook of experimental pharmacology, 341-366.

Remme, W.J., and Swedberg, K. (2001). Guidelines for the diagnosis and treatment of chronic heart failure. European heart journal *22*, 1527-1560.

Richards, A.M., Crozier, I.G., Yandle, T.G., Espiner, E.A., Ikram, H., and Nicholls, M.G. (1993). Brain natriuretic factor: regional plasma concentrations and correlations with haemodynamic state in cardiac disease. British heart journal *69*, 414-417.

Richards, A.M., Lainchbury, J.G., Nicholls, M.G., Troughton, R.W., and Yandle, T.G. (2002). BNP in hormone-guided treatment of heart failure. Trends in endocrinology and metabolism: TEM *13*, 151-155.

Richards, A.M., McDonald, D., Fitzpatrick, M.A., Nicholls, M.G., Espiner, E.A., Ikram, H., Jans, S., Grant, S., and Yandle, T. (1988). Atrial natriuretic hormone has biological effects in man at physiological plasma concentrations. The Journal of clinical endocrinology and metabolism *67*, 1134-1139.

Richer, C., Pratz, J., Mulder, P., Mondot, S., Giudicelli, J.F., and Cavero, I. (1990). Cardiovascular and biological effects of K+ channel openers, a class of drugs with vasorelaxant and cardioprotective properties. Life sciences *47*, 1693-1705.

Robinson, J.W., and Potter, L.R. (2011). ATP potentiates competitive inhibition of guanylyl cyclase A and B by the staurosporine analog, Go6976: reciprocal regulation of ATP and GTP binding. The Journal of biological chemistry *286*, 33841-33844.

Robinson, J.W., and Potter, L.R. (2012). Guanylyl cyclases A and B are asymmetric dimers that are allosterically activated by ATP binding to the catalytic domain. Science signaling *5*, ra65.

Robinson, M.A., Herron, A.J., Goodwin, B.S., and Grill, R.J. (2012). Suprapubic bladder catheterization of male spinal-cord-injured Sprague-Dawley rats. Journal of the American Association for Laboratory Animal Science : JAALAS *51*, 76-82.

Rockwell, N.C., Krysan, D.J., Komiyama, T., and Fuller, R.S. (2002). Precursor processing by kex2/furin proteases. Chemical reviews *102*, 4525-4548.

Rubattu, S., Sciarretta, S., Valenti, V., Stanzione, R., and Volpe, M. (2008). Natriuretic peptides: an update on bioactivity, potential therapeutic use, and implication in cardiovascular diseases. American journal of hypertension *21*, 733-741.

Rybalkin, S.D., Yan, C., Bornfeldt, K.E., and Beavo, J.A. (2003). Cyclic GMP phosphodiesterases and regulation of smooth muscle function. Circulation research *93*, 280-291.

Sabrane, K., Kruse, M.N., Fabritz, L., Zetsche, B., Mitko, D., Skryabin, B.V., Zwiener, M., Baba, H.A., Yanagisawa, M., and Kuhn, M. (2005). Vascular endothelium is critically involved in the hypotensive and hypovolemic actions of atrial natriuretic peptide. The Journal of clinical investigation *115*, 1666-1674.

Sabrane, K., Kruse, M.N., Gazinski, A., and Kuhn, M. (2009). Chronic endothelium-dependent regulation of arterial blood pressure by atrial natriuretic peptide: role of nitric oxide and endothelin-1. Endocrinology *150*, 2382-2387.

Sackner-Bernstein, J.D., Skopicki, H.A., and Aaronson, K.D. (2005). Risk of worsening renal function with nesiritide in patients with acutely decompensated heart failure. Circulation *111*, 1487-1491.

Saito, Y., Nakao, K., Nishimura, K., Sugawara, A., Okumura, K., Obata, K., Sonoda, R., Ban, T., Yasue, H., and Imura, H. (1987). Clinical application of atrial natriuretic polypeptide in patients with congestive heart failure: beneficial effects on left ventricular function. Circulation *76*, 115-124.

Sasaki, A., Kida, O., Kangawa, K., Matsuo, H., and Tanaka, K. (1985). Hemodynamic effects of alpha-human atrial natriuretic polypeptide (alpha-hANP) in rats. European journal of pharmacology *109*, 405-407.

Sautebin, L., Ialenti, A., Ianaro, A., and Di Rosa, M. (1995). Modulation by nitric oxide of prostaglandin biosynthesis in the rat. British journal of pharmacology *114*, 323-328.

Schlossmann, J., Feil, R., and Hofmann, F. (2005). Insights into cGMP signalling derived from cGMP kinase knockout mice. Frontiers in bioscience : a journal and virtual library *10*, 1279-1289.

Schmitt, M., Gunaruwan, P., Payne, N., Taylor, J., Lee, L., Broadley, A.J., Nightingale, A.K., Cockcroft, J.R., Struthers, A.D., Tyberg, J.V., *et al.* (2004). Effects of exogenous and endogenous natriuretic peptides on forearm vascular function in chronic heart failure. Arteriosclerosis, thrombosis, and vascular biology *24*, 911-917.

Schroter, J., Zahedi, R.P., Hartmann, M., Gassner, B., Gazinski, A., Waschke, J., Sickmann, A., and Kuhn, M. (2010). Homologous desensitization of guanylyl cyclase A, the receptor for atrial natriuretic peptide, is associated with a complex phosphorylation pattern. The FEBS journal *277*, 2440-2453.

Schweitz, H., Vigne, P., Moinier, D., Frelin, C., and Lazdunski, M. (1992). A new member of the natriuretic peptide family is present in the venom of the green mamba (Dendroaspis angusticeps). The Journal of biological chemistry *267*, 13928-13932.

Shapiro, J.T., DeLeonardis, V.M., Needleman, P., and Hintze, T.H. (1986). Integrated cardiac and peripheral vascular response to atriopeptin 24 in conscious dogs. The American journal of physiology *251*, H1292-1297.

Sheng, J.Z., Ella, S., Davis, M.J., Hill, M.A., and Braun, A.P. (2009). Openers of SKCa and IKCa channels enhance agonist-evoked endothelial nitric oxide synthesis and arteriolar vasodilation. FASEB journal : official publication of the Federation of American Societies for Experimental Biology *23*, 1138-1145.

Shi, S.J., Nguyen, H.T., Sharma, G.D., Navar, L.G., and Pandey, K.N. (2001). Genetic disruption of atrial natriuretic peptide receptor-A alters renin and angiotensin II levels. American journal of physiology Renal physiology *281*, F665-673.

Siang, A.S., Doley, R., Vonk, F.J., and Kini, R.M. (2010). Transcriptomic analysis of the venom gland of the red-headed krait (Bungarus flaviceps) using expressed sequence tags. BMC molecular biology *11*.

Singh, G., Maguire, J.J., Kuc, R.E., Skepper, J.N., Fidock, M., and Davenport, A.P. (2006). Characterization of the snake venom ligand [125I]-DNP binding to natriuretic peptide receptor-A in human artery and potent DNP mediated vasodilatation. British journal of pharmacology *149*, 838-844.

Skryabin, B.V., Holtwick, R., Fabritz, L., Kruse, M.N., Veltrup, I., Stypmann, J., Kirchhof, P., Sabrane, K., Bubikat, A., Voss, M., *et al.* (2004). Hypervolemic hypertension in mice with systemic inactivation of the (floxed) guanylyl cyclase-A gene by alphaMHC-Cre-mediated recombination. Genesis *39*, 288-298.

St Pierre, L., Flight, S., Masci, P.P., Hanchard, K.J., Lewis, R.J., Alewood, P.F., de Jersey, J., and Lavin, M.F. (2006). Cloning and characterisation of natriuretic peptides from the venom glands of Australian elapids. Biochimie *88*, 1923-1931.

Stankevicius, E., Kevelaitis, E., Vainorius, E., and Simonsen, U. (2003). [Role of nitric oxide and other endothelium-derived factors]. Medicina (Kaunas) *39*, 333-341.

Stephenson, S.L., and Kenny, A.J. (1987). The hydrolysis of alpha-human atrial natriuretic peptide by pig kidney microvillar membranes is initiated by endopeptidase-24.11. The Biochemical journal *243*, 183-187.

Stingo, A.J., Clavell, A.L., Aarhus, L.L., and Burnett, J.C., Jr. (1992). Cardiovascular and renal actions of C-type natriuretic peptide. The American journal of physiology *262*, H308-312.

Strobaek, D., Teuber, L., Jorgensen, T.D., Ahring, P.K., Kjaer, K., Hansen, R.S., Olesen, S.P., Christophersen, P., and Skaaning-Jensen, B. (2004). Activation of human IK and SK Ca2+ -activated K+ channels by NS309 (6,7-dichloro-1H-indole-2,3-dione 3-oxime). Biochimica et biophysica acta *1665*, 1-5.

Sudoh, T., Kangawa, K., Minamino, N., and Matsuo, H. (1988). A new natriuretic peptide in porcine brain. Nature *332*, 78-81.

Sudoh, T., Minamino, N., Kangawa, K., and Matsuo, H. (1990). C-type natriuretic peptide (CNP): a new member of natriuretic peptide family identified in porcine brain. Biochemical and biophysical research communications *168*, 863-870.

Suga, S., Itoh, H., Komatsu, Y., Ogawa, Y., Hama, N., Yoshimasa, T., and Nakao, K. (1993). Cytokine-induced C-type natriuretic peptide (CNP) secretion from vascular endothelial cells--evidence for CNP as a novel autocrine/paracrine regulator from endothelial cells. Endocrinology *133*, 3038-3041.

Suga, S., Nakao, K., Hosoda, K., Mukoyama, M., Ogawa, Y., Shirakami, G., Arai, H., Saito, Y., Kambayashi, Y., Inouye, K., *et al.* (1992). Receptor selectivity of natriuretic peptide family, atrial natriuretic peptide, brain natriuretic peptide, and C-type natriuretic peptide. Endocrinology *130*, 229-239.

Sunagawa, K., Ikeda, Y., Kawada, T., Sugimachi, M., Shishido, T., Sato, T., Miyano, H., Matsuura, W., Inagaki, M., and Alexander, J., Jr. (1998). Dynamic control of

arterial blood pressure by the sympathetic baroreflex. Fundamental & clinical pharmacology *12 Suppl 1*, 23s-28s.

Suwa, M., Seino, Y., Nomachi, Y., Matsuki, S., and Funahashi, K. (2005). Multicenter prospective investigation on efficacy and safety of carperitide for acute heart failure in the 'real world' of therapy. Circulation Journal *69*, 283-290.

Swedberg, K., Cleland, J., Dargie, H., Drexler, H., Follath, F., Komajda, M., Tavazzi, L., Smiseth, O.A., Gavazzi, A., Haverich, A., *et al.* (2005). Guidelines for the diagnosis and treatment of chronic heart failure: executive summary (update 2005): The Task Force for the Diagnosis and Treatment of Chronic Heart Failure of the European Society of Cardiology. European heart journal *26*, 1115-1140.

Takahashi, N., Saito, Y., Kuwahara, K., Harada, M., Kishimoto, I., Ogawa, Y., Kawakami, R., Nakagawa, Y., Nakanishi, M., and Nakao, K. (2003). Angiotensin II-induced ventricular hypertrophy and extracellular signal-regulated kinase activation are suppressed in mice overexpressing brain natriuretic peptide in circulation. Hypertension research : official journal of the Japanese Society of Hypertension *26*, 847-853.

Takayanagi, R., Inagami, T., Snajdar, R.M., Imada, T., Tamura, M., and Misono, K.S. (1987). Two distinct forms of receptors for atrial natriuretic factor in bovine adrenocortical cells. Purification, ligand binding, and peptide mapping. The Journal of biological chemistry *262*, 12104-12113.

Tamura, N., Ogawa, Y., Chusho, H., Nakamura, K., Nakao, K., Suda, M., Kasahara, M., Hashimoto, R., Katsuura, G., Mukoyama, M., *et al.* (2000). Cardiac fibrosis in mice lacking brain natriuretic peptide. Proceedings of the National Academy of Sciences of the United States of America *97*, 4239-4244.

Thoren, P., Mark, A.L., Morgan, D.A., O'Neill, T.P., Needleman, P., and Brody, M.J. (1986). Activation of vagal depressor reflexes by atriopeptins inhibits renal sympathetic nerve activity. The American journal of physiology *251*, H1252-1259.

Thorpe, D.S., Niu, S., and Morkin, E. (1996). The guanylyl cyclase core of an atrial natriuretic peptide receptor: enzymatic properties and basis for cooperativity. Biochemical and biophysical research communications *218*, 670-673.

Tsuji, T., and Kunieda, T. (2005). A loss-of-function mutation in natriuretic peptide receptor 2 (Npr2) gene is responsible for disproportionate dwarfism in cn/cn mouse. The Journal of biological chemistry *280*, 14288-14292.

Ueda, S., Sudoh, T., Fukuda, K., Kangawa, K., Minamino, N., and Matsuo, H. (1987). Identification of alpha atrial natriuretic peptide [4-28] and [5-28] in porcine brain. Biochemical and biophysical research communications *149*, 1055-1062.

van den Akker, F., Zhang, X., Miyagi, M., Huo, X., Misono, K.S., and Yee, V.C. (2000). Structure of the dimerized hormone-binding domain of a guanylyl-cyclase-coupled receptor. Nature *406*, 101-104.

van den Meiracker, A.H., Lameris, T.W., van de Ven, L.L., and Boomsma, F. (2003). Increased plasma concentration of natriuretic peptides by selective beta1-blocker bisoprolol. Journal of cardiovascular pharmacology *42*, 462-468.

van der Zander, K., Houben, A.J., Kroon, A.A., and de Leeuw, P.W. (1999). Effects of brain natriuretic peptide on forearm vasculature: comparison with atrial natriuretic peptide. Cardiovascular research *44*, 595-600.

van Veldhuisen, D.J., Linssen, G.C., Jaarsma, T., van Gilst, W.H., Hoes, A.W., Tijssen, J.G., Paulus, W.J., Voors, A.A., and Hillege, H.L. (2013). B-type natriuretic peptide and prognosis in heart failure patients with preserved and reduced ejection fraction. Journal of the American College of Cardiology *61*, 1498-1506.

Vanneste, Y., Michel, A., Dimaline, R., Najdovski, T., and Deschodt-Lanckman, M. (1988). Hydrolysis of alpha-human atrial natriuretic peptide in vitro by human kidney membranes and purified endopeptidase-24.11. Evidence for a novel cleavage site. The Biochemical journal *254*, 531-537.

Vuolteenaho, O., Arjamaa, O., and Ling, N. (1985). Atrial natriuretic polypeptides (ANP): rat atria store high molecular weight precursor but secrete processed peptides of 25-35 amino acids. Biochemical and biophysical research communications *129*, 82-88.

Waldman, S.A., Rapoport, R.M., and Murad, F. (1984). Atrial natriuretic factor selectively activates particulate guanylate cyclase and elevates cyclic GMP in rat tissues. The Journal of biological chemistry *259*, 14332-14334.

Wang, W., Ou, Y., and Shi, Y. (2004). AlbuBNP, a recombinant B-type natriuretic peptide and human serum albumin fusion hormone, as a long-term therapy of congestive heart failure. Pharmaceutical research *21*, 2105-2111.

Wegner, M., Stasch, J.P., Hirth-Dietrich, C., Dressel, J., Voges, K.P., and Kazda, S. (1995). Interaction of a neutral endopeptidase inhibitor with an ANP-C receptor ligand in anesthetized dogs. Clin Exp Hypertens *17*, 861-876.

Wei, C.M., Kim, C.H., Miller, V.M., and Burnett, J.C., Jr. (1993). Vasonatrin peptide: a unique synthetic natriuretic and vasorelaxing peptide. The Journal of clinical investigation *92*, 2048-2052.

Wennberg, P.W., Miller, V.M., Rabelink, T., and Burnett, J.C., Jr. (1999). Further attenuation of endothelium-dependent relaxation imparted by natriuretic peptide receptor antagonism. The American journal of physiology *277*, H1618-1621.

Winquist, R.J., Faison, E.P., Waldman, S.A., Schwartz, K., Murad, F., and Rapoport, R.M. (1984). Atrial natriuretic factor elicits an endothelium-independent relaxation and activates particulate guanylate cyclase in vascular smooth muscle. Proceedings of the National Academy of Sciences of the United States of America *81*, 7661-7664.

Wu, C., Wu, F., Pan, J., Morser, J., and Wu, Q. (2003). Furin-mediated processing of Pro-C-type natriuretic peptide. The Journal of biological chemistry *278*, 25847-25852.

Yamahara, K., Itoh, H., Chun, T.H., Ogawa, Y., Yamashita, J., Sawada, N., Fukunaga, Y., Sone, M., Yurugi-Kobayashi, T., Miyashita, K., *et al.* (2003). Significance and therapeutic potential of the natriuretic peptides/cGMP/cGMP-dependent protein kinase pathway in vascular regeneration. Proceedings of the National Academy of Sciences of the United States of America *100*, 3404-3409.

Yan, W., Wu, F., Morser, J., and Wu, Q. (2000). Corin, a transmembrane cardiac serine protease, acts as a pro-atrial natriuretic peptide-converting enzyme. Proceedings of the National Academy of Sciences of the United States of America *97*, 8525-8529.

Yancy, C.W., Jessup, M., Bozkurt, B., Butler, J., Casey, D.E., Jr., Drazner, M.H., Fonarow, G.C., Geraci, S.A., Horwich, T., Januzzi, J.L., *et al.* (2013). 2013 ACCF/AHA guideline for the management of heart failure: executive summary: a

report of the American College of Cardiology Foundation/American Heart Association Task Force on practice guidelines. Circulation *128*, 1810-1852.

Yandle, T.G., Richards, A.M., Nicholls, M.G., Cuneo, R., Espiner, E.A., and Livesey, J.H. (1986). Metabolic clearance rate and plasma half life of alpha-human atrial natriuretic peptide in man. Life sciences *38*, 1827-1833.

Yanoshita, R., Ogawa, Y., Murayama, N., Omori-Satoh, T., Saguchi, K., Higuchi, S., Khow, O., Chanhome, L., Samejima, Y., and Sitprija, V. (2006). Molecular cloning of the major lethal toxins from two kraits (Bungarus flaviceps and Bungarus candidus). Toxicon : official journal of the International Society on Toxinology *47*, 416-424.

Yoshimoto, T., Naruse, M., Tanabe, A., Naruse, K., Seki, T., Imaki, T., Muraki, T., Matsuda, Y., and Demura, H. (1998). Potentiation of natriuretic peptide action by the beta-adrenergic blocker carvedilol in hypertensive rats: a new antihypertensive mechanism. Endocrinology *139*, 81-88.

Yoshimura, M., Yasue, H., Morita, E., Sakaino, N., Jougasaki, M., Kurose, M., Mukoyama, M., Saito, Y., Nakao, K., and Imura, H. (1991). Hemodynamic, renal, and hormonal responses to brain natriuretic peptide infusion in patients with congestive heart failure. Circulation *84*, 1581-1588.

Appendix

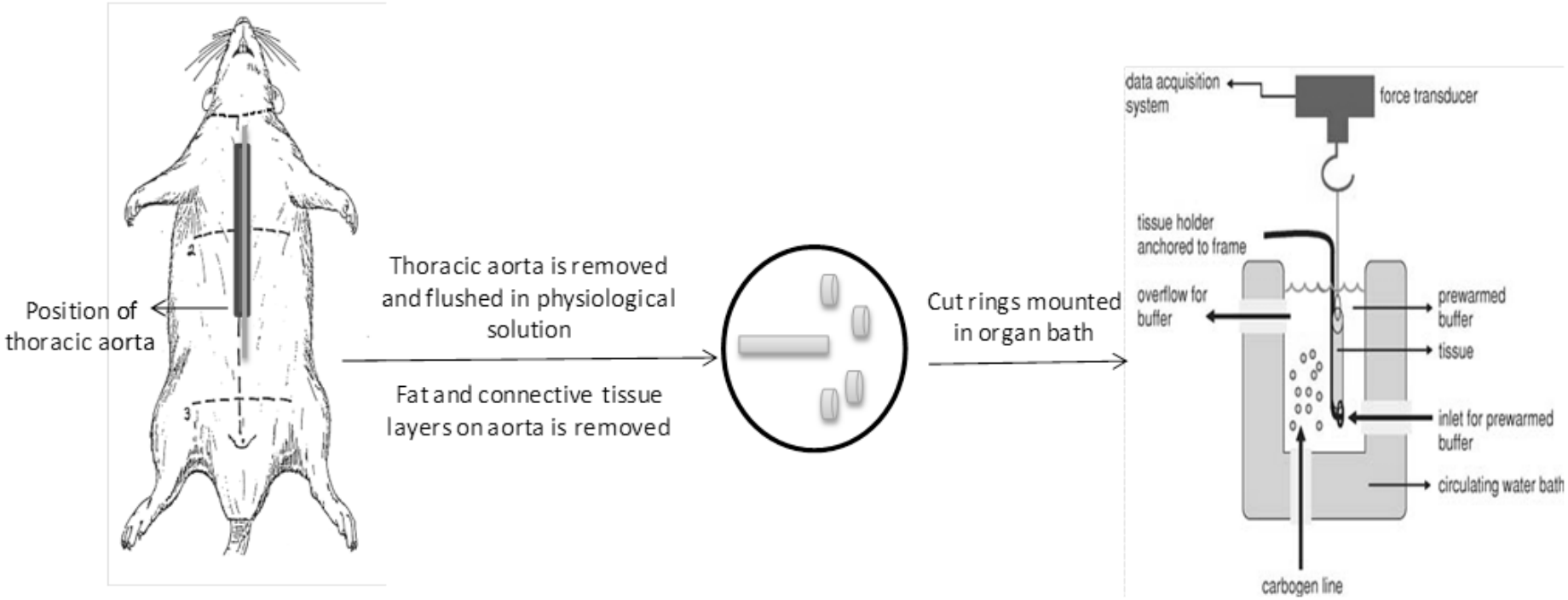

Figure A.1. Ex-vivo organ bath experiment setup for vasorelaxation assay

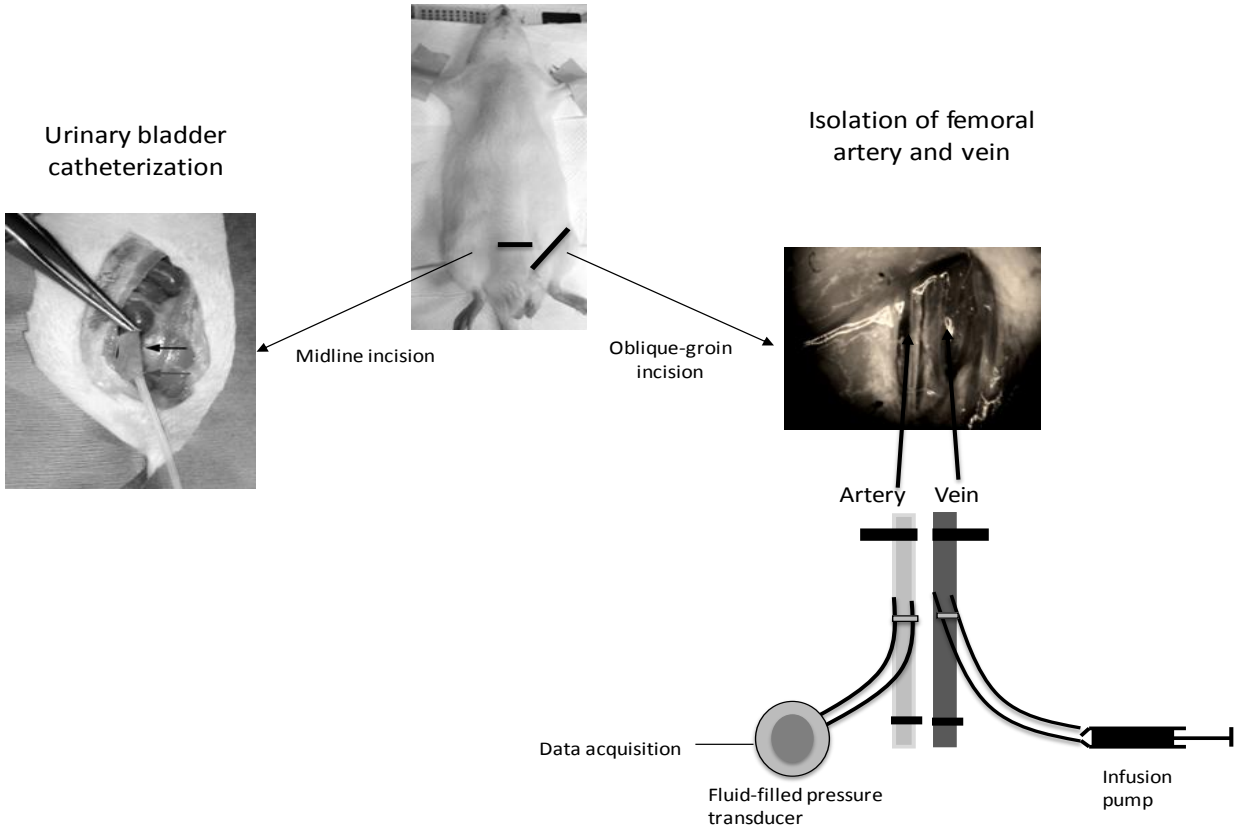

Figure A.2. Experimental setup for measurement of blood pressure and urine output in anesthetized rats (de Bold *et al.*, 1981)